



A precise measurement of the Z-boson double-differential transverse momentum and rapidity distributions in the full phase space of the decay leptons with the ATLAS experiment at $\sqrt{s} = 8 \text{ TeV}$

The ATLAS Collaboration

This paper presents for the first time a precise measurement of the production properties of the Z boson in the full phase space of the decay leptons. The measurement is obtained from proton–proton collision data collected by the ATLAS experiment in 2012 at $\sqrt{s} = 8 \text{ TeV}$ at the LHC and corresponding to an integrated luminosity of 20.2 fb^{-1} . The results, based on a total of 15.3 million Z-boson decays to electron and muon pairs, extend and improve a previous measurement of the full set of angular coefficients describing Z-boson decay. The double-differential cross-section distributions in Z-boson transverse momentum p_T and rapidity y are measured in the pole region, defined as $80 < m < 100 \text{ GeV}$, over the range $|y| < 3.6$. The total uncertainty of the normalised cross-section measurements in the peak region of the p_T distribution is dominated by statistical uncertainties over the full range and increases as a function of rapidity from $0.5 - 1.0\%$ for $|y| < 2.0$ to $2 - 7\%$ at higher rapidities. The results for the rapidity-dependent transverse momentum distributions are compared to state-of-the-art QCD predictions, which combine in the best cases approximate $N^4\text{LL}$ resummation with $N^3\text{LO}$ fixed-order perturbative calculations. The differential rapidity distributions integrated over p_T are even more precise, with accuracies from $0.2 - 0.3\%$ for $|y| < 2.0$ to $0.4 - 0.9\%$ at higher rapidities, and are compared to fixed-order QCD predictions using the most recent parton distribution functions. The agreement between data and predictions is quite good in most cases.

1 Introduction and motivation

The production of Z bosons and their decay to lepton pairs at the Large Hadron Collider (LHC) through the Drell–Yan mechanism [1] has been the topic of very fruitful and detailed studies in the LHC experiments [2–8]. The precision of the measurements has motivated over the past decade impressive theoretical developments, mostly in the area of higher-accuracy quantum chromodynamic (QCD) predictions, but also in the area of parton distribution functions (PDFs). The sub-percent precision achieved for the absolute and normalised fiducial cross-section measurements of the Z -boson transverse momentum, p_T , as a function of its rapidity, $|y|$, at the Z pole strongly constrains state-of-the-art theoretical calculations. In the best cases, these calculations combine approximate next-to-next-to-next-to-next-to-leading logarithm (N⁴LL) perturbative resummation at low p_T with $\mathcal{O}(\alpha_s^3)$ (N³LO) fixed-order perturbative calculations at high p_T , where α_s denotes the strong coupling constant. Similarly, the precision obtained for the fiducial cross-section measurements of $|y|$ provides strong constraints on the parton distribution functions.

This paper presents for the first time a double-differential measurement in $(p_T, |y|)$ of absolute and normalised cross-sections at the Z pole within the full phase space of the decay leptons. The measurement uses the full coverage of the ATLAS detector to combine 6.2 million electron and 7.8 million muon pairs from Z -boson decays in the central region (ee_{CC} and $\mu\mu_{CC}$ channels), complemented by 1.3 million electron pairs with one electron in the forward region of the detector (ee_{CF} channel). Such a measurement is possible using the methodology already developed and published for the extraction of the Z boson polarisation [6]. It relies on the decomposition of the lepton angular $\cos\theta$ and ϕ distributions in the Collins-Soper frame [9] into nine spherical harmonic polynomials, P_i , multiplied by angular coefficients, A_i [10–13]. For pure Z -boson production, the full five-dimensional differential cross section describing the kinematics of the two Born-level leptons can be written as:

$$\frac{d\sigma}{dp_T dy dm d\cos\theta d\phi} = \frac{3}{16\pi} \frac{d\sigma^{U+L}}{dp_T dy dm} \left\{ (1 + \cos^2\theta) + \frac{1}{2} A_0(1 - 3\cos^2\theta) + A_1 \sin 2\theta \cos\phi \right. \quad (1)$$

$$+ \frac{1}{2} A_2 \sin^2\theta \cos 2\phi + A_3 \sin\theta \cos\phi + A_4 \cos\theta$$

$$\left. + A_5 \sin^2\theta \sin 2\phi + A_6 \sin 2\theta \sin\phi + A_7 \sin\theta \sin\phi \right\}.$$

The dependence of the differential cross section on $\cos\theta$ and ϕ is analytical and is fully contained in the harmonic polynomials. On the other hand, the dependence on p_T , $|y|$ and m is entirely contained in the unpolarised cross section, denoted by σ^{U+L} , and in the A_i angular coefficients. Therefore, all hadronic dynamics from the production mechanism are factorised from the decay kinematics in the Z -boson rest frame. This allows the measurement precision to be essentially insensitive to all uncertainties in QCD, quantum electrodynamics (QED), and electroweak (EW) effects related to Z -boson production and decay. In particular, EW corrections that couple the initial-state quarks to the final-state leptons have a negligible impact (below 0.05%) at the Z -boson pole. This has been shown for the LEP precision measurements [14, 15], when calculating the interference between initial-state and final-state QED radiation and more recently for Z -boson measurements at the LHC [16]. The small fraction of γ^* production in the Z -boson pole region and its interference with the Z boson can also be described by Eq. (1), but with different coefficients, so the A_i coefficients discussed in this paper are effective coefficients, containing the small γ^* contribution at the Z pole.

The decomposition is based on a simple and model-independent ansatz: the spin-one nature of the intermediate gauge boson, and the spin one-half nature of the decay leptons, and on the assumption of angular momentum conservation and quantisation. It removes the need for predictions to model accurately the polarisation and decay of the Z -boson; only its production properties are of interest for comparison to the measurements. Therefore, any phenomenological interpretation of this measurement avoids the theoretical uncertainties and ambiguities related to spin correlations and to the resummation of fiducial power corrections [17–20].

One striking example of the advantage of exploiting measurement in the full phase space of the decay leptons is the rapidity dependence of the Z -boson transverse momentum spectrum: whereas the fiducial measurements of Ref. [2] are insensitive to this production property because the fiducial lepton selections essentially remove the rapidity dependence of the spectrum, the measurements reported here probe this dependence very precisely. Equally importantly, the differential angular distributions provide extra constraints on experimental systematic uncertainties since they are not used in the calibration procedures of the detectors and have even less sensitivity to theoretical systematic uncertainties than the fiducial measurements.

Finally, these measurements pave the way for very clean interpretations in terms of QCD. A precise determination of the Z -boson transverse momentum spectrum leads to excellent sensitivity to the strong coupling constant at the m_Z scale, while the even more precise rapidity-dependent cross-sections, obtained after integrating over p_T , can be compared directly to state-of-the-art fixed-order predictions with excellent sensitivity to the parton distribution functions.

This paper is structured as follows. Section 2 first presents an overview of the measurement methodology and of the likelihood fit performed to extract the observables of interest from the experimental distributions. Section 3 describes briefly the data analysis, and Section 4 discusses the systematic uncertainties in the measured differential cross-sections. Section 5 compares the $\frac{d^2\sigma}{dp_T dy}$ measurements to theoretical predictions combining perturbative resummation with fixed-order calculations, and then compares the $\frac{d\sigma}{dy}$ and the total cross-section measurements to the predictions from QCD N³LO calculations using different PDF sets. Finally, Section 6 summarises and concludes the paper.

2 Measurement methodology

The angular coefficients are extracted from the data by fitting templates of the P_i polynomial terms, defined in Eq. (1), to the reconstructed angular distributions using 8×8 bins in $(\cos \theta, \phi)$ space (see Ref. [6] for a detailed description). Each template is normalised by a free parameter for its corresponding polynomial coefficient A_i and a common parameter representing the unpolarised cross section. The polynomial $P_8 = 1 + \cos^2 \theta$ in Eq. (1) is only normalised by the parameter for the unpolarised cross-section. All the angular coefficients together with the corresponding unpolarised cross section parameters are measured in each of the analysis bins in $(p_T, |y|)$ space.

In the absence of selections for the final state leptons, the angular distributions in the gauge boson rest frame are defined by its polarisation. In the presence of selection criteria applied to the leptons, the distributions are sculpted by kinematic effects, and can no longer be described by the sum of the nine P_i polynomials as in Eq. (1). Templates of the P_i terms are therefore constructed to account for this, which requires fully simulated signal Monte-Carlo (MC) samples to model the acceptance, efficiency, and migration of events. Reference A_i coefficients are extracted in a simple way from the predicted shapes

of the angular distributions in the full phase space of the decay leptons, using the orthogonality of the P_i polynomials (see Ref. [11] describing the underlying moment method used to extract the coefficients). Together with the reference unpolarised cross-section, they are used in a folding procedure based on the signal MC simulation. The folded polynomial templates (or simply templates) are built in $(\cos \theta, \phi)$ space for each of the nine original polynomials and for each of the measurement bins in $(p_T^{\ell\ell}, y^{\ell\ell})$ space. They are then used to extract the angular coefficients and the unpolarised cross section in the full phase space of the leptons from Z -boson decay. The observables $m^{\ell\ell}$, $p_T^{\ell\ell}$, and $y^{\ell\ell}$, which are defined using reconstructed lepton pairs, as described in Section 3.3, are to be distinguished from m , p_T and $|y|$, which are defined at generator level using lepton pairs at the Born level.

A likelihood is built from the nominal templates and the varied templates reflecting the systematic uncertainties, which are represented by two categories of nuisance parameters (NP), β and γ . The first category, β , represents experimental and theoretical uncertainties. Each β^m in the set $\beta = \{\beta^1, \dots, \beta^M\}$ is constrained by a unit Gaussian probability density function, $G(0|\beta^m, 1)$, and linearly interpolates between the nominal and varied templates. The second category, γ^n , represents systematic uncertainties from the limited size of the MC signal and background samples, which are constrained by Poisson probability density functions, $P(N_{\text{eff}}^n|\gamma^n N_{\text{eff}}^n)$ where N_{eff}^n is the effective number of MC events in bin n , in each of the $N_{\text{bins}} = 22528$ bins of the measurement. After including these auxiliary parameters, and after all signal and background templates (see Section 3 for details of the samples) are summed over (with their respective normalisations), the expected number of events N_{exp}^n in bin n of the measurement can be written as:

$$N_{\text{exp}}^n(A, \sigma^{U+L}, \beta, \gamma) = \left\{ \sum_j \sigma_j^{U+L} \times L \times \left[t_{8j}^n(\beta) + \sum_{i=0}^7 A_{ij} \times t_{ij}^n(\beta) \right] \right\} \times \gamma^n + \sum_B^{\text{bkg}} T_B^n(\beta), \quad (2)$$

where:

- index i runs over the eight angular coefficients and the corresponding P_i polynomials, while index j runs over all 352 bins in $(p_T, |y|)$ space
- A is the set of all angular coefficients, A_{ij}
- σ^{U+L} is the set of all unpolarised cross sections, σ_j^{U+L}
- β is the set of all Gaussian-constrained nuisance parameters representing the systematic uncertainties
- γ is the set of all Poisson-constrained nuisance parameters representing the statistical uncertainties in the simulated samples and in the background estimates
- t is the set of all signal P_i polynomial templates, t_{ij}
- T_B is the set of background templates, where the sum runs over all background sources
- L is the total integrated luminosity.

The summation over index j accounts for the contributions from all analysis bins at generator level that migrate into other analysis bins at the reconstruction level. The likelihood is then constructed as a product of Poisson probabilities across all N_{bins} and of auxiliary constraints for each nuisance parameter β^m :

$$\mathcal{L}(A, \sigma^{U+L}, \theta|N_{\text{obs}}) = \prod_n^{N_{\text{bins}}} \{P(N_{\text{obs}}^n|N_{\text{exp}}^n(A, \sigma^{U+L}, \theta))P(N_{\text{eff}}^n|\gamma^n N_{\text{eff}}^n)\} \times \prod_m^M G(0|\beta^m, 1). \quad (3)$$

A profile likelihood ratio method is used to extract the best fit values of the parameters of interest (POIs) and their uncertainties. The POIs include the angular coefficients A_{ij} and the cross sections σ_j^{U+L} in each measurement bin. This procedure extends that presented in Ref. [6], in which only the angular coefficients were extracted as a function of p_T and $|y|$ without any fit constraints based on the σ_j^{U+L} POIs. The results from the full fit focus on the differential cross-section results in each channel and each measurement bin. The results of the fit for the angular coefficients involving only central leptons are compatible with those of Ref. [6] within the uncertainties resulting from the slightly different selections and calibrations applied here. As explained in Section 3.3, the analysis of the forward electrons is significantly improved here with respect to that documented in Ref. [21]. As a result, the measurements of the ee_{CF} angular coefficients reported in this paper are published in HEPDATA and supersede those of Ref. [6].

3 Analysis

3.1 ATLAS detector

The ATLAS experiment [22] at the LHC is a multipurpose particle detector with a forward–backward symmetric cylindrical geometry and a near 4π coverage in solid angle.¹ It consists of an inner tracking detector, electromagnetic (EM) and hadronic calorimeters, and a muon spectrometer. The inner detector provides precision tracking of charged particles in the pseudorapidity range $|\eta| < 2.5$. This region is matched to a high-granularity EM sampling calorimeter covering the pseudorapidity range $|\eta| < 3.2$ and a coarser granularity calorimeter up to $|\eta| = 4.9$. A hadronic calorimeter system covers the entire pseudorapidity range up to $|\eta| = 4.9$. The muon spectrometer provides triggering and tracking capabilities in the range $|\eta| < 2.4$ and $|\eta| < 2.7$, respectively.

A first-level trigger is implemented in hardware, followed by two software-based trigger levels that together reduce the accepted event rate to 400 Hz on average. An extensive software suite [23] is used in the reconstruction and analysis of real and simulated data, in detector operations, and in the trigger and data acquisition systems of the experiment.

3.2 Data and Monte Carlo samples

The data were collected by the ATLAS detector in 2012 at a centre-of-mass energy of $\sqrt{s} = 8$ TeV, and correspond to an integrated luminosity of 20.2 fb^{-1} . The mean number of additional pp interactions per bunch crossing (pile-up events) in the data set is approximately 20.

The event generators used to produce the $Z/\gamma^* \rightarrow \ell\ell$ signal events and the backgrounds estimated from simulation are listed in Table 1. The baseline POWHEG Box (v1/r2129) signal sample [24–26], using the CT10 NLO set of PDFs [28], is interfaced to PYTHIA 8 (v.8.170) [27] with the AU2 set of tuned parameters [36] to simulate the parton shower, hadronisation and underlying event, and to Photos (v2.154) [37] to simulate QED final-state radiation (FSR) in the Z -boson decay. The simulated line-shape of the Z -boson is

¹ ATLAS uses a right-handed coordinate system with its origin at the nominal interaction point (IP) in the centre of the detector and the z -axis along the beam pipe. The x -axis points from the IP to the centre of the LHC ring, and the y -axis points upwards. Cylindrical coordinates (r, ϕ) are used in the transverse plane, ϕ being the azimuthal angle around the z -axis. The pseudorapidity is defined in terms of the polar angle θ as $\eta = -\ln \tan(\theta/2)$. Angular distance is measured in units of $\Delta R \equiv \sqrt{(\Delta\eta)^2 + (\Delta\phi)^2}$.

Process	Generator	PDF
$Z/\gamma^* \rightarrow \ell\ell$	POWHEG BOX [24–26] + PYTHIA 8 [27]	CT10 NLO [28]
$Z/\gamma^* \rightarrow \tau\tau$	SHERPA [29–32]	CT10 NLO
$t\bar{t}$	POWHEG BOX + PYTHIA 6 [33]	CT10 NLO
Single top quark (Wt channel)	POWHEG BOX + PYTHIA 8	CT10 NLO
Dibosons	HERWIG [34]	CTEQ6L1
$\gamma\gamma \rightarrow \ell\ell$	PYTHIA 8	MRST2004QED NLO [35]

Table 1: MC samples used to estimate the signal and backgrounds in the analysis.

reweighted to account for the running width and for mass-dependent NNLO QCD [38] effects, following the recipe described in Ref. [8]. This is a percent-level effect within the mass range used by the measurement, and provides the best possible leading-order EW prediction of the line-shape of the Z boson. The number of events available in the baseline POWHEG BOX + PYTHIA 8 signal sample corresponds to approximately four times that in the data.

Backgrounds from EW (diboson, $Z/\gamma^* \rightarrow \tau\tau$, and $\gamma\gamma \rightarrow \ell\ell$ production) and top-quark (production of top-quark pairs and of single top quarks) processes are evaluated from the MC samples listed in Table 1. All MC samples are processed through a full ATLAS detector simulation [39], based on GEANT4 [40], and reconstructed with the same software as that used for the data. Pile-up events, occurring in the same and neighbouring bunch crossings are simulated and overlaid at the detector hit level on top of the hard-scattering process from the MC simulation.

3.3 Analysis overview and event selection

For this paper, a central lepton (electron or muon) is one found in the region $|\eta| < 2.4$ (excluding, for electrons, the electromagnetic calorimeter barrel/end-cap transition region $1.37 < |\eta| < 1.52$), while a forward electron is one found in the region $2.5 < |\eta| < 4.9$ (excluding a transition region $3.00 < |\eta| < 3.35$ between the end-cap and forward calorimeters). The analysis is split into three orthogonal channels that are analysed independently, and then combined for the last stages of the analysis, after verifying their compatibility.

The ee_{CC} channel consists of candidate events with two central electrons, obtained using a logical OR of a dielectron trigger, requiring two electron candidates, each having $p_T > 12$ GeV, with two high- p_T single-electron triggers, the main one corresponding to a p_T threshold of 24 GeV. Electron candidates are required offline to have $p_T > 20$ GeV and $|\eta| < 2.4$, and are reconstructed from clusters of energy in the electromagnetic calorimeter matched to inner detector tracks. The electron candidates must satisfy a set of “medium” selection criteria [21], which have been optimised for the level of pile-up present in the 2012 data.

The $\mu\mu_{CC}$ channel consists of candidate events with two central muons, obtained using a logical OR of a dimuon trigger requiring two muon candidates with $p_T > 18$ GeV and 8 GeV, respectively, and of two high- p_T single-muon triggers, the main one corresponding to a p_T threshold of 24 GeV. Muon candidates

are required offline to have $p_T > 20$ GeV and $|\eta| < 2.4$, and are identified as tracks in the inner detector, which are matched and combined with track segments in the muon spectrometer [41]. Track-quality, and longitudinal and transverse impact-parameter requirements are imposed to suppress backgrounds, and to ensure that the muon candidates originate from a common primary pp interaction vertex.

The ee_{CF} channel consists of candidate events with one central and one forward electron, obtained using the logical OR of the two high- p_T single-electron triggers used for the ee_{CC} events, as described above. The central electron candidate is required to have $p_T > 25$ GeV and $|\eta| < 2.4$. Because the expected background from multijet events is larger in this channel than in the ee_{CC} channel, the central electron candidate is required in addition to satisfy a set of “tight” selection criteria [21], including an explicit isolation requirement, which are optimised for the level of pile-up observed in the 2012 data. The forward electron candidate is required to have $p_T > 20$ GeV and to satisfy a set of “medium” selection criteria, based only on the shower shapes in the calorimeters, since this region is outside the acceptance of the inner detector [42].

In the case of the ee_{CF} channel, the analysis of the forward electron candidates, in terms of the data quality, alignment, identification criteria, and calibration of the electromagnetic compartments of the calorimeters outside the acceptance of the inner detector, was improved significantly from those documented in Ref. [21]. A few examples illustrating these improvements are:

- misalignments of a few mm between the inner wheels of the electromagnetic end-cap calorimeters and the inner detector and a rotation of a few mrad between one of the forward calorimeters and the inner detector were found and corrected for when studying the azimuthal angle difference between the central and forward electrons. As a result, the two angular coefficients (A_1, A_6), for which the fully two-dimensional ($\cos \theta, \phi$) measurement is necessary, can now be measured for the ee_{CF} channel, and are found to be in agreement with the SM predictions.
- an azimuthal inter-calibration of the forward electrons was performed to improve the baseline calibration. This corrected for large inhomogeneities of up to 10–15% in the energy response due to material from inner-detector services in front of the calorimeters not accounted for correctly in the simulation, and for high-voltage problems in some cells, which were inadequately corrected for online during data-taking.
- the largest correction was obtained by adjusting the simulated lateral shower shapes in the calorimeters to data and then calibrating carefully each region of the calorimeters. This resulted in both improved efficiencies for the forward electrons in certain regions of phase space and improved energy calibration. As a result, the p-value for the agreement between the combined ee_{CC} and $\mu\mu_{CC}$ channels and the ee_{CF} channel in the $|y|$ range where they overlap, $1.6 < |y| < 2.4$, was improved from $< 10^{-4}$ to 3% (see Fig. 6 in Section 5.1).

In each channel, the events are required to contain exactly two lepton candidates satisfying the criteria described above. For the central-central channels, where the charges of both leptons are measured, the two lepton candidates are required to be of opposite charge.

As described in Section 1, this analysis is focused on the Z -boson pole region, and the lepton pair is required to have an invariant mass, $m^{\ell\ell}$, within a window around the Z -boson mass, $80 < m^{\ell\ell} < 100$ GeV. The simulated events are required to satisfy the same selection criteria as the data, after applying small corrections to account for the differences between data and simulation in terms of reconstruction, identification and trigger efficiencies and of energy scale and resolution for electrons and muons [41–43]. All simulated

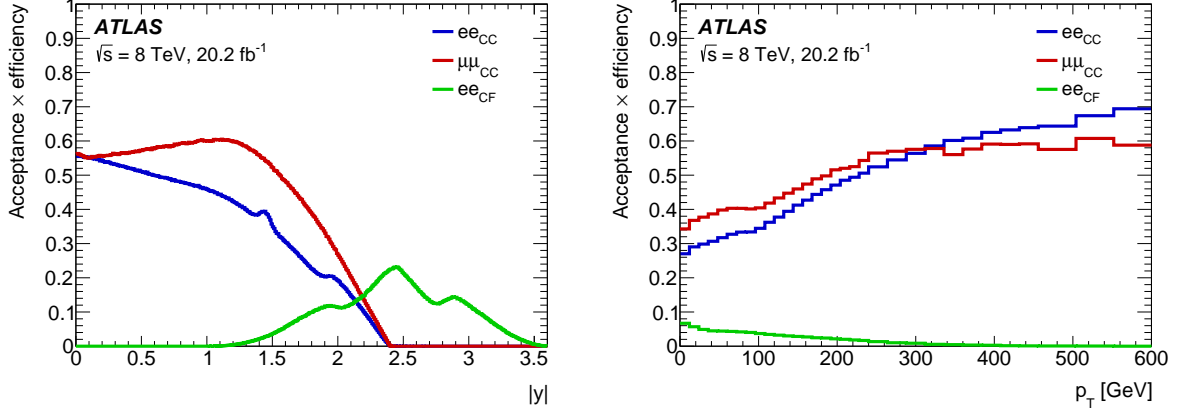


Figure 1: Expected Z-boson acceptance times selection efficiencies as a function of $|y|$ (left) and p_T (right) for the ee_{CC} , $\mu\mu_{CC}$ and ee_{CF} analysis channels.

events are reweighted to match the distributions observed in data for the level of pile-up and for the primary vertex longitudinal position.

The measurements are binned in p_T and $|y|$, with fine bins in p_T and coarse bins in $|y|$, as follows:

1. ee_{CC} and $\mu\mu_{CC}$ channels:

- 23 bins in p_T with bin boundaries $\{0, 2.5, 5.0, 8.0, 11.4, 14.9, 18.5, 22.0, 25.5, 29.0, 32.6, 36.4, 40.4, 44.9, 50.2, 56.4, 63.9, 73.4, 85.4, 105.0, 132.0, 173.0, 253.0, 4000\}$ GeV,
- 6 bins in $|y|$ with bin boundaries $\{0, 0.4, 0.8, 1.2, 1.6, 2.0, 2.4\}$;

2. ee_{CF} channel:

- 19 bins in p_T with bin boundaries $\{0, 2.5, 5.0, 8.0, 11.4, 14.9, 18.5, 22.0, 25.5, 29.0, 32.6, 36.4, 40.4, 44.9, 50.2, 56.4, 63.9, 73.4, 85.4, 105.0\}$ GeV,
- 4 bins in $|y|$ with bin boundaries $\{1.6, 2.0, 2.4, 2.8, 3.6\}$.

The choice of bin boundaries in p_T is the result of an optimisation with respect to the limited resolution of the measurements at low p_T and the limited statistics at high p_T .

The angular coefficients and unpolarised cross-section results are extracted taking into account the correlations and migrations between the measurement bins. Figure 1 shows the expected products of the acceptance and the selection efficiency, defined as the ratio of the number of selected events to the number of events in the full decay lepton phase space, as functions of both $|y|$ and p_T . The shape of this product of acceptance and efficiency in $|y|$ results in part from the differences in reconstruction and identification efficiencies between central electrons and muons. The ee_{CF} channel covers a higher range in $|y|$ and overlaps with the central-central channels for $1.6 < |y| < 2.4$. In each of the analysis measurement bins, two-dimensional $(\cos \theta, \phi)$ angular distributions are computed (eight equal-sized bins in each observable) and they serve as the basis for the simultaneous extraction of all the angular coefficients and of the unpolarised cross-sections, following the methodology described in Section 2.

3.4 Background estimates and signal yields

Table 2 shows the event yields and breakdowns of the fraction of events originating from background sources, for the ee_{CC} , $\mu\mu_{CC}$, and ee_{CF} channels, respectively. The numbers are shown in each $|y|$ analysis bin integrated over p_T . The backgrounds are divided into three major groups:

- the backgrounds containing a prompt isolated lepton, from top ($t\bar{t}$ and Wt), diboson, $Z \rightarrow \tau\tau$, and $\gamma\gamma \rightarrow ll$ processes, estimated from simulation samples (see Section 3.2),
- the multijet and W +jet backgrounds, estimated from data using a method very similar to that described in Ref. [6], and
- the non-fiducial Z background, which is estimated from simulation and consists almost entirely of events outside the full mass range considered for the analysis at generator level, but passing the selection cuts at reconstruction level owing to migrations.

The background contamination from other processes for the ee_{CC} and $\mu\mu_{CC}$ channels is very small and amounts to about 0.3%. The multijet background in the ee_{CF} channel is larger, amounting to about 1.0%. The non-fiducial Z background amounts to about 1% in all channels. Templates of the angular distributions of the sum of all these backgrounds are used in the fit to extract the angular coefficients, as described in Section 2.

3.5 Angular distributions

The criteria described above are applied to the data, leading to totals of 6.2 (ee_{CC}), 7.8 ($\mu\mu_{CC}$), and 1.3 (ee_{CF}) million selected events (see Table 2 for a more detailed breakdown as a function of $y^{\ell\ell}$). The reconstructed differential angular distributions, integrated over $p_T^{\ell\ell}$ and $y^{\ell\ell}$, are shown in Fig. 2 for the three channels. Small normalisation differences between the data and the MC distributions are observed at the level of a few percent, compatible with the combination of uncertainties in integrated luminosity and signal cross section. The measurement of the angular coefficients is, however, independent of the normalisation between data and simulation in each measurement bin. Overall, the agreement in shape between the observed and predicted distributions of $\cos\theta$ and ϕ is good.

Table 2: Data yields integrated over $p_T^{\ell\ell}$ in each $|y^{\ell\ell}|$ analysis bin along with estimated background fractions in % for the ee_{CC} , $\mu\mu_{CC}$, and ee_{CF} channels.

ee_{CC} channel				
$ y^{\ell\ell} $ range	Data (yield)	Top+EW (%)	Multijets (%)	Non-fiducial Z (%)
0 – 0.4	1 573 411	0.2	0.1	0.8
0.4 – 0.8	1 441 923	0.2	0.1	0.9
0.8 – 1.2	1 285 026	0.2	0.2	0.9
1.2 – 1.6	1 025 043	0.2	0.1	0.9
1.6 – 2.0	621 017	0.1	0.2	1.0
2.0 – 2.4	248 261	0.1	0.3	0.9
$ y^{\ell\ell} < 2.4$	6 194 681	0.2	0.1	0.9
$\mu\mu_{CC}$ channel				
$ y^{\ell\ell} $ range	Data (yield)	Top+EW (%)	Multijets (%)	Non-fiducial Z (%)
0 – 0.4	1 617 521	0.3	< 0.1	0.7
0.4 – 0.8	1 657 881	0.2	< 0.1	0.7
0.8 – 1.2	1 680 981	0.2	< 0.1	0.8
1.2 – 1.6	1 503 977	0.2	< 0.1	0.8
1.6 – 2.0	1 010 432	0.2	< 0.1	0.9
2.0 – 2.4	335 788	0.2	< 0.1	0.9
$ y^{\ell\ell} < 2.4$	7 806 580	0.2	< 0.1	0.8
ee_{CF} channel				
$ y^{\ell\ell} $ range	Data (yield)	Top+EW (%)	Multijets (%)	Non-fiducial Z (%)
1.6 – 2.0	245 869	0.2	1.3	1.0
2.0 – 2.4	388 183	0.1	0.9	1.1
2.4 – 2.8	391 405	0.1	0.7	1.1
2.8 – 3.6	228 867	< 0.1	1.1	1.2
$1.6 < y^{\ell\ell} < 3.6$	1 254 324	0.1	1.0	1.1

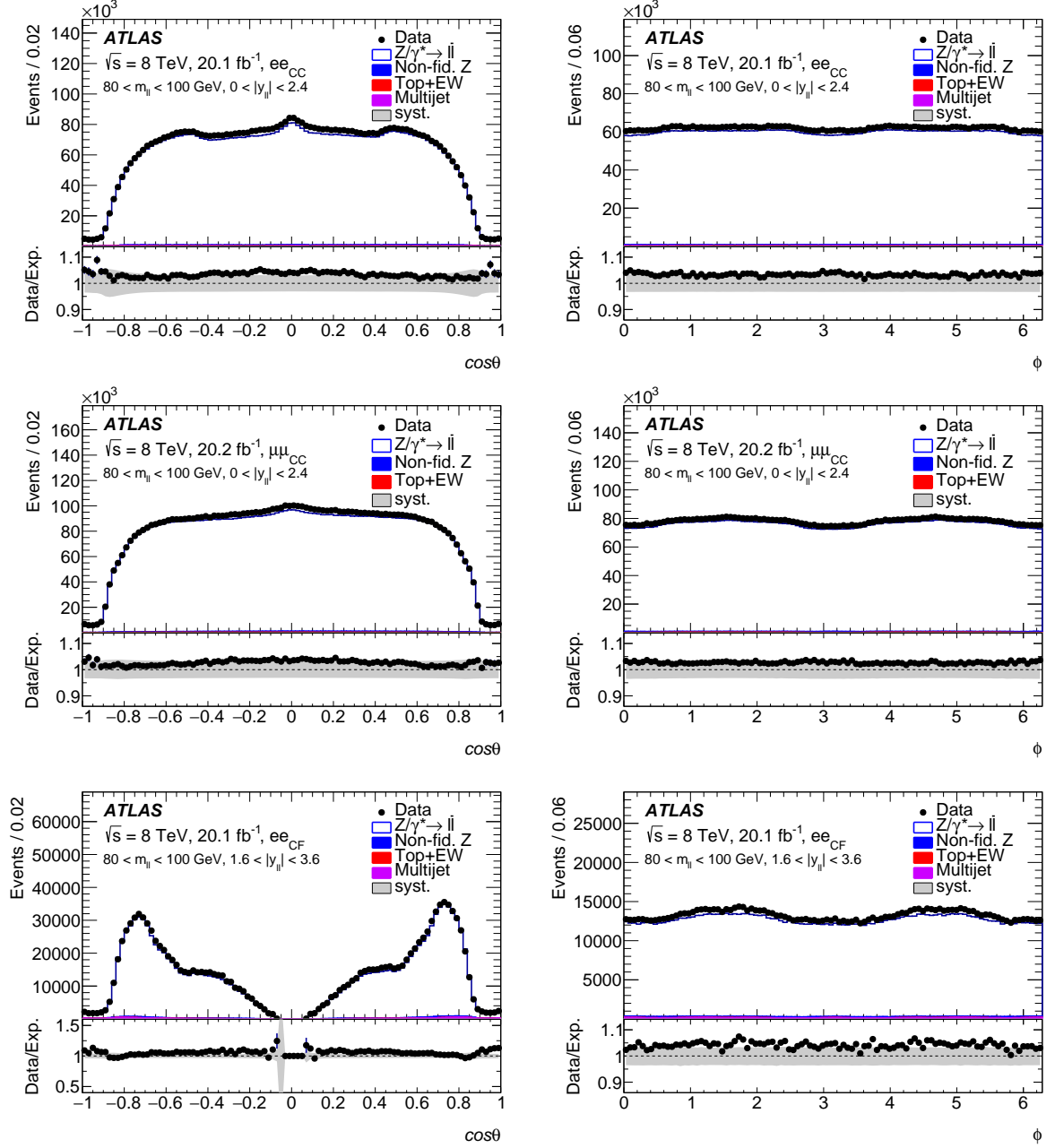


Figure 2: The $\cos\theta$ (left) and ϕ (right) angular distributions, integrated over $p_T^{\ell\ell}$ and $y^{\ell\ell}$, for the ee_{CC} (top), $\mu\mu_{CC}$ (middle) and ee_{CF} (bottom) channels. The pre-fit expected distributions are shown separately for the signal and the different small background sources contributing to each channel. The multijet background is determined from data, using a method very similar to that described in Ref. [6]. The grey band represents the experimental systematic uncertainties in the total expected yields from signal plus background.

Table 3: Examples of breakdown of relative uncertainties in the measured absolute differential cross-sections, as obtained from the full fit. The values are given in % for the region near the peak of the p_T distribution and are shown for two y bins in the case of the ee_{CC} and $\mu\mu_{CC}$ channels and for one y bin in the case of the ee_{CF} channel. Also shown are the total uncertainties. The uncertainty of 1.8% in the integrated luminosity is not included.

Uncertainty source	ee_{CC} channel (%)	$\mu\mu_{CC}$ channel (%)	ee_{CC} channel (%)	$\mu\mu_{CC}$ channel (%)	ee_{CF} channel (%)
Rapidity range	$0 < y < 0.4$	$0 < y < 0.4$	$1.2 < y < 1.6$	$1.2 < y < 1.6$	$2.4 < y < 2.8$
Data stat.	0.5	0.5	0.8	0.6	2.7
MC stat.	0.3	0.3	0.4	0.3	1.5
Leptons	0.2	0.3	0.2	0.4	0.6
Background	< 0.1	< 0.1	< 0.1	< 0.1	< 0.1
PDF	< 0.1	< 0.1	< 0.1	< 0.1	< 0.1
Total	0.6	0.6	1.0	0.8	3.0

4 Systematic uncertainties

This section describes the systematic uncertainties in the measurements of the absolute and normalised differential cross-sections, $\frac{d^2\sigma}{dp_T dy}$ and $\frac{d\sigma}{dy}$, as extracted from the angular observables presented in Fig. 2. These systematic uncertainties are grouped according to their source, and their typical relative values over most of the kinematic range of the measured observables are listed in Table 3 in the case of the absolute cross-section measurements, $\frac{d^2\sigma}{dp_T dy}$. The overall uncertainty of 1.8% in the integrated luminosity is not shown in this table nor in the figures below, but affects of course all the absolute cross-section measurements presented in this paper. The variations of the uncertainties as a function of p_T and $|y|$ are shown in Figs. 3 (absolute cross-sections) and 4 (normalised cross-sections). The statistical uncertainty in the data is the dominant uncertainty over most of the measurement bins, followed by the statistical uncertainty in the MC samples. The variations are shown after combining the different channels together, so the uncertainties are correlated through the fit procedure. This explains for example why the forward electron systematic uncertainties do not vanish for $|y| < 1.6$. The breakdown between the different groups of uncertainties is obtained after freezing all the nuisance parameters of each group to their best-fit values, and then subtracting in quadrature the total uncertainty obtained by performing the fit in these conditions from the total uncertainty obtained by the full fit. Because of the correlations between the nuisance parameters, each of the resulting contributions is rescaled such that their sum in quadrature remains equal to the total uncertainty from the full fit.

Once these cross-sections are integrated over p_T , the statistical uncertainties obtained for $\frac{d\sigma}{dy}$ are significantly reduced and the experimental systematic uncertainties in the lepton measurements [21, 41] become dominant, especially in the central region, as shown in Fig. 5. In all cases, theoretical uncertainties, arising essentially only from PDFs, are negligible (see Ref. [6] for a more detailed discussion). In particular, as mentioned in Section 1, higher-order QED/EW effects, such as initial-final state interference diagrammes, which break the factorisation assumption underlying the expression of the differential cross-section in Eq. (1), have a negligible impact in the Z -boson pole region studied here [16].

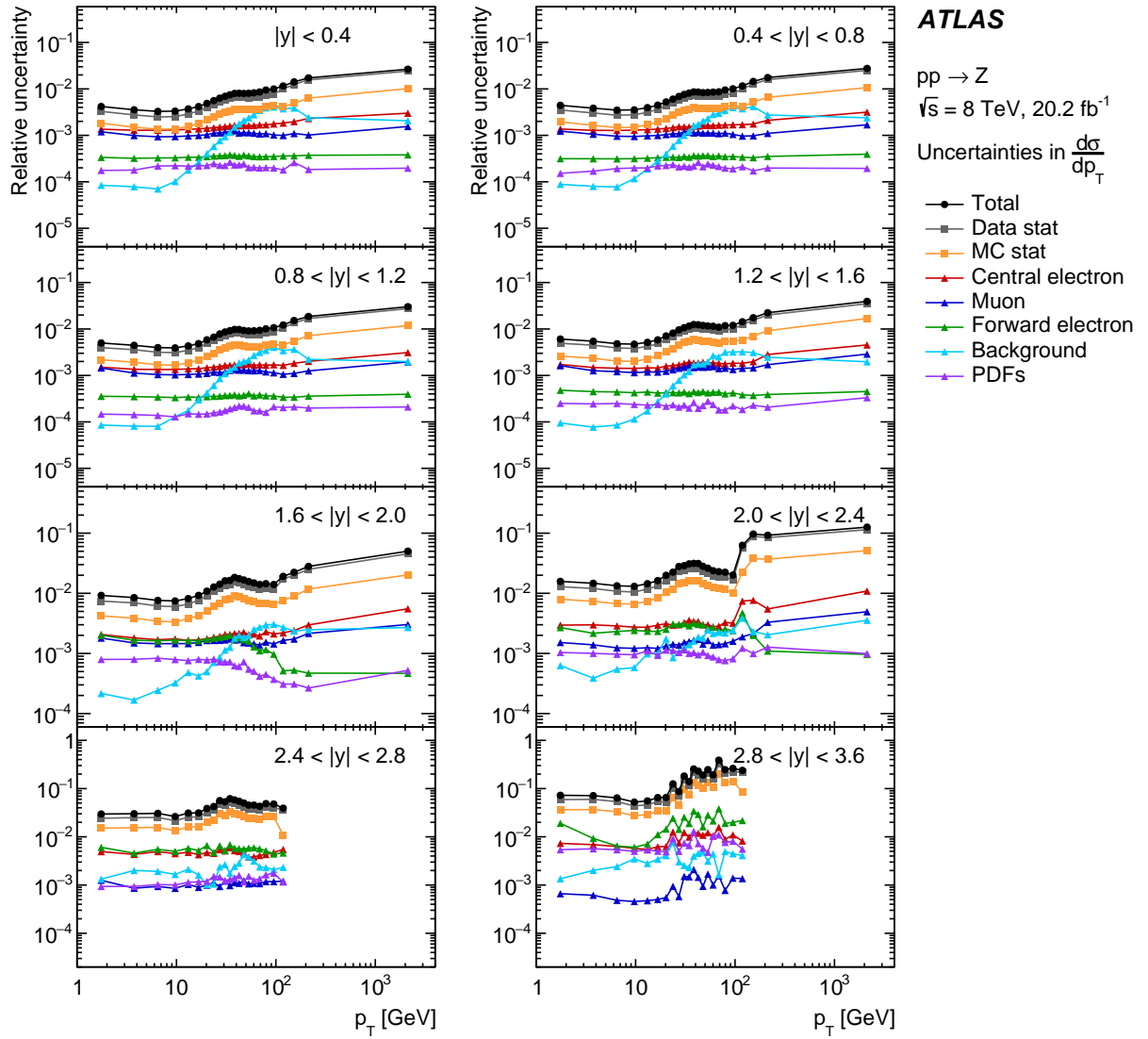


Figure 3: Breakdown of relative uncertainties in the measured absolute differential cross-sections, $\frac{d^2\sigma}{dp_T dy}$, as a function of p_T . The values are shown, as obtained from the full fit and for each $|y|$ bin, for the combination of the ee_{CC} and $\mu\mu_{CC}$ channels for $|y| < 1.6$, for the combination of all three channels for $1.6 < |y| < 2.4$, and for the ee_{CF} channel alone for $2.4 < |y| < 3.6$. The uncertainty of 1.8% in the integrated luminosity is not included.

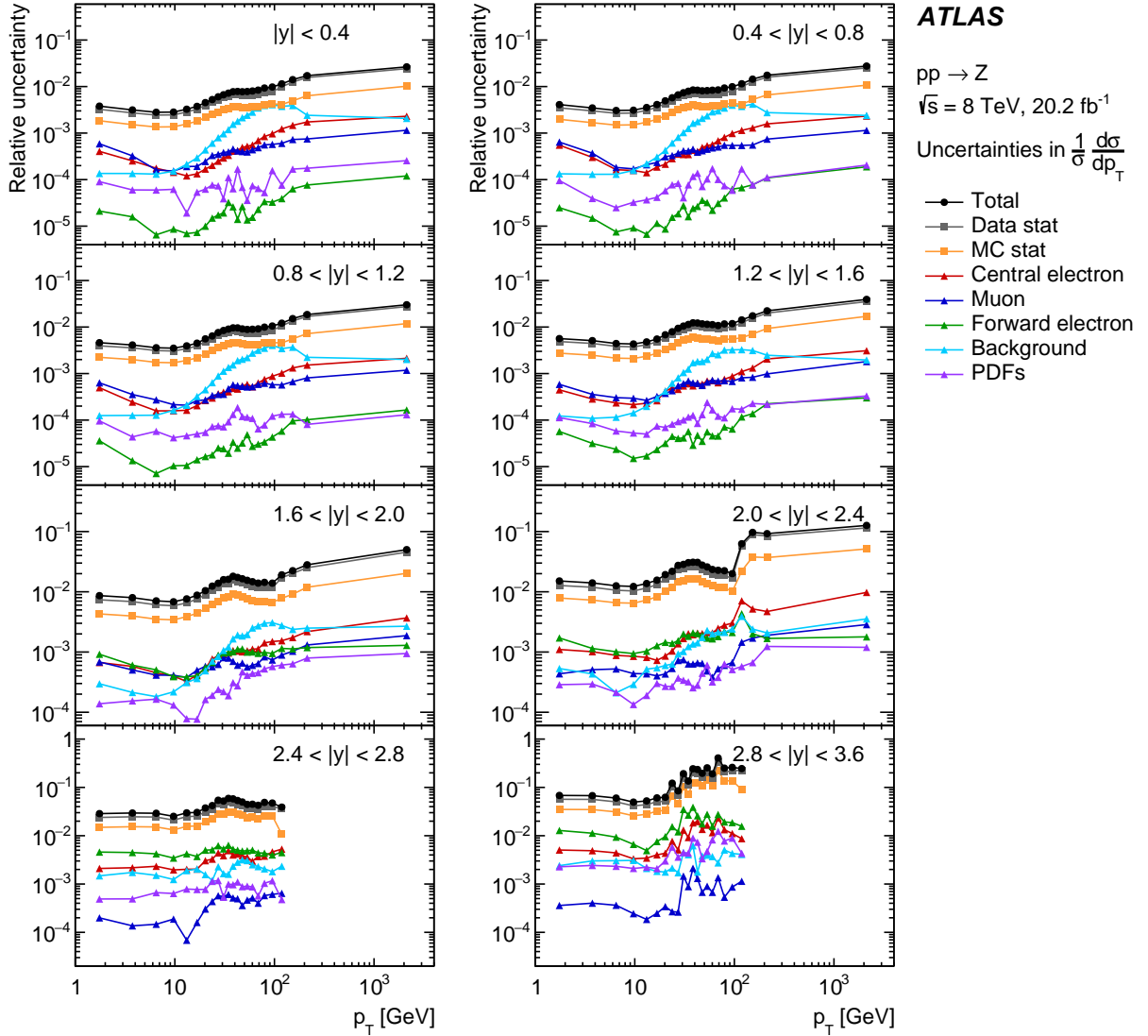


Figure 4: Breakdown of relative uncertainties in the measured normalised differential cross-sections, $\frac{1}{\sigma} \frac{d^2\sigma}{dp_T dy}$, as a function of p_T . The values are shown, as obtained from the full fit and for each $|y|$ bin, for the combination of the ee_{CC} and $\mu\mu_{CC}$ channels for $|y| < 1.6$, for the combination of all three channels for $1.6 < |y| < 2.4$, and for the ee_{CF} channel alone for $2.4 < |y| < 3.6$.

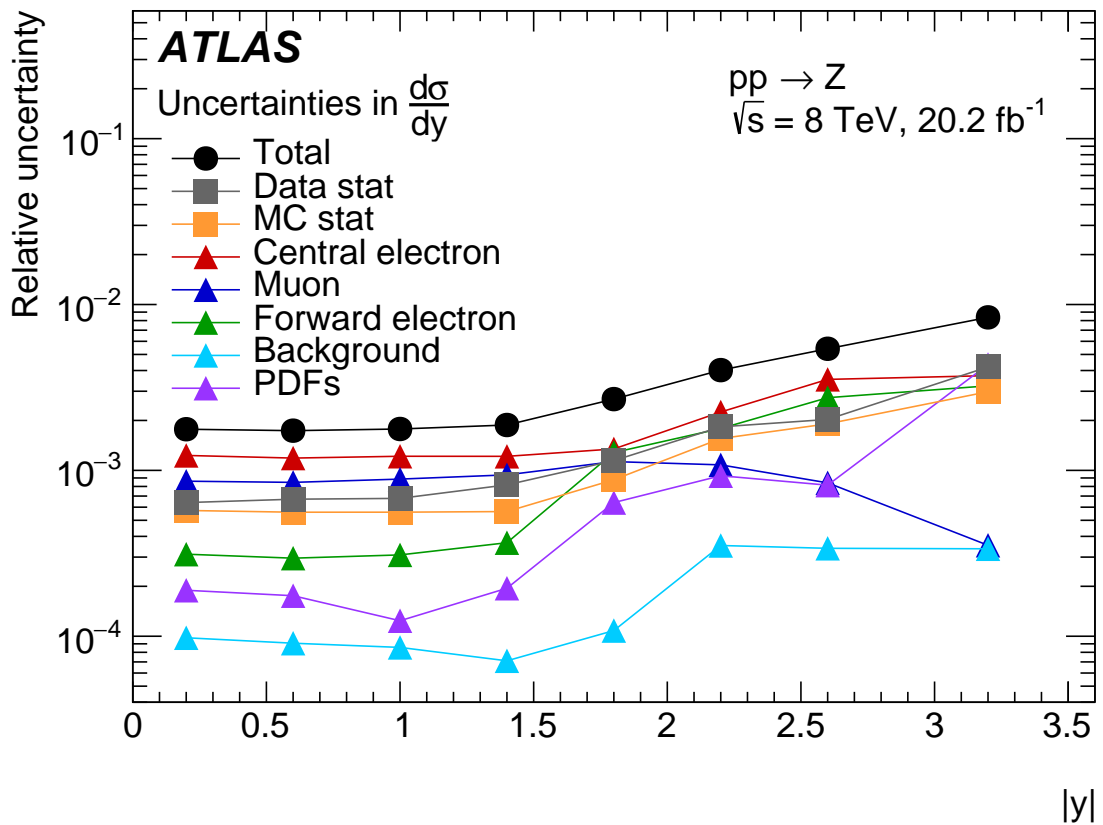


Figure 5: Breakdown of relative uncertainties in the measured absolute differential cross-section, $\frac{d\sigma}{dy}$, as a function of $|y|$. The values are shown, as obtained from the full fit, for the combination of the ee_{CC} and $\mu\mu_{CC}$ channels for $|y| < 1.6$, for the combination of all three channels for $1.6 < |y| < 2.4$, and for the ee_{CF} channel alone for $2.4 < |y| < 3.6$. The uncertainty of 1.8% in the integrated luminosity is not included.

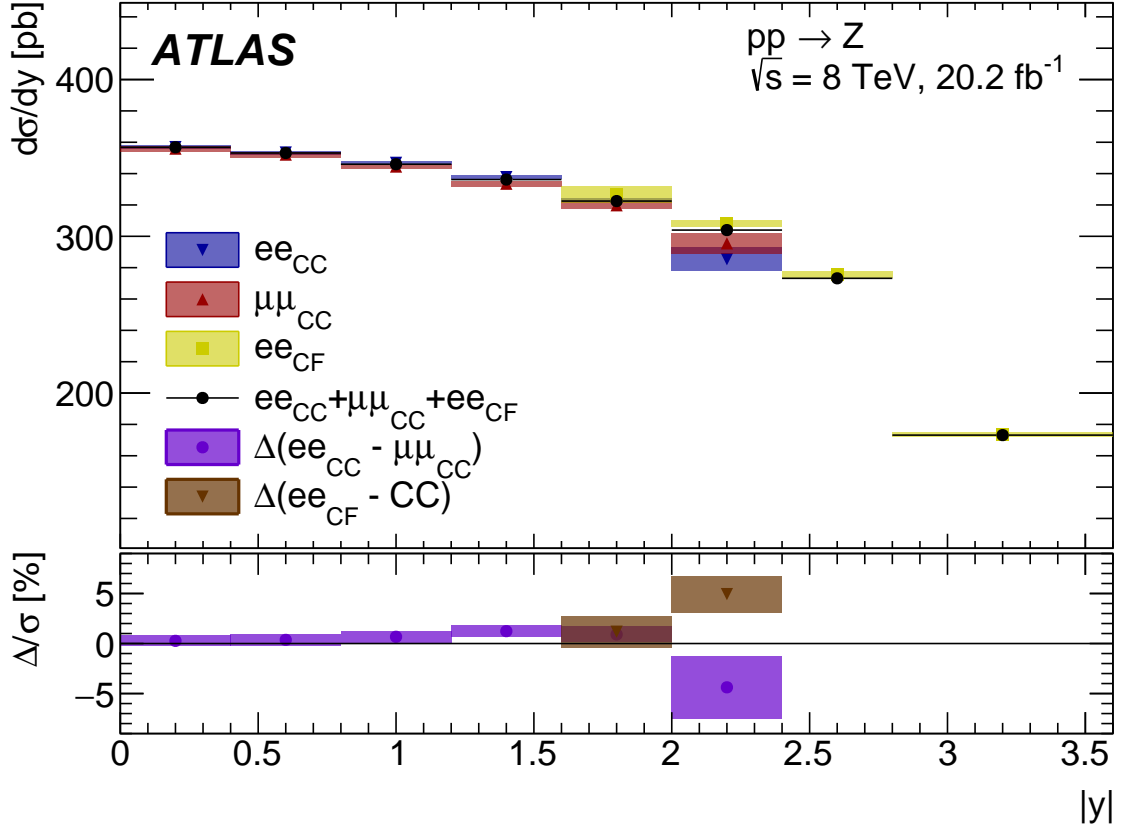


Figure 6: Compatibility test between the different channels for the differential $\frac{d\sigma}{dy}$ cross-section measurements integrated over p_T . The top panel shows the measurements with their total uncertainties (except for the uncertainty of 1.8% in the integrated luminosity) for the three channels and their overall combination. The bottom panel shows, for the relevant $|y|$ bins, the relative $\frac{d\sigma}{dy}$ differences, Δ/σ , in % between the ee_{CC} and $\mu\mu_{CC}$ channels, $\Delta(ee_{CC} - \mu\mu_{CC})$, and between the ee_{CF} channel and the combination of the ee_{CC} and $\mu\mu_{CC}$ channels, $\Delta(ee_{CF} - CC)$.

5 Results and comparisons to predictions

5.1 Compatibility between measurements

Before considering the measurement results themselves, an important step is to evaluate the compatibility between the different channels. This is first done for $\frac{d^2\sigma}{dp_T dy}$ for the ee_{CC} versus $\mu\mu_{CC}$ channels, which are found to be compatible within their dominant statistical uncertainties in all cases, and are then combined into overall central-central (CC) measurements. In the results presented in this paper, there are two rapidity bins where the central-central and central-forward measurements overlap, namely in the range $1.6 < |y| < 2.4$. The $\frac{d^2\sigma}{dp_T dy}$ measurements from the ee_{CF} channel are compared in this overlap region with those from the CC channel. The distributions are found to be compatible within their dominant statistical uncertainties, and all three channels are then finally combined. The overall p-value of the combined fit is 4%, while the overall p-values of fits performed separately for each channel are found to be 11% for the ee_{CC} channel, 90% for the $\mu\mu_{CC}$ channel and 2% for the ee_{CF} channel.

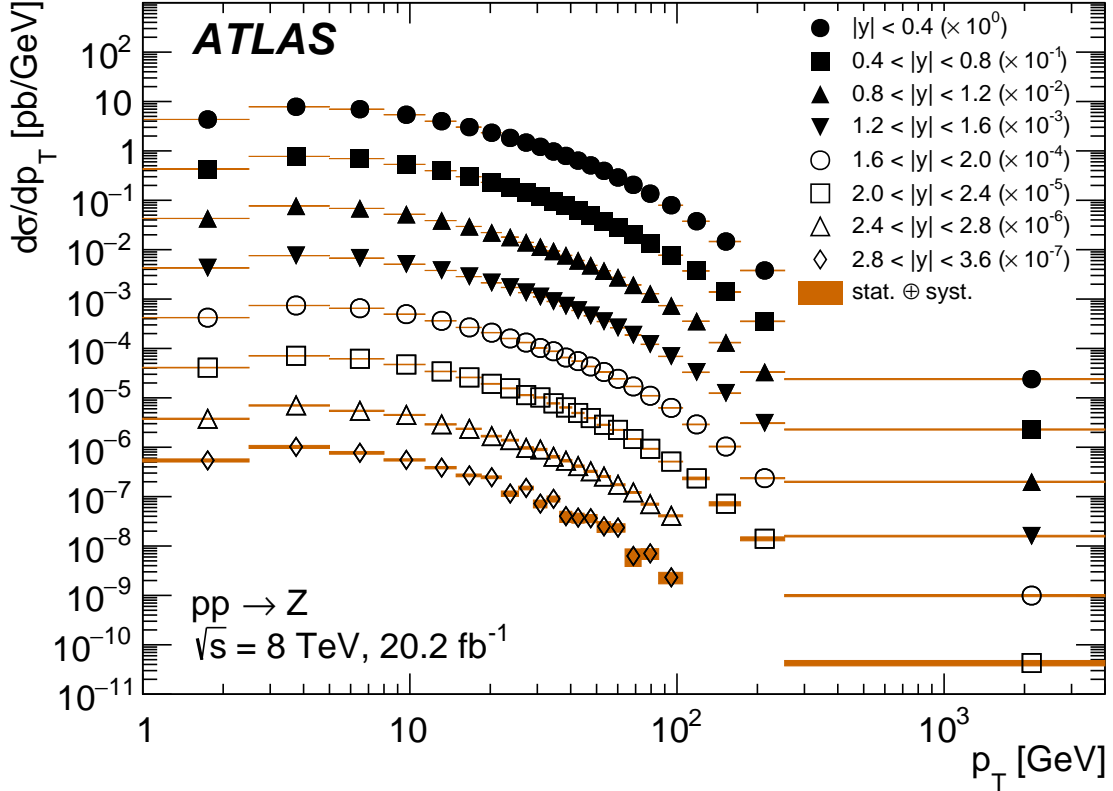


Figure 7: Measured absolute differential $\frac{d\sigma}{dp_T}$ cross-sections with their total uncertainties shown as a function of p_T for each $|y|$ bin. The uncertainty of 1.8% in the integrated luminosity is not included. For each successive $|y|$ bin, the differential cross section is divided by a factor of ten for plotting purposes.

A stringent test of the compatibility between channels can be performed for the $\frac{d\sigma}{dy}$ measurements after integration over p_T , since the statistical uncertainties are strongly reduced as shown in Fig. 5. The results of this test are shown as a function of $|y|$ in Fig. 6. The top panel of Fig. 6 shows comparisons between separate fits done to each of the three channels. The overall p-value for the compatibility between the ee_{CC} and $\mu\mu_{CC}$ channels is found to be 2%, while that between the ee_{CF} and CC channels is found to be 3%. The bottom panel of Fig. 6 shows the relative cross-section differences after performing the full combination of all channels between the ee_{CC} and $\mu\mu_{CC}$ channels for $|y| < 2.4$ and between the ee_{CF} and CC channels for $1.6 < |y| < 2.4$. The residual tensions between channels arise mostly from the highest $|y|$ bin.

5.2 Comparison between $\frac{d^2\sigma}{dp_T dy}$ measurements and predictions

For the double-differential $\frac{d^2\sigma}{dp_T dy}$ measurements, the predictions are obtained by different state-of-the-art QCD perturbative calculations based on q_T resummation [44] at approximate approximate N^4LL accuracy. All these calculations, DYTurbo [45–47], CuTe-MCFM [48], Artemide [49], NangaParbat [50], RadISH [51–53], and SCETlib [54], are currently being benchmarked in the LHC Standard Model working group.

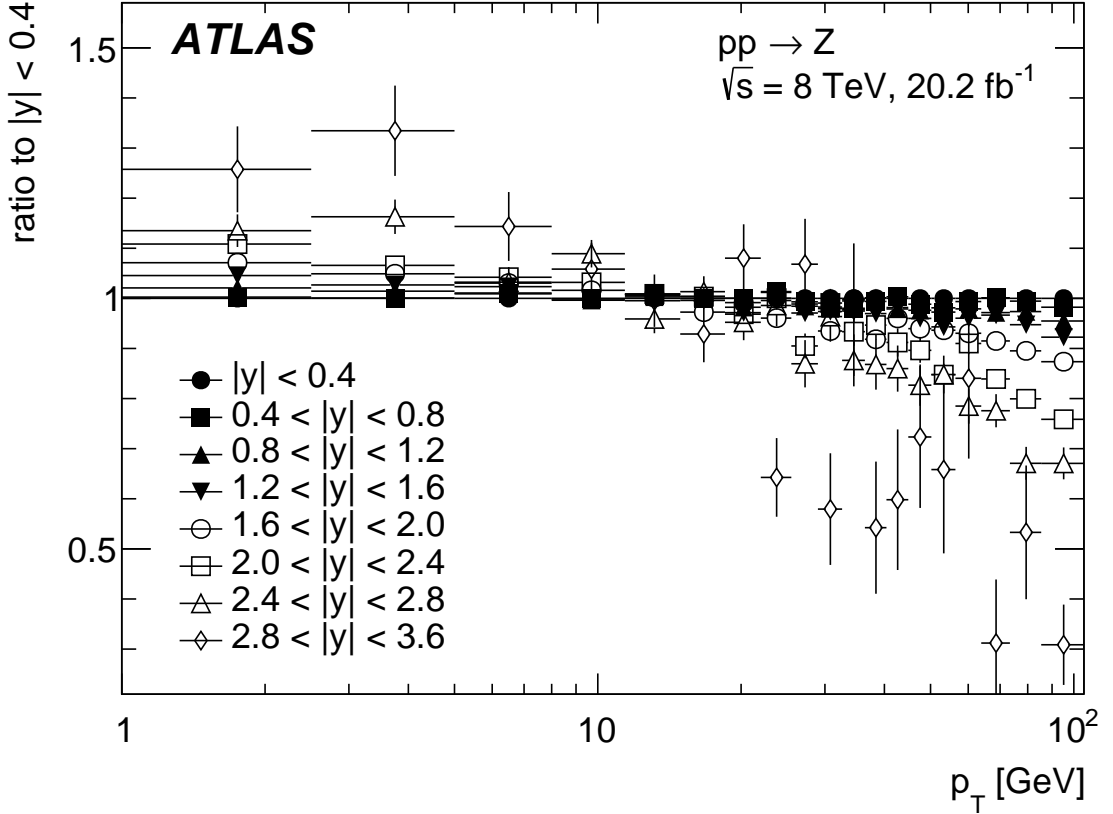


Figure 8: Ratio of measured differential $\frac{d\sigma}{dp_T}$ cross-sections in each $|y|$ bin to a reference one taken to be the most central one, $0 < |y| < 0.4$.

Except for Artemide, they are matched at high values of p_T to a common state-of-the-art $O(\alpha_s^3)$ fixed-order perturbative calculation from MCFM [48, 55]. Each one of these perturbative resummation calculations has its own recipe for defining a total uncertainty in the prediction based on variations of several QCD scales related to the resummation and fixed-order contributions and the procedure used to match them such that the summed prediction is well behaved. It is beyond the scope of this paper to explain the differences between the various approaches and the theory predictions are therefore shown below with total uncertainty envelopes provided by the authors.

Figure 7 shows all the absolute differential $\frac{d^2\sigma}{dp_T dy}$ cross-section measurements with their total uncertainties (except for the uniform uncertainty of 1.8% in the integrated luminosity). This complete set of cross-section numbers with the full covariance matrix are published in HEPDATA and contain all the information required for comparisons to theory and for interpretation in terms of PDF fits or of the strong coupling constant. As $|y|$ increases, the p_T spectrum becomes softer and this is illustrated in Fig. 8, which presents a normalised ratio of the measurements, for which the reference is taken to be the measurement in the most central $|y|$ bin, namely $0 < |y| < 0.4$. Here the luminosity uncertainty cancels, and the softening of the p_T spectrum is clearly visible for the higher $|y|$ bins. This feature, measured for the first time, is expected and well reproduced by the predictions, as shown below. The standard fiducial measurements published for example using the same ATLAS data in Ref. [2] do not see this kinematic effect because the lepton

fiducial selections in p_T and pseudorapidity largely compensate for it, resulting in a flat dependence of the differential fiducial measurement versus rapidity of the Z -boson.

Figure 9 shows the ratio of the absolute differential $\frac{d^2\sigma}{dp_T dy}$ cross-section measurements presented in Fig. 7 to the predictions from DYTurbo. In all $|y|$ bins, the predictions are a few percent lower than the measurements, a feature that is discussed more in detail in Section 5.3. In the region near the peak of the p_T distribution however, the shape of the predictions is in agreement with that of the measurements within the predominantly theoretical uncertainties. To illustrate this agreement in shape, Fig. 10 shows the ratios between the normalised differential measurements and predictions in the range $0 < p_T < 100$ GeV. Over the full $|y|$ range measured, the data and predictions are found to be in agreement within better than 5%. There are rather strong anti-correlation terms between neighbouring bins, inducing for example the large fluctuations from bin to bin seen for the highest $|y|$ bin at high p_T , where the limited statistics induce terms as large as 40%.

Figures 11, 12, 13, 14, and 15 show the same ratios as in Fig. 9, successively for the CuTe-MCFM, Artemide, NangaParbat, RadISH, and SCETlib predictions. In all cases, the predictions agree with the measurements within their uncertainties, which range between 2% and 5% at the peak of the p_T distribution. The theory uncertainties in all the calculations are arguably incomplete at this stage, since variations between PDF sets are not included nor are uncertainties at low p_T related to heavy quark and non-perturbative effects.

To better assess the degree of accuracy with which the different resummation calculations agree with the data, the $\frac{d^2\sigma}{dp_T dy}$ cross-sections are integrated over $|y| < 1.6$. This improves considerably the statistical uncertainty in the measurements. Figure 16 shows these normalised $|y|$ -integrated $\frac{d\sigma}{dp_T}$ spectra for the data and the predictions with their respective uncertainties, together with the ratios between each prediction and the data. The agreement of the predictions with the data is excellent, well within the scale variation uncertainties of 2–3% over most of the p_T range, except for two points in the lowest p_T bins from the RadISH predictions that are somewhat discrepant.

Finally, Fig. 17 shows a comparison between the measured absolute $\frac{d\sigma}{dp_T}$ differential cross-section in each $|y|$ bin and two fixed-order $O(\alpha_s^3)$ predictions, that from MCFM, as used by the different calculations discussed above, and that from NNLOJET [56]. As expected, these fixed-order calculations are in agreement with the data at high p_T , and do not describe the data well at the lower values of p_T , where resummation is expected to play a major role, as shown for the case of the RadISH predictions matched to each of these fixed-order $O(\alpha_s^3)$ predictions in Fig. 18. The larger uncertainties seen in the case of MCFM are mostly due to limited statistics.

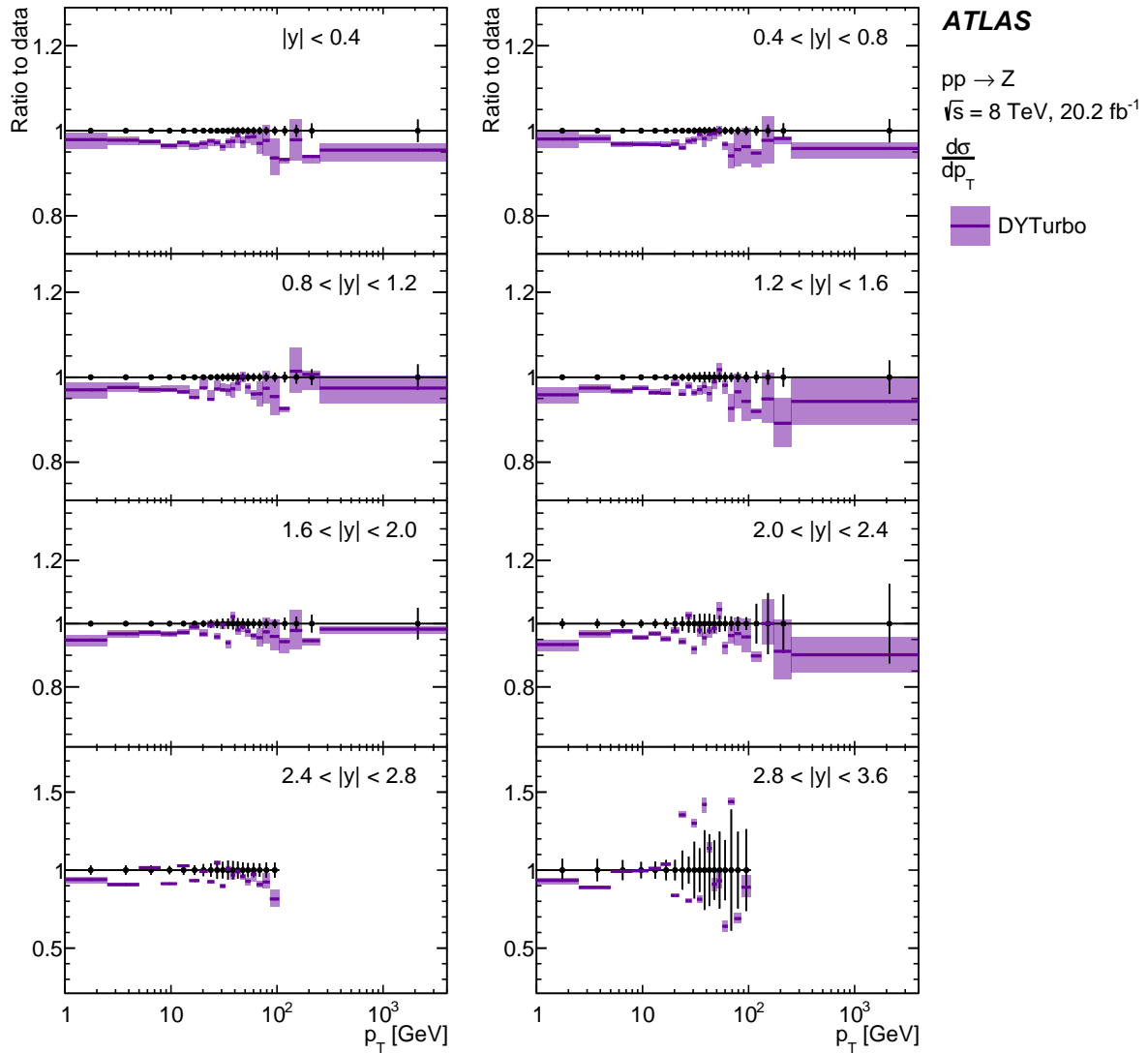


Figure 9: Comparison between the measured absolute differential $\frac{d\sigma}{dp_T}$ cross-sections in each of the eight $|y|$ bins and the predictions from DYTurbo [45]. Shown are the ratios between the predictions with their uncertainties as obtained from renormalisation/factorisation/resummation scale variations and the data with their overall uncertainties (except for the uncertainty of 1.8% in the integrated luminosity). The predictions from DYTurbo are matched to the fixed-order $O(\alpha_s^3)$ contributions from MCFM [48, 55].

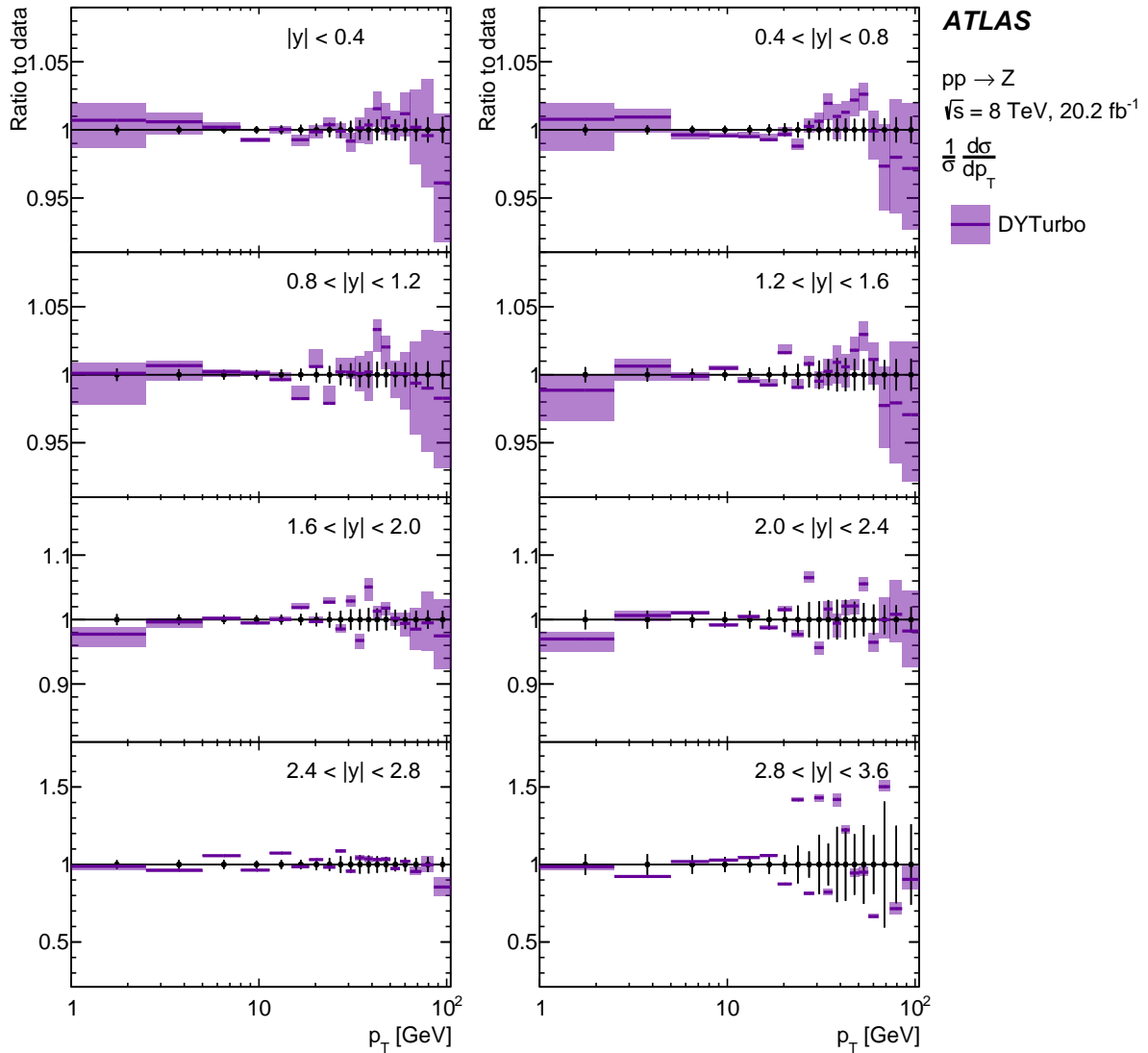


Figure 10: Comparison between the measured normalised differential $\frac{1}{\sigma} \frac{d\sigma}{dp_T}$ cross-sections in each of the eight $|y|$ bins and the predictions from DYTurbo [45]. Shown are the ratios between the predictions with their uncertainties as obtained from renormalisation/factorisation/resummation scale variations and the data with their overall uncertainties. The predictions from DYTurbo are matched to the fixed-order $O(\alpha_s^3)$ contributions from MCFM [48, 55].

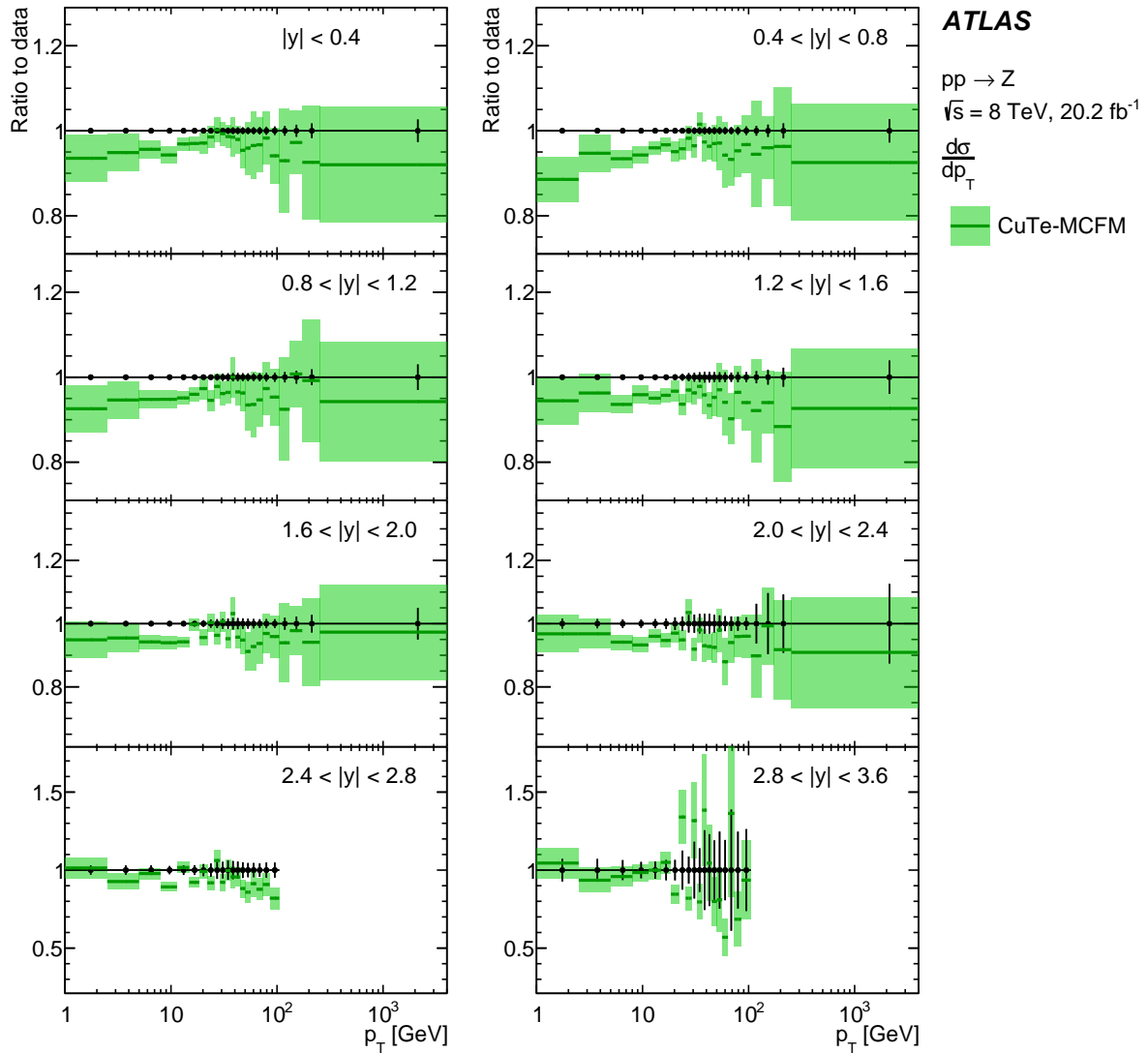


Figure 11: Comparison between the measured absolute differential $\frac{d\sigma}{dp_T}$ cross-sections in each of the eight $|y|$ bins and the predictions from CuTe-MCFM [48]. Shown are the ratios between the predictions with their uncertainties as obtained from renormalisation/factorisation/resummation scale variations and the data with their overall uncertainties (except for the uncertainty of 1.8% in the integrated luminosity). The predictions from CuTe-MCFM are matched to the fixed-order $O(\alpha_s^3)$ contributions from MCFM [48, 55].

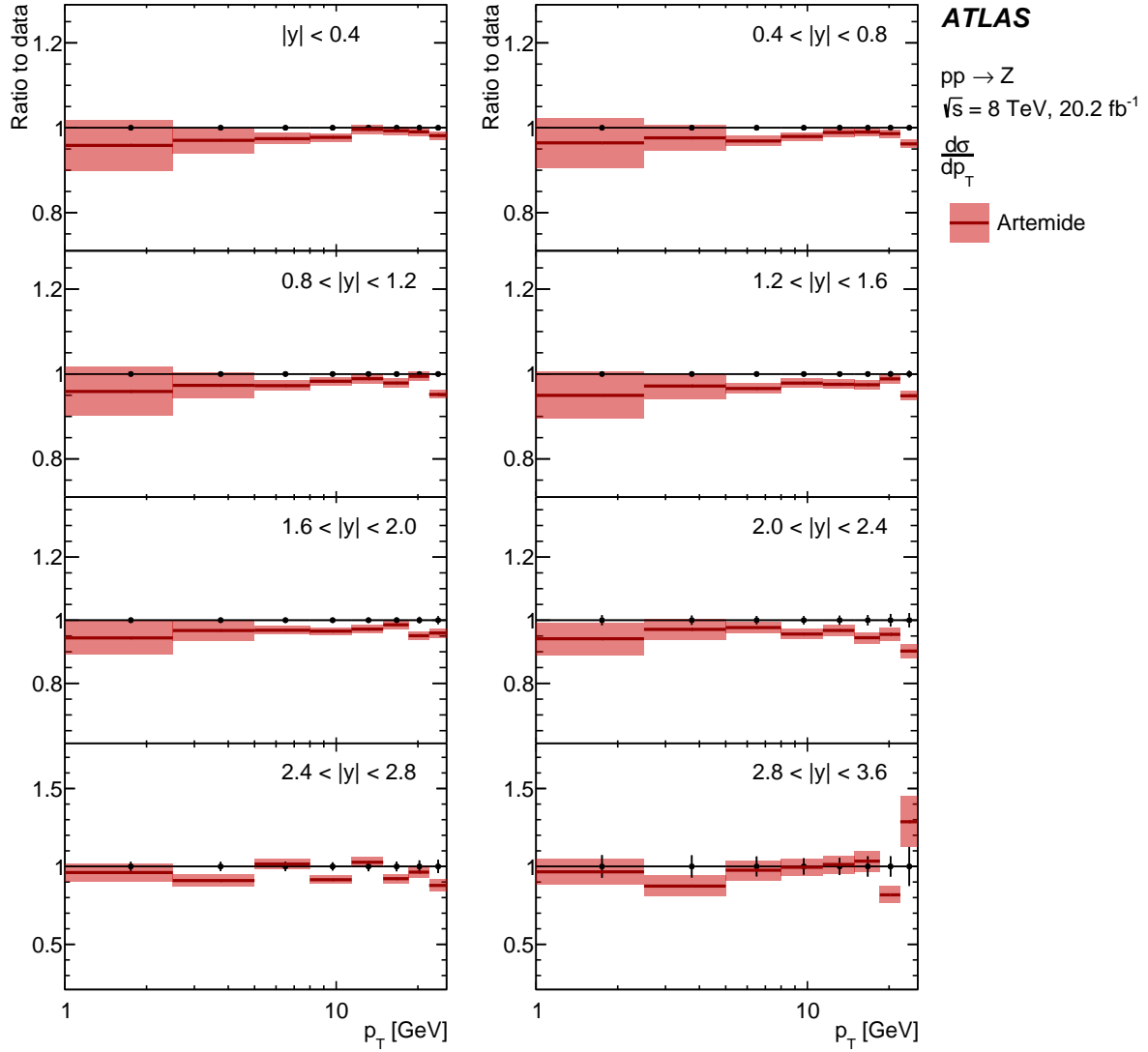


Figure 12: Comparison between the measured absolute differential $\frac{d\sigma}{dp_T}$ cross-sections in each of the eight $|y|$ bins and the predictions from Artemide [49]. Shown are the ratios between the predictions with their uncertainties as obtained from renormalisation/factorisation/resummation scale variations and the data with their overall uncertainties (except for the uncertainty of 1.8% in the integrated luminosity). The predictions from Artemide are from pure resummation and are therefore shown only over the p_T range for which the contribution from fixed-order is below a few %.

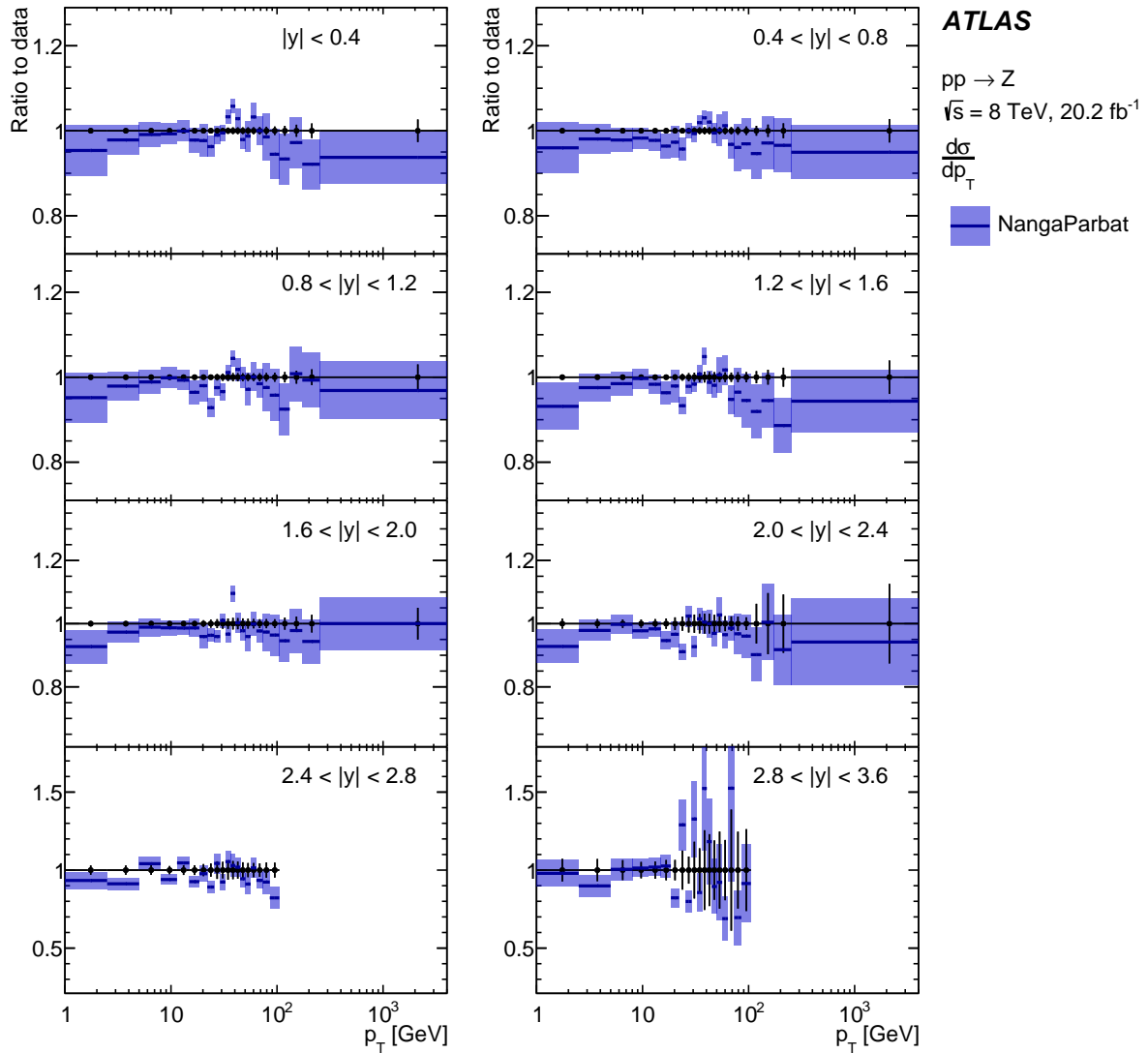


Figure 13: Comparison between the measured absolute differential $\frac{d\sigma}{dp_T}$ cross-sections in each of the eight $|y|$ bins and the predictions from NangaParbat [50]. Shown are the ratios between the predictions with their uncertainties as obtained from renormalisation/factorisation/resummation scale variations and the data with their overall uncertainties (except for the uncertainty of 1.8% in the integrated luminosity). The predictions from NangaParbat are matched to the fixed-order $O(\alpha_s^3)$ contributions from MCFM [48, 55].

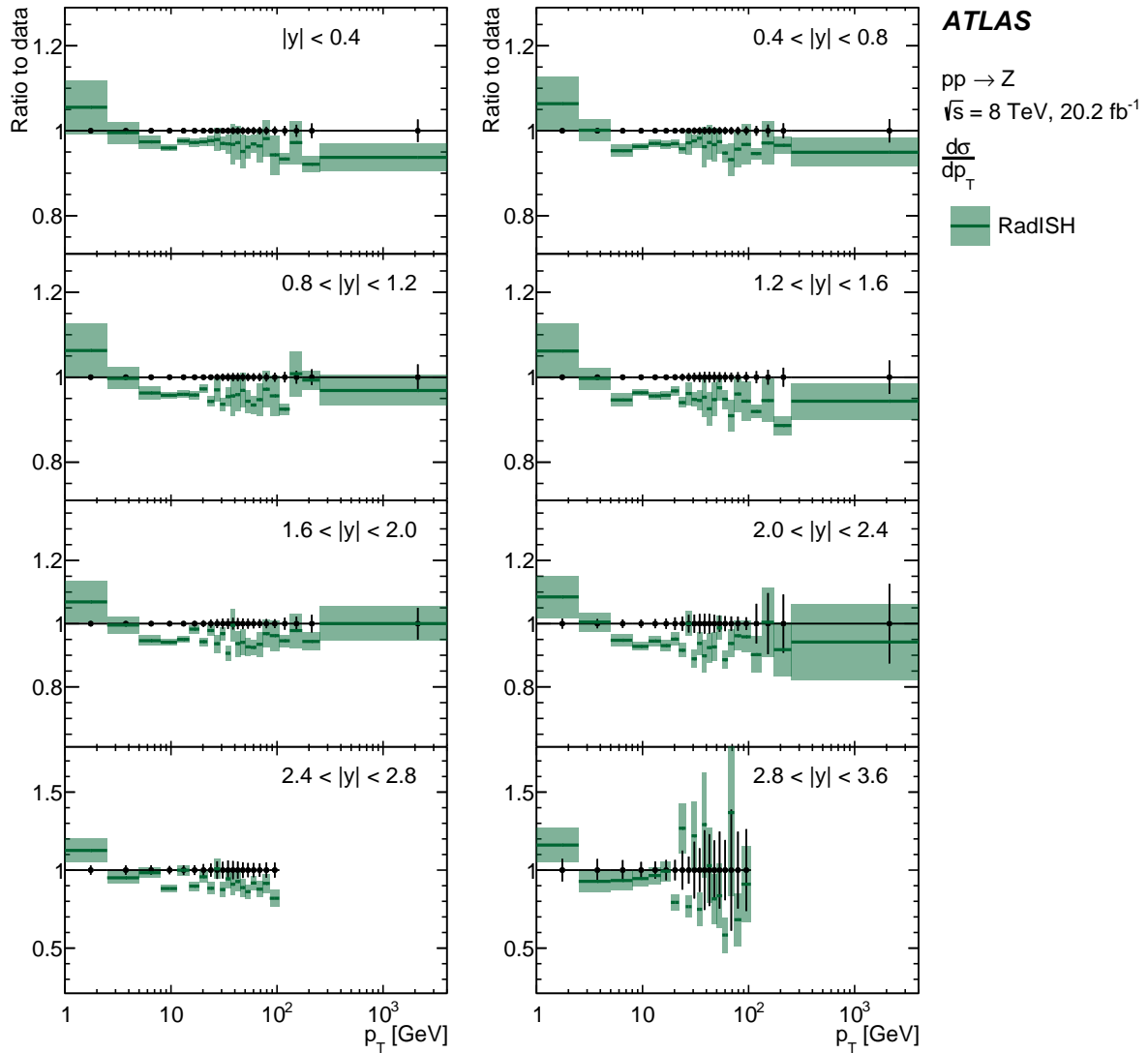


Figure 14: Comparison between the measured absolute differential $\frac{d\sigma}{dp_T}$ cross-sections in each of the eight $|y|$ bins and the predictions from RadISH [53]. Shown are the ratios between the predictions with their uncertainties as obtained from renormalisation/factorisation/resummation scale variations and the data with their overall uncertainties (except for the uncertainty of 1.8% in the integrated luminosity). The predictions from RadISH are matched to the fixed-order $O(\alpha_s^3)$ contributions from MCFM [48, 55].

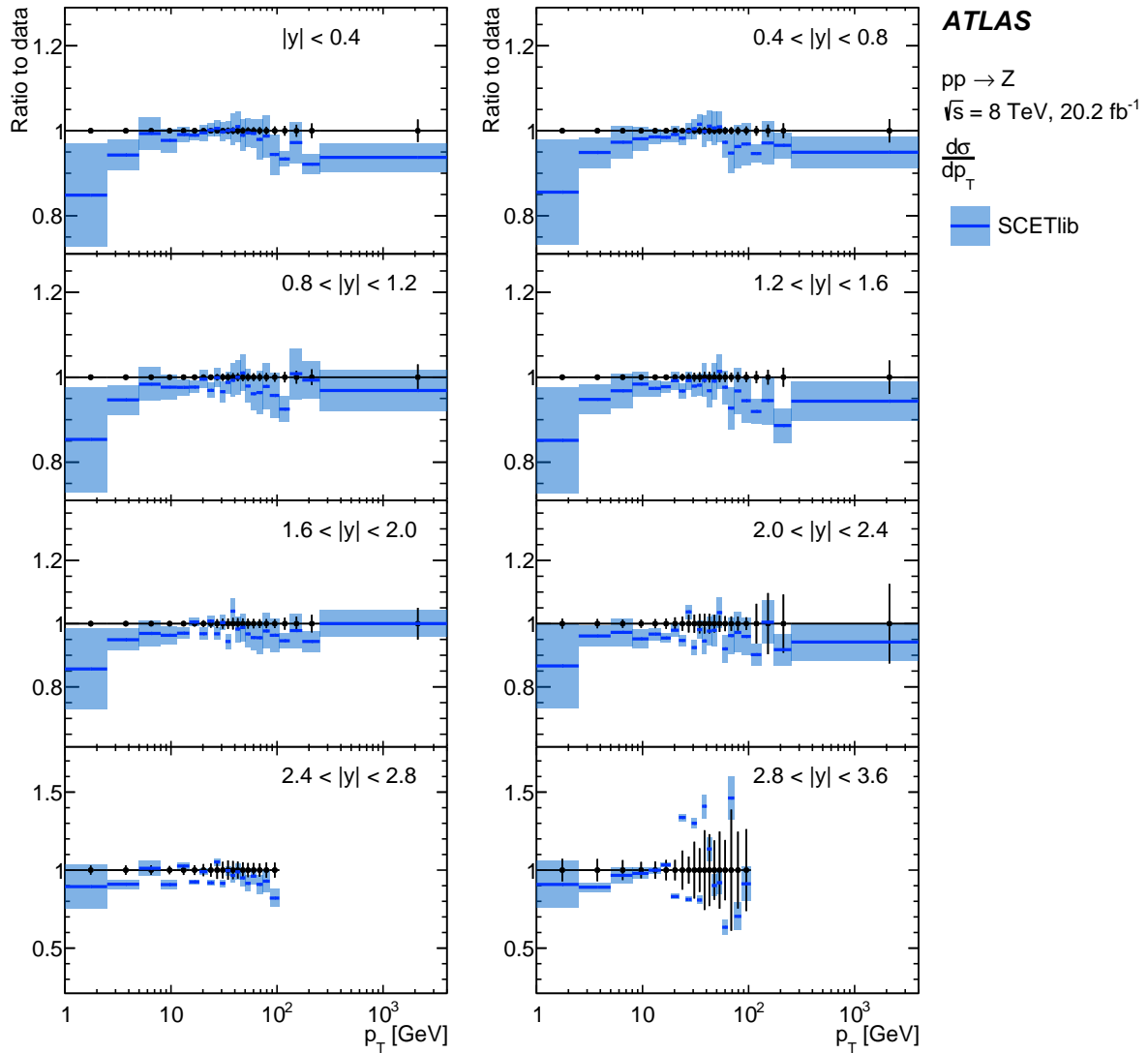


Figure 15: Comparison between the measured absolute differential $\frac{d\sigma}{dp_T}$ cross-sections in each of the eight $|y|$ bins and the predictions from SCETlib [54]. Shown are the ratios between the predictions with their uncertainties as obtained from renormalisation/factorisation/resummation scale variations and the data with their overall uncertainties (except for the uncertainty of 1.8% in the integrated luminosity). The predictions from SCETlib are matched to the fixed-order $O(\alpha_s^3)$ contributions from MCFM [48, 55].

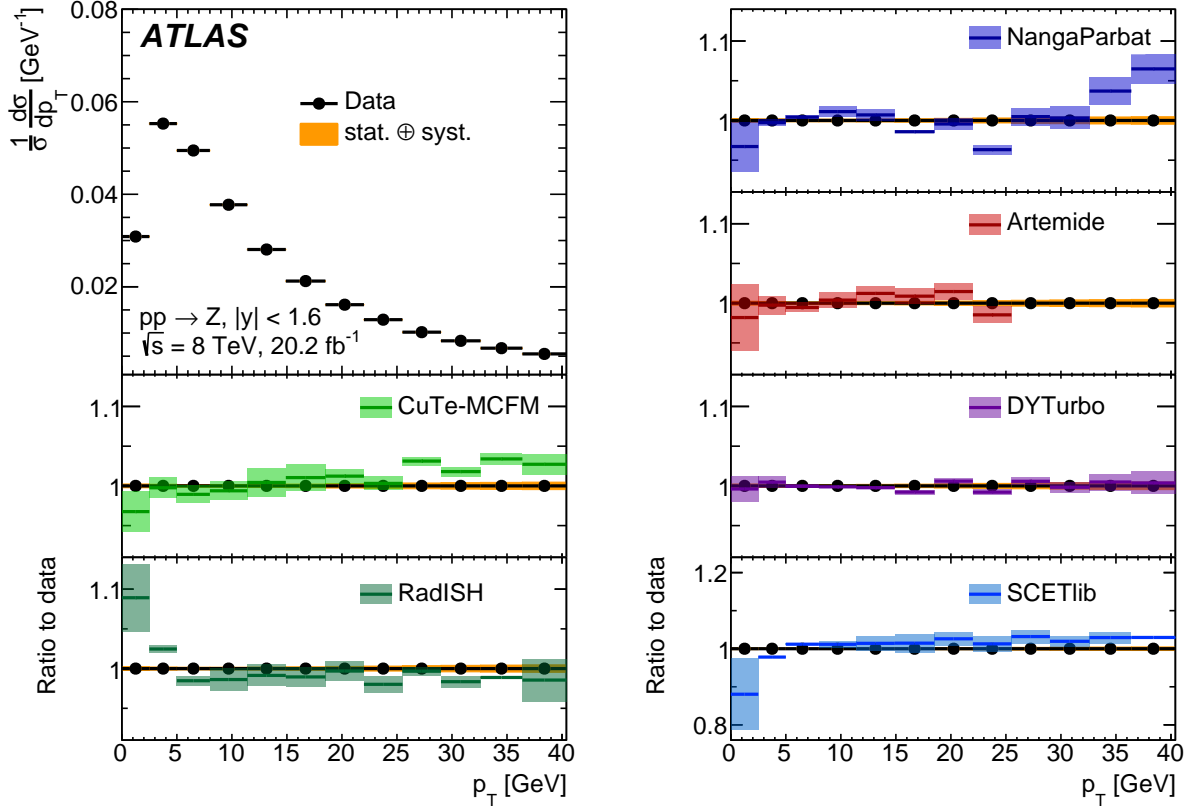


Figure 16: Comparison between the measured normalised differential $\frac{1}{\sigma} \frac{d\sigma}{dp_T}$ cross-sections, integrated over $|y| < 1.6$, with their total uncertainties and the predictions from the various resummation calculations. The top left panel shows the data, while the next panels show one by one the ratios between each prediction with its uncertainties as obtained from renormalisation/factorisation/resummation scale variations and the data. Except for Artemide, the predictions are matched to the fixed-order $O(\alpha_s^3)$ contributions from MCFM [48, 55].

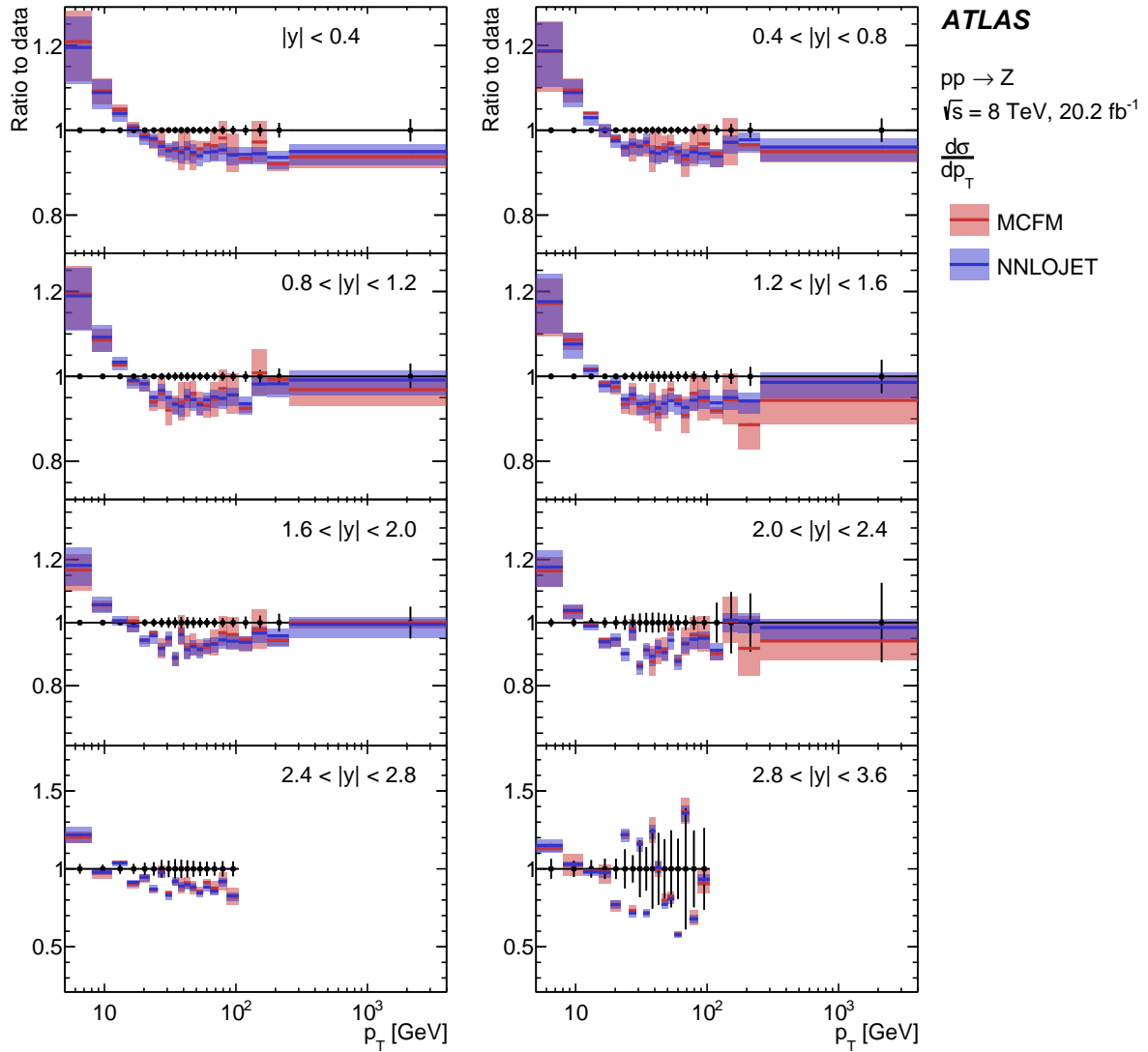


Figure 17: Comparison between the absolute differential $\frac{d\sigma}{dp_T}$ cross-sections with their total uncertainties in each $|y|$ bin and the predictions from the two fixed-order $O(\alpha_s^3)$ calculations from MCFM [48, 55] and NNLOJET [56].

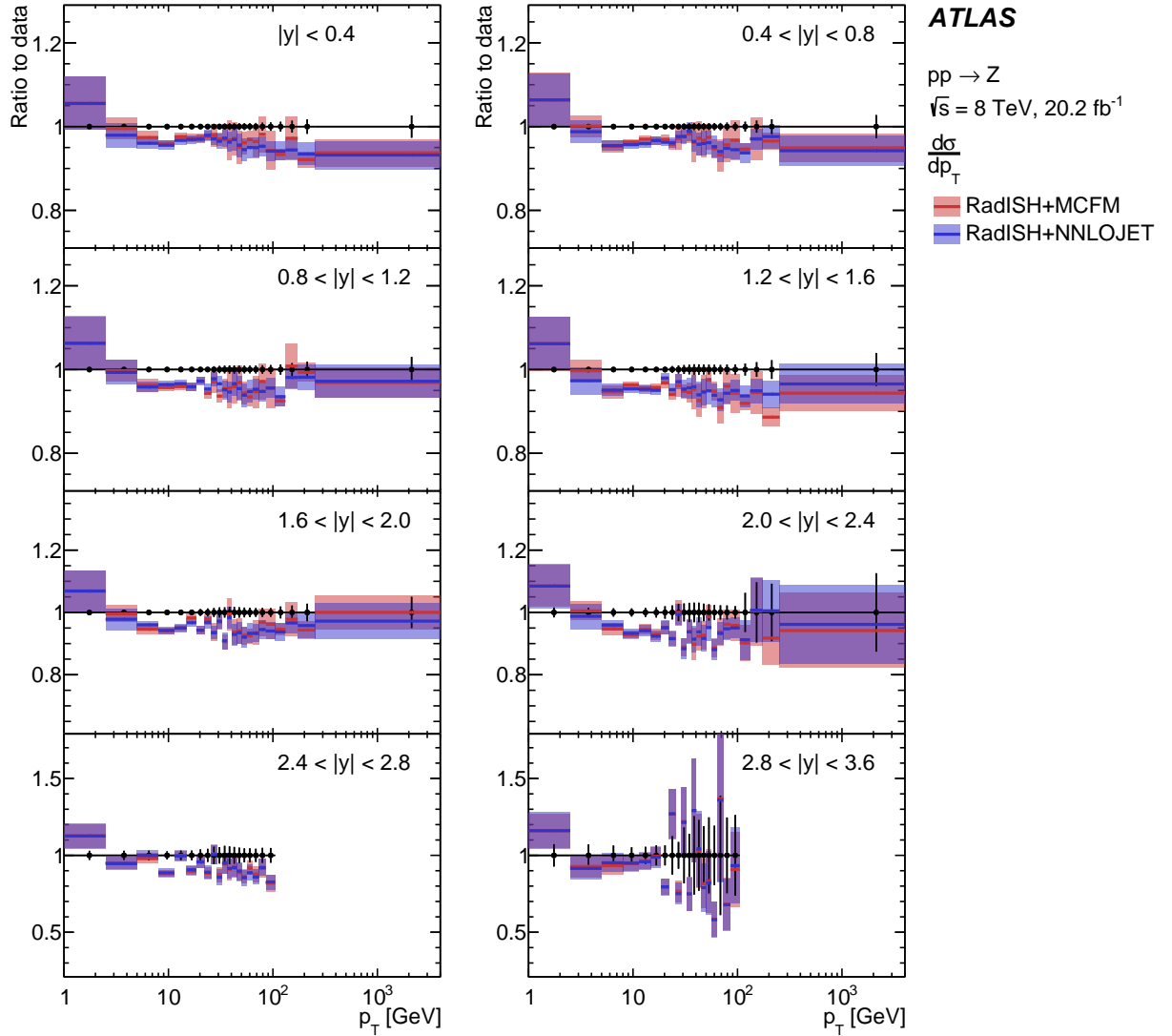


Figure 18: Comparison between the absolute differential $\frac{d\sigma}{dp_T}$ cross-sections with their total uncertainties in each $|y|$ bin and the predictions from RadISH [53] matched to the two fixed-order $O(\alpha_s^3)$ calculations from MCFM [48, 55] and NNLOJET [56, 57].

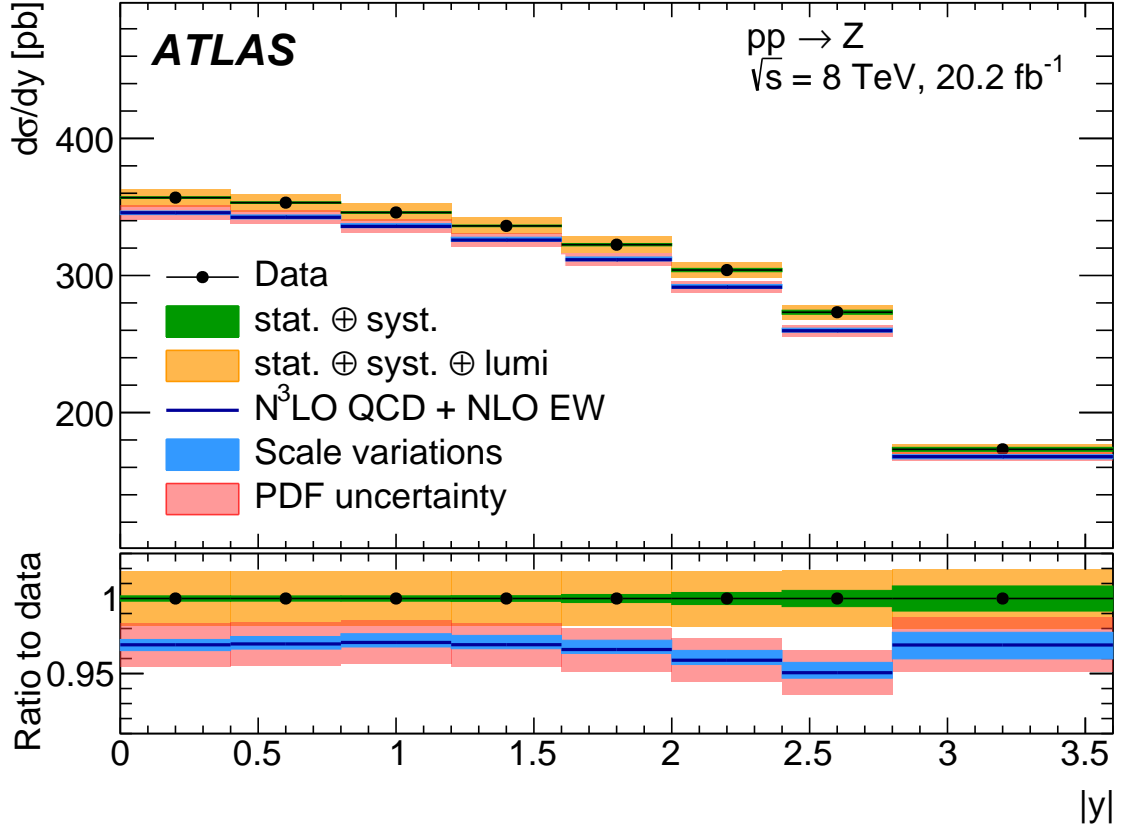


Figure 19: Comparison between the $\frac{d\sigma}{dy}$ measurements and N³LO QCD predictions obtained from DYTurbo using the recent aN³LO MSHT PDF set. The N³LO QCD theory prediction includes a negative correction of 0.4% from NLO EW effects and the theoretical uncertainty bands from QCD renormalisation/factorisation scale variations and from the aN³LO PDF set are shown separately. The bottom panel shows the ratios between predictions and data, where the data uncertainty bands with and without inclusion of the dominant uncertainty of 1.8% in the integrated luminosity are shown separately.

5.3 Comparison between $\frac{d\sigma}{dy}$ measurements and predictions

This section focuses on the $\frac{d\sigma}{dy}$ measurements obtained after integrating the $\frac{d^2\sigma}{dp_T dy}$ distributions shown above over p_T . As shown in Fig. 5, the experimental measurement is significantly more precise with a total uncertainty below 0.2% in the central rapidity region, owing to the large reduction of the uncertainties of a statistical nature. One also expects the theoretical uncertainties in the predictions to be significantly reduced compared to those shown for the $\frac{d^2\sigma}{dp_T dy}$ measurements. As a consequence, the focus of the comparisons between data and predictions in this section are on the PDFs, which are expected to provide the dominant uncertainty in the predictions.

Given the experimental accuracy achieved for the measurements presented in this section, higher-order effects from QED initial-state radiation (ISR) and from so-called genuine electroweak (EW) virtual corrections are considered at next-to-leading order and their sum is labelled NLO EW. These are directly

Table 4: Compatibility test between $\frac{d\sigma}{dy}$ measurements and predictions obtained from DYTurbo using different PDF sets. Based on the total uncertainties in the measurements and on the PDF uncertainties in the predictions shown in Figs. 19 and 20, the χ^2 per degree of freedom (d.o.f.) and corresponding p-values are shown for each PDF set (the uncertainties from CT18A have been rescaled from 95% to 68% confidence level). Also shown is the pull on the integrated luminosity in units of its total uncertainty of 1.8%.

PDF set	Total χ^2 / d.o.f.	χ^2 p-value	Pull on luminosity
MSHT20aN ³ LO [58]	13/8	0.11	1.2 ± 0.6
CT18A [59]	12/8	0.17	0.9 ± 0.7
MSHT20 [60]	10/8	0.26	0.9 ± 0.6
NNPDF4.0 [61]	30/8	0.0002	0.0 ± 0.2
ABMP16 [62, 63]	30/8	0.0002	1.8 ± 0.4
HERAPDF2.0 [64]	22/8	0.005	-1.3 ± 0.8
ATLASpdf21 [65]	20/8	0.01	-1.1 ± 0.8

computed using the code from Ref. [66], and are in agreement with earlier results from calculations benchmarked in the LHC EW working group [16, 67–70]. At the Z pole, the virtual effects decrease the predicted cross-sections by 0.8%, while the QED ISR effects increase them by 0.4%. These corrections are found to be independent of rapidity. All QCD predictions shown below have therefore been decreased by a $|y|$ -independent amount of 0.4% labelled as NLO EW corrections.

In this case, the comparisons to predictions do not depend on q_T resummation which, through unitarity constraints, does not affect the p_T -integrated differential cross-sections. The measurements are thus directly compared to the $O(\alpha_s^3)$ fixed-order perturbative predictions from DYTurbo, supplemented by MCFM [48, 55] for the Z+jet contribution at $O(\alpha_s^3)$. These predictions are formally N³LO in QCD and are obtained using the very recent aN³LO PDF set of Ref. [58]. For the first time, such a comparison between experimental measurements and predictions of this formal accuracy is possible and shown in Figure 19. The theoretical uncertainty bands from QCD renormalisation/factorisation scale variations and from the aN³LO PDF set are shown separately. The uncertainty arising from the scale variations rises slowly from 0.4% to 1.0% as $|y|$ increases, while the MSHT PDF uncertainty is constant at around 1.5%. As shown in the first line of Table 4, the compatibility of the theory with the data is reasonable, with a p-value of 11% if one only includes the uncertainties in the PDFs for the predictions, a standard practice for many publications because most PDF sets do not usually provide scale variation uncertainties. If one combines the PDF uncertainties with a combined scale variation uncertainty from DYTurbo, assumed to be uncorrelated with that from the PDFs, the p-value obtained is 12%.

To assess how the aN³LO MSHT20-specific PDF uncertainty band compares to the presumably non-negligible spread between different PDF sets, the calculation has been performed one order lower, at NNLO in QCD using six of the most recent NNLO PDF sets. These comprise CT18A [59], MSHT20 [60], NNPDF4.0 [61], ABMP16 [62, 63], HERAPDF2.0 [64], and ATLASpdf21 [65].

Figure 20 shows the results of these comparisons as ratios between the predictions and the data. The uncertainties in the theory predictions reflect here only the PDF specific uncertainties (the uncertainties from CT18A have been rescaled from 95% to 68% confidence level). Table 4 quantifies the quality of the agreement between the data and the predictions through the total χ^2 and its corresponding p-value. Also shown is the pull on the integrated luminosity of the experiment for each PDF set. Only the aN³LO MSHT,

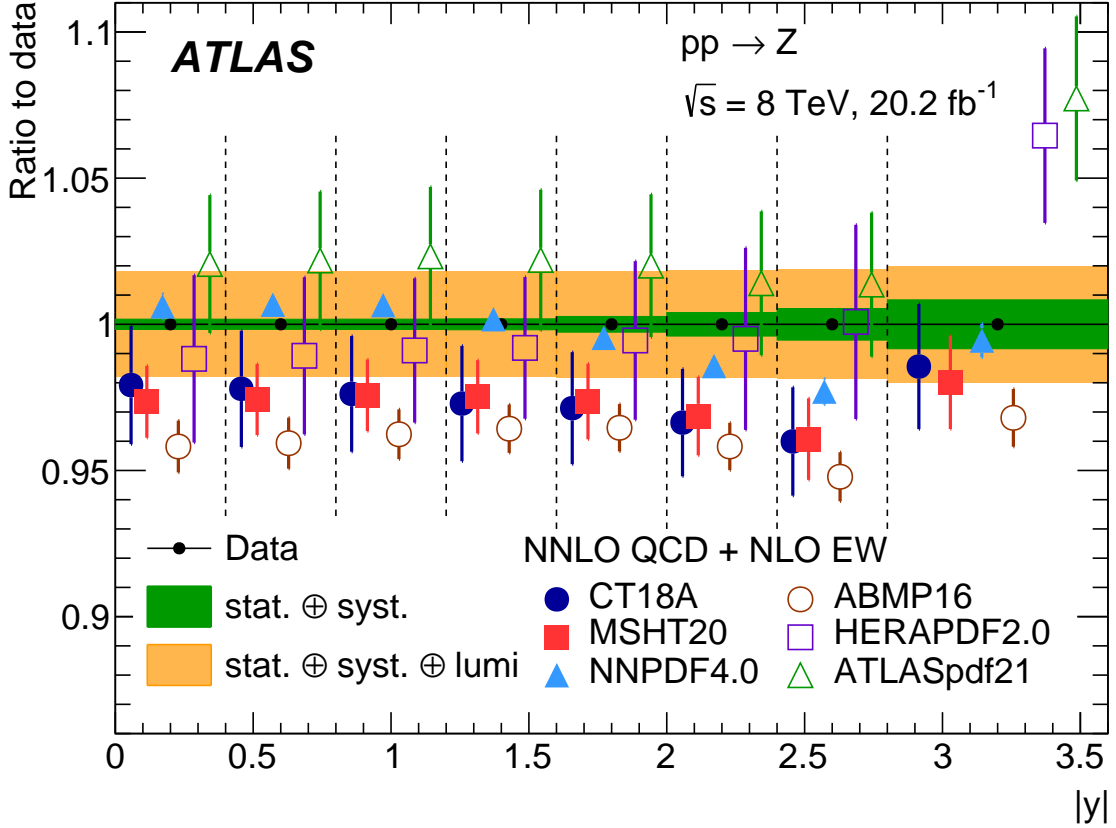


Figure 20: Ratio comparison between the $\frac{d\sigma}{dy}$ measurements and NNLO QCD predictions obtained from DYTURBO using different NNLO PDF sets. The uncertainty bands in the predictions only show the uncertainties specific to each PDF set (the uncertainties from CT18A have been rescaled from 95% to 68% confidence level). In each $|y|$ bin, the ratios for each PDF set are gradually displaced to the right for plotting purposes.

NNLO CT18A and NNLO MSHT PDF sets show reasonable agreement with the data, with a positive pull close to one standard deviation on the luminosity, corresponding to predictions approximately 1.6% lower than the data. The NNPDF4.0 PDF set with its much smaller uncertainties displays poor agreement with the data. This is due to the shape of the predicted distribution since the pull on the integrated luminosity is small. The ABMP16 PDF set is the one that most strongly pulls the integrated luminosity but its poor agreement with the data is also due to its significant difference in shape with respect to the data. The HERAPDF2.0 set and, to a lesser extent, the ATLASpdf21 set also display poor agreement because of a large discrepancy with the data in the highest $|y|$ bin due to the limited set of data used in these fits.

Finally, the total cross-section times branching ratio of $Z \rightarrow \ell\ell$, σ_Z , for Z/γ^* production in the Z -boson pole region, $80 < m < 100$ GeV, and within $|y| < 3.6$ is extracted from the integration of the measured differential $\frac{d\sigma}{dy}$ cross-section:

$$\sigma_Z = 1055.3 \pm 0.7 \text{ (stat.)} \pm 2.2 \text{ (syst.)} \pm 19.0 \text{ (lumi.) pb}$$

Aside from the dominant uncertainty in the integrated luminosity, the overall systematic uncertainty of 0.2% in this measurement is dominated by experimental lepton efficiency systematic uncertainties and has a

Table 5: Comparison between the measured total cross-section times branching ratio of $Z \rightarrow \ell\ell$, σ_Z , for Z/γ^* production with its uncertainty and predictions obtained from DYTurbo using different PDF sets. The prediction using the MSHTaN³LO PDF from Ref. [58] shows separately the scale variation and PDF uncertainties. The uncertainties in the NNLO predictions include only the PDF uncertainties from each specific PDF set (the uncertainties from CT18A have been rescaled from 95% to 68% confidence level).

	σ_Z (pb)
Data	1055 ± 19
MSHT20aN ³ LO [58]	1023^{+6}_{-4} (scale) ± 15 (PDF)
CT18A [59]	1028 ± 19
MSHT20 [60]	1027 ± 13
NNPDF4.0 [61]	1054 ± 4
ABMP16 [62]	1014 ± 9
HERAPDF2.0 [64]	1058 ± 25
ATLASpdf21 [65]	1084 ± 25

negligible contribution from theory uncertainties, which are below 0.1% and arise essentially from PDFs. Table 5 compares this measurement to the predictions obtained from DYTurbo with the same PDF sets as those shown in Table 4 for the rapidity-dependent cross-section $\frac{d\sigma}{dy}$.

6 Conclusions

This paper presents for the first time a double-differential measurement in $(p_T, |y|)$ of absolute and normalised cross-sections at the Z pole within the full phase space of the decay leptons. The measurements in this paper are obtained through a four-dimensional measurement of the lepton angular distributions as a function of $p_T^{\ell\ell}$ and $y^{\ell\ell}$ for a total sample of approximately 15 million Z -boson decays measured within the pole region, $80 < m^{\ell\ell} < 100$ GeV, and within the range $|y^{\ell\ell}| < 3.6$. Such a measurement is achieved by extending and improving the methodology already developed and published for the extraction of the Z -boson angular coefficients. A profile likelihood fit extracts at the same time these eight angular coefficients and the corresponding unpolarised cross-section as parameters of interest in each measurement bin in $(p_T, |y|)$ space. The uncertainties in these measurements are mostly statistical in nature and the experimental and theoretical systematics are at the few per mille level over most of the range.

The $\frac{d^2\sigma}{dp_T dy}$ measurements are compared to several state-of-the-art QCD perturbative predictions based on q_T -resummation at approximate N⁴LL accuracy matched to fixed-order $\mathcal{O}(\alpha_s^3)$ calculations at high p_T . The agreement between the data and the predictions is within 5% over the whole range of the measurements except in kinematic regions with limited statistics.

Once integrated over p_T , the rapidity-dependent cross-sections are measured with an overall accuracy of 0.2–0.5% before accounting for the uncertainty in the integrated luminosity of 1.8%. They are compared to the predictions from different PDF sets, which display a varying degree of agreement with the data.

The total cross-section times branching ratio of $Z \rightarrow \ell\ell$, σ_Z , for Z/γ^* production in the Z -boson pole region, $80 < m < 100$ GeV, and within $|y| < 3.6$, is found to be:

$$\sigma_Z = 1055.3 \pm 0.7 \text{ (stat.)} \pm 2.2 \text{ (syst.)} \pm 19.0 \text{ (lumi.) pb,}$$

in agreement with state-of-the-art predictions at $N^3\text{LO}$ in QCD.

Acknowledgements

We thank CERN for the very successful operation of the LHC, as well as the support staff from our institutions without whom ATLAS could not be operated efficiently.

We acknowledge the support of ANPCyT, Argentina; YerPhI, Armenia; ARC, Australia; BMWFW and FWF, Austria; ANAS, Azerbaijan; CNPq and FAPESP, Brazil; NSERC, NRC and CFI, Canada; CERN; ANID, Chile; CAS, MOST and NSFC, China; Minciencias, Colombia; MEYS CR, Czech Republic; DNRF and DNSRC, Denmark; IN2P3-CNRS and CEA-DRF/IRFU, France; SRNSFG, Georgia; BMBF, HGF and MPG, Germany; GSRI, Greece; RGC and Hong Kong SAR, China; ISF and Benoziyo Center, Israel; INFN, Italy; MEXT and JSPS, Japan; CNRST, Morocco; NWO, Netherlands; RCN, Norway; MEiN, Poland; FCT, Portugal; MNE/IFA, Romania; MESTD, Serbia; MSSR, Slovakia; ARRS and MIZŠ, Slovenia; DSI/NRF, South Africa; MICINN, Spain; SRC and Wallenberg Foundation, Sweden; SERI, SNSF and Cantons of Bern and Geneva, Switzerland; MOST, Taiwan; TENMAK, Türkiye; STFC, United Kingdom; DOE and NSF, United States of America. In addition, individual groups and members have received support from BCKDF, CANARIE, Compute Canada and CRC, Canada; PRIMUS 21/SCI/017 and UNCE SCI/013, Czech Republic; COST, ERC, ERDF, Horizon 2020 and Marie Skłodowska-Curie Actions, European Union; Investissements d’Avenir Labex, Investissements d’Avenir IDEX and ANR, France; DFG and AvH Foundation, Germany; Herakleitos, Thales and Aristeia programmes co-financed by EU-ESF and the Greek NSRF, Greece; BSF-NSF and MINERVA, Israel; Norwegian Financial Mechanism 2014-2021, Norway; NCN and NAWA, Poland; La Caixa Banking Foundation, CERCA Programme Generalitat de Catalunya and PROMETEO and GenT Programmes Generalitat Valenciana, Spain; Göran Gustafssons Stiftelse, Sweden; The Royal Society and Leverhulme Trust, United Kingdom.

The crucial computing support from all WLCG partners is acknowledged gratefully, in particular from CERN, the ATLAS Tier-1 facilities at TRIUMF (Canada), NDGF (Denmark, Norway, Sweden), CC-IN2P3 (France), KIT/GridKA (Germany), INFN-CNAF (Italy), NL-T1 (Netherlands), PIC (Spain), ASGC (Taiwan), RAL (UK) and BNL (USA), the Tier-2 facilities worldwide and large non-WLCG resource providers. Major contributors of computing resources are listed in Ref. [71].

References

- [1] S. D. Drell and T. M. Yan, *Massive Lepton-Pair Production in Hadron-Hadron Collisions at High Energies*, *Phys. Rev. Lett.* **25** (1970) 316.
- [2] ATLAS Collaboration, *Measurement of the transverse momentum and ϕ_{η}^* distributions of Drell-Yan lepton pairs in proton-proton collisions at $\sqrt{s} = 8$ TeV with the ATLAS detector*, *Eur. Phys. J. C* **76** (2016) 291, arXiv: [1512.02192](#).
- [3] ATLAS Collaboration, *Measurement of the transverse momentum distribution of Drell-Yan lepton pairs in proton-proton collisions at $\sqrt{s} = 13$ TeV with the ATLAS detector*, *Eur. Phys. J. C* **80** (2020) 616, arXiv: [1912.02844](#) [[hep-ex](#)].
- [4] CMS Collaboration, *Measurement of the Z boson differential cross section in transverse momentum and rapidity in proton-proton collisions at 8 TeV*, *Phys. Lett. B* **749** (2015) 187, arXiv: [1504.03511](#) [[hep-ex](#)].
- [5] CMS Collaboration, *Measurements of differential Z boson production cross sections in proton-proton collisions at $\sqrt{s} = 13$ TeV*, *JHEP* **12** (2019) 061, arXiv: [1909.04133](#).
- [6] ATLAS Collaboration, *Measurement of the angular coefficients in Z-boson events using electron and muon pairs from data taken at $\sqrt{s} = 8$ TeV with the ATLAS detector*, *JHEP* **08** (2016) 159, arXiv: [1606.00689](#).
- [7] CMS Collaboration, *Angular coefficients of Z bosons produced in pp collisions at $\sqrt{s} = 8$ TeV and decaying to $\mu^+\mu^-$ as a function of transverse momentum and rapidity*, *Phys. Lett. B* **750** (2015) 154, arXiv: [1504.03512](#) [[hep-ex](#)].
- [8] ATLAS Collaboration, *Measurement of the Drell-Yan triple-differential cross section in pp collisions at $\sqrt{s} = 8$ TeV*, *JHEP* **12** (2017) 059, arXiv: [1710.05167](#) [[hep-ex](#)].
- [9] J. C. Collins and D. E. Soper, *Angular distribution of dileptons in high-energy hadron collisions*, *Phys. Rev. D* **16** (7 1977) 2219.
- [10] E. Mirkes, *Angular decay distribution of leptons from W-bosons at NLO in hadronic collisions*, *Nucl. Phys. B* **387** (1992) 3.
- [11] E. Mirkes and J. Ohnemus, *W and Z Polarization Effects in Hadronic Collisions*, *Phys. Rev. D* **50** (1994) 5692, arXiv: [9406381](#) [[hep-ph](#)].
- [12] E. Mirkes and J. Ohnemus, *Angular distributions of Drell-Yan lepton pairs at the Tevatron: Order α_s^2 corrections and Monte Carlo studies*, *Phys. Rev. D* **51** (1995) 4891, arXiv: [hep-ph/9412289](#) [[hep-ph](#)].
- [13] E. Mirkes and J. Ohnemus, *Polarization Effects in Drell-Yan Type Processes $h_1 + h_2 \rightarrow (W, Z, \gamma^*, J/\psi) + X$* , (1994), arXiv: [hep-ph/9408402](#) [[hep-ph](#)].
- [14] S. Jadach and Z. Was, *Suppression of QED interference contributions to the charge asymmetry at the Z^0 resonance*, *Phys. Lett. B* **219** (1989) 103.
- [15] S. Jadach et al., *Initial-final-state interference in the Z line shape*, *Phys. Lett. B* **465** (1999) 254, arXiv: [9907547](#) [[hep-ph](#)].

- [16] S. Jadach, B. F. L. Ward, Z. A. Was and S. A. Yost, *KK MC-hh: Systematic studies of exact $O(\alpha^2 L)$ CEEX EW corrections in a hadronic MC for precision Z/γ^* physics at LHC Energies*, [Phys. Rev. D **99** \(2019\) 076016](#).
- [17] M. A. Ebert, J. K. L. Michel, I. W. Stewart and F. J. Tackmann, *Drell-Yan q_T resummation of fiducial power corrections at N^3LL* , [JHEP **04** \(2021\) 102](#), arXiv: [2006.11382 \[hep-ph\]](#).
- [18] A. Glazov, *Defiducialization: Providing Experimental Measurements for Accurate Fixed-Order Predictions*, [Eur. Phys. J. C **80** \(2020\) 875](#), arXiv: [2001.02933 \[hep-ex\]](#).
- [19] G. P. Salam and E. Slade, *Cuts for two-body decays at colliders*, [JHEP **11** \(2021\) 220](#), arXiv: [2106.08329 \[hep-ph\]](#).
- [20] S. Alekhin, A. Kardos, S. Moch and Z. Trócsányi, *Precision studies for Drell–Yan processes at NNLO*, [Eur. Phys. J. C **81** \(2021\) 573](#), arXiv: [2104.02400 \[hep-ph\]](#).
- [21] ATLAS Collaboration, *Electron efficiency measurements with the ATLAS detector using 2012 LHC proton–proton collision data*, [Eur. Phys. J. C **77** \(2017\) 195](#), arXiv: [1612.01456 \[hep-ex\]](#).
- [22] ATLAS Collaboration, *The ATLAS Experiment at the CERN Large Hadron Collider*, [JINST **3** \(2008\) S08003](#).
- [23] ATLAS Collaboration, *The ATLAS Collaboration Software and Firmware*, ATL-SOFT-PUB-2021-001, 2021, URL: <https://cds.cern.ch/record/2767187>.
- [24] P. Nason, *A new method for combining NLO QCD with shower Monte Carlo algorithms*, [JHEP **11** \(2004\) 040](#).
- [25] S. Frixione, P. Nason and C. Oleari, *Matching NLO QCD computations with parton shower simulations: the POWHEG method*, [JHEP **11** \(2007\) 070](#), arXiv: [0709.2092 \[hep-ph\]](#).
- [26] S. Alioli, P. Nason, C. Oleari and E. Re, *A general framework for implementing NLO calculations in shower Monte Carlo programs: the POWHEG BOX*, [JHEP **06** \(2010\) 043](#), arXiv: [1002.2581 \[hep-ph\]](#).
- [27] T. Sjöstrand, S. Mrenna and P. Skands, *A Brief Introduction to PYTHIA 8.1*, [Computer Physics Communications **178** \(2008\) 852](#).
- [28] H.-L. Lai, M. Guzzi, J. Huston, Z. Li, P. M. Nadolsky et al., *New parton distributions for collider physics*, [Phys.Rev. **D82** \(2010\) 074024](#), arXiv: [1007.2241 \[hep-ph\]](#).
- [29] T. Gleisberg, S. Höche, F. Krauss et al., *Event generation with SHERPA 1.1*, [JHEP **02** \(2009\) 007](#), arXiv: [0811.4622 \[hep-ph\]](#).
- [30] S. Höche, F. Krauss, S. Schumann and F. Siegert, *QCD matrix elements and truncated showers*, [JHEP **05** \(2009\) 053](#), arXiv: [0903.1219 \[hep-ph\]](#).
- [31] T. Gleisberg and S. Höche, *Comix, a new matrix element generator*, [JHEP **12** \(2008\) 039](#), arXiv: [0808.3674 \[hep-ph\]](#).
- [32] S. Schumann and F. Krauss, *A Parton shower algorithm based on Catani-Seymour dipole factorisation*, [JHEP **03** \(2008\) 038](#), arXiv: [0709.1027 \[hep-ph\]](#).

- [33] T. Sjöstrand, S. Mrenna and P. Z. Skands, *PYTHIA 6.4 physics and manual*, *JHEP* **05** (2006) 026, arXiv: [hep-ph/0603175](#).
- [34] G. Corcella et al., *HERWIG 6: An Event generator for hadron emission reactions with interfering gluons (including supersymmetric processes)*, *JHEP* **01** (2001) 010, arXiv: [0011363 \[hep-ph\]](#).
- [35] A. D. Martin et al., *Parton distributions incorporating QED contributions*, *Eur. Phys. J. C* **39** (2005) 155, arXiv: [0411040](#).
- [36] ATLAS Collaboration, *Summary of ATLAS Pythia 8 tunes*, ATL-PHYS-PUB-2012-003, 2012, URL: <https://cds.cern.ch/record/1474107>.
- [37] P. Golonka and Z. Was, *PHOTOS Monte Carlo: A precision tool for QED corrections in Z and W decays*, *Eur. Phys. J. C* **45** (2006) 97, arXiv: [hep-ph/0506026](#).
- [38] Y. Li and F. Petriello, *Combining QCD and electroweak corrections to dilepton production in the framework of the FEWZ simulation code*, *Phys. Rev. D* **86** (2012) 094034, arXiv: [1208.5967 \[hep-ph\]](#).
- [39] ATLAS Collaboration, *The ATLAS Simulation Infrastructure*, *Eur. Phys. J. C* **70** (2010) 823, arXiv: [1005.4568 \[physics.ins-det\]](#).
- [40] S. Agostinelli et al., *GEANT4 – a simulation toolkit*, *Nucl. Instrum. Meth. A* **506** (2003) 250.
- [41] ATLAS Collaboration, *Measurement of the muon reconstruction performance of the ATLAS detector using 2011 and 2012 LHC proton–proton collision data*, *Eur. Phys. J. C* **74** (2014) 3130, arXiv: [1407.3935](#).
- [42] ATLAS Collaboration, *Electron reconstruction and identification efficiency measurements with the ATLAS detector using the 2011 LHC proton–proton collision data*, *Eur. Phys. J. C* **74** (2014) 2941, arXiv: [1404.2240 \[hep-ex\]](#).
- [43] ATLAS Collaboration, *Electron and photon energy calibration with the ATLAS detector using LHC Run 1 data*, *Eur. Phys. J. C* **74** (2014) 3071, arXiv: [1407.3935](#).
- [44] G. Bozzi, S. Catani, D. de Florian and M. Grazzini, *Transverse-momentum resummation and the spectrum of the Higgs boson at the LHC*, *Nucl. Phys. B* **737** (2006) 73, arXiv: [hep-ph/0508068](#).
- [45] S. Camarda et al., *DYTurbo: Fast predictions for Drell-Yan processes*, *Eur. Phys. J. C* **80** (2020) 251, [Erratum: *Eur.Phys.J.C* 80, 440 (2020)], arXiv: [1910.07049 \[hep-ph\]](#).
- [46] S. Camarda, L. Cieri and G. Ferrera, *Drell–Yan lepton-pair production: q_T resummation at N^3LL accuracy and fiducial cross sections at N^3LO* , *Phys. Rev. D* **104** (2021) L111503, arXiv: [2103.04974 \[hep-ph\]](#).
- [47] S. Camarda, L. Cieri and G. Ferrera, *Drell-Yan lepton-pair production: q_T resummation at approximate N^4LL+N^4LO accuracy*, (2023), arXiv: [2303.12781 \[hep-ph\]](#).
- [48] T. Neumann and J. Campbell, *Fiducial Drell-Yan production at the LHC improved by transverse-momentum resummation at $N^4LL_p+N^3LO$* , *Phys. Rev. D* **107** (2023) L011506, arXiv: [2207.07056 \[hep-ph\]](#).

- [49] I. Scimemi and A. Vladimirov, *Analysis of vector boson production within TMD factorization*, *Eur. Phys. J. C* **78** (2018) 89, arXiv: [1706.01473 \[hep-ph\]](#).
- [50] A. Bacchetta et al., *Transverse-momentum-dependent parton distributions up to N^3LL from Drell-Yan data*, *JHEP* **07** (2020) 117, arXiv: [1912.07550 \[hep-ph\]](#).
- [51] P. F. Monni, E. Re and P. Torrielli, *Higgs Transverse-Momentum Resummation in Direct Space*, *Phys. Rev. Lett.* **116** (2016) 242001, arXiv: [1604.02191 \[hep-ph\]](#).
- [52] W. Bizon, P. F. Monni, E. Re, L. Rottoli and P. Torrielli, *Momentum-space resummation for transverse observables and the Higgs p_\perp at $N^3LL+NNLO$* , *JHEP* **02** (2018) 108, arXiv: [1705.09127 \[hep-ph\]](#).
- [53] E. Re, L. Rottoli and P. Torrielli, *Fiducial Higgs and Drell-Yan distributions at $N^3LL'+NNLO$ with RadISH*, *JHEP* **9** (2021) 108, arXiv: [2104.07509 \[hep-ph\]](#).
- [54] G. Billis, B. Dehnadi, M. A. Ebert, J. K. L. Michel and F. J. Tackmann, *Higgs p_T Spectrum and Total Cross Section with Fiducial Cuts at Third Resummed and Fixed Order in QCD*, *Phys. Rev. Lett.* **127** (2021) 072001, arXiv: [2102.08039 \[hep-ph\]](#).
- [55] R. Boughezal et al., *Z-boson production in association with a jet at next-to-next-to-leading order in perturbative QCD*, *Phys. Rev. Lett.* **116** (2016) 152001, arXiv: [1512.01291 \[hep-ph\]](#).
- [56] A. G.-D. Ridder, T. Gehrmann, E. Glover, A. Huss and T. Morgan, *Precise QCD Predictions for the Production of a Z Boson in Association with a Hadronic Jet*, *Phys. Rev. Lett.* **117** (2016), arXiv: [1507.02850 \[hep-ph\]](#).
- [57] X. Chen et al., *Third-Order Fiducial Predictions for Drell-Yan Production at the LHC*, *Phys. Rev. Lett.* **128** (2022) 252001, arXiv: [2203.01565 \[hep-ph\]](#).
- [58] J. McGowan, T. Cridge, L. A. Harland-Lang and R. S. Thorne, *Approximate N^3LO Parton Distribution Functions with Theoretical Uncertainties: MSHT20a N^3LO PDFs*, *Eur. Phys. J. C* **83** (2023), arXiv: [2207.04739 \[hep-ph\]](#).
- [59] T.-J. Hou et al., *New CTEQ global analysis of quantum chromodynamics with high-precision data from the LHC*, *Phys. Rev. D* **103** (2021), arXiv: [1912.10053](#).
- [60] S. Bailey, T. Cridge, L. A. Harland-Lang, A. D. Martin and R. S. Thorne, *Parton distributions from LHC, HERA, Tevatron and fixed target data: MSHT20 PDFs*, *Eur. Phys. J. C* **81** (2021).
- [61] Richard D. Ball et al., *The path to proton structure at 1% accuracy*, *Eur. Phys. J. C* **82** (2022).
- [62] S. Alekhin, J. Blümlein, S. Moch and R. Placakyte, *Parton distribution functions, α_s , and heavy-quark masses for LHC Run II*, *Phys. Rev. D* **96** (2017) 014011, arXiv: [1701.05838 \[hep-ph\]](#).
- [63] S. Alekhin, J. Blümlein and S. Moch, *An Update of the ABMP16 PDF Fit*, 2019, arXiv: [1909.03533 \[hep-ph\]](#).
- [64] H1 and ZEUS Collaborations, *Combination of Measurements of Inclusive Deep Inelastic $e^\pm p$ Scattering Cross Sections and QCD Analysis of HERA Data*, *Eur. Phys. J. C* **75** (2015).

- [65] ATLAS Collaboration, *Determination of the parton distribution functions of the proton using diverse ATLAS data from pp collisions at $\sqrt{s} = 7, 8$ and 13 TeV*, *Eur. Phys. J. C* **82** (2022).
- [66] S. Bondarenko, Y. Dydyshka, L. Kalinovskaya, R. Sadykov and V. Yermolchuk, *Hadron-hadron collision mode in ReneSANCe-v1.3.0*, *Comput. Phys. Commun.* **285** (2023) 108646, arXiv: [2207.04332](https://arxiv.org/abs/2207.04332) [[hep-ph](#)].
- [67] M. Chiesa, F. Piccinini and A. Vicini, *Direct determination of $\sin^2\theta_{\text{eff}}^\ell$ at hadron colliders*, *Phys. Rev. D* **100** (7 2019) 071302, arXiv: [1906.11569](https://arxiv.org/abs/1906.11569) [[hep-ph](#)].
- [68] A. Arbuzov et al., *Update of the MCSANC Monte Carlo integrator, v. 1.20*, *JETP Lett.* **103** (2016) 131, arXiv: [1509.03052](https://arxiv.org/abs/1509.03052) [[hep-ph](#)].
- [69] S. Dittmaier, A. Huss and C. Schwinn, *Mixed QCD-electroweak $O(\alpha_s\alpha)$ corrections to Drell-Yan processes in the resonance region: Pole approximation and non-factorizable corrections*, *Nucl. Phys. B* **885** (2014) 318, arXiv: [1403.3216](https://arxiv.org/abs/1403.3216) [[hep-ph](#)].
- [70] E. Richter-Was and Z. Was, *Adequacy of Effective Born for electroweak effects and TauSpinner algorithms for high energy physics simulated samples*, *Eur. Phys. J. C.* **137** (2022) 95, arXiv: [2012.10997](https://arxiv.org/abs/2012.10997) [[hep-ph](#)].
- [71] ATLAS Collaboration, *ATLAS Computing Acknowledgements*, ATL-SOFT-PUB-2023-001, 2023, URL: <https://cds.cern.ch/record/2869272>.

The ATLAS Collaboration

G. Aad ¹⁰², B. Abbott ¹²⁰, K. Abeling ⁵⁵, N.J. Abicht ⁴⁹, S.H. Abidi ²⁹, A. Aboulhorma ^{35e}, H. Abramowicz ¹⁵¹, H. Abreu ¹⁵⁰, Y. Abulaiti ¹¹⁷, A.C. Abusleme Hoffman ^{137a}, B.S. Acharya ^{69a,69b,p}, C. Adam Bourdarios ⁴, L. Adamczyk ^{86a}, L. Adamek ¹⁵⁵, S.V. Addepalli ²⁶, M.J. Addison ¹⁰¹, J. Adelman ¹¹⁵, A. Adiguzel ^{21c}, T. Adye ¹³⁴, A.A. Affolder ¹³⁶, Y. Afik ³⁶, M.N. Agaras ¹³, J. Agarwala ^{73a,73b}, A. Aggarwal ¹⁰⁰, C. Agheorghiesei ^{27c}, A. Ahmad ³⁶, F. Ahmadov ^{38,ad}, W.S. Ahmed ¹⁰⁴, S. Ahuja ⁹⁵, X. Ai ^{62a}, G. Aielli ^{76a,76b}, M. Ait Tamliah ^{35e}, B. Aitbenkikh ^{35a}, I. Aizenberg ¹⁶⁹, M. Akbiyik ¹⁰⁰, T.P.A. Åkesson ⁹⁸, A.V. Akimov ³⁷, D. Akiyama ¹⁶⁸, N.N. Akolkar ²⁴, K. Al Houry ⁴¹, G.L. Alberghi ^{23b}, J. Albert ¹⁶⁵, P. Albicocco ⁵³, G.L. Albouy ⁶⁰, S. Alderweireldt ⁵², M. Aleksa ³⁶, I.N. Aleksandrov ³⁸, C. Alexa ^{27b}, T. Alexopoulos ¹⁰, A. Alfonsi ¹¹⁴, F. Alfonsi ^{23b}, M. Algren ⁵⁶, M. Alhroob ¹²⁰, B. Ali ¹³², H.M.J. Ali ⁹¹, S. Ali ¹⁴⁸, S.W. Alibocus ⁹², M. Aliev ³⁷, G. Alimonti ^{71a}, W. Alkahi ⁵⁵, C. Allaire ⁶⁶, B.M.M. Allbrooke ¹⁴⁶, J.F. Allen ⁵², C.A. Allendes Flores ^{137f}, P.P. Allport ²⁰, A. Aloisio ^{72a,72b}, F. Alonso ⁹⁰, C. Alpigiani ¹³⁸, M. Alvarez Estevez ⁹⁹, A. Alvarez Fernandez ¹⁰⁰, M.G. Alvigi ^{72a,72b}, M. Aly ¹⁰¹, Y. Amaral Coutinho ^{83b}, A. Ambler ¹⁰⁴, C. Amelung ³⁶, M. Amerl ¹⁰¹, C.G. Ames ¹⁰⁹, D. Amidei ¹⁰⁶, S.P. Amor Dos Santos ^{130a}, K.R. Amos ¹⁶³, V. Ananiev ¹²⁵, C. Anastopoulos ¹³⁹, T. Andeen ¹¹, J.K. Anders ³⁶, S.Y. Andreev ^{47a,47b}, A. Andreazza ^{71a,71b}, S. Angelidakis ⁹, A. Angerami ^{41,ag}, A.V. Anisenkov ³⁷, A. Annovi ^{74a}, C. Antel ⁵⁶, M.T. Anthony ¹³⁹, E. Antipov ¹⁴⁵, M. Antonelli ⁵³, D.J.A. Antrim ^{17a}, F. Anulli ^{75a}, M. Aoki ⁸⁴, T. Aoki ¹⁵³, J.A. Aparisi Pozo ¹⁶³, M.A. Aparo ¹⁴⁶, L. Aperio Bella ⁴⁸, C. Appelt ¹⁸, A. Apyan ²⁶, N. Aranzabal ³⁶, C. Arcangeletti ⁵³, A.T.H. Arce ⁵¹, E. Arena ⁹², J-F. Arguin ¹⁰⁸, S. Argyropoulos ⁵⁴, J.-H. Arling ⁴⁸, A.J. Armbruster ³⁶, O. Arnaez ⁴, H. Arnold ¹¹⁴, Z.P. Arrubarrena Tame ¹⁰⁹, G. Artoni ^{75a,75b}, H. Asada ¹¹¹, K. Asai ¹¹⁸, S. Asai ¹⁵³, N.A. Asbah ⁶¹, J. Assahsah ^{35d}, K. Assamagan ²⁹, R. Astalos ^{28a}, S. Atashi ¹⁶⁰, R.J. Atkin ^{33a}, M. Atkinson ¹⁶², N.B. Atlay ¹⁸, H. Atmani ^{62b}, P.A. Atlasiddha ¹⁰⁶, K. Augsten ¹³², S. Auricchio ^{72a,72b}, A.D. Auriol ²⁰, V.A. Austrup ¹⁰¹, G. Avolio ³⁶, K. Axiotis ⁵⁶, G. Azuelos ^{108,ak}, D. Babal ^{28b}, H. Bachacou ¹³⁵, K. Bachas ^{152,t}, A. Bachiu ³⁴, F. Backman ^{47a,47b}, A. Badea ⁶¹, P. Bagnaia ^{75a,75b}, M. Bahmani ¹⁸, A.J. Bailey ¹⁶³, V.R. Bailey ¹⁶², J.T. Baines ¹³⁴, L. Baines ⁹⁴, C. Bakalis ¹⁰, O.K. Baker ¹⁷², E. Bakos ¹⁵, D. Bakshi Gupta ⁸, R. Balasubramanian ¹¹⁴, E.M. Baldin ³⁷, P. Balek ^{86a}, E. Ballabene ^{23b,23a}, F. Balli ¹³⁵, L.M. Baltes ^{63a}, W.K. Balunas ³², J. Balz ¹⁰⁰, E. Banas ⁸⁷, M. Bandieramonte ¹²⁹, A. Bandyopadhyay ²⁴, S. Bansal ²⁴, L. Barak ¹⁵¹, M. Barakat ⁴⁸, E.L. Barberio ¹⁰⁵, D. Barberis ^{57b,57a}, M. Barbero ¹⁰², G. Barbour ⁹⁶, K.N. Barends ^{33a}, T. Barillari ¹¹⁰, M-S. Barisits ³⁶, T. Barklow ¹⁴³, P. Baron ¹²², D.A. Baron Moreno ¹⁰¹, A. Baroncelli ^{62a}, G. Barone ²⁹, A.J. Barr ¹²⁶, J.D. Barr ⁹⁶, L. Barranco Navarro ^{47a,47b}, F. Barreiro ⁹⁹, J. Barreiro Guimarães da Costa ^{14a}, U. Barron ¹⁵¹, M.G. Barros Teixeira ^{130a}, S. Barsov ³⁷, F. Bartels ^{63a}, R. Bartoldus ¹⁴³, A.E. Barton ⁹¹, P. Bartos ^{28a}, A. Basan ¹⁰⁰, M. Baselga ⁴⁹, A. Bassalat ^{66,b}, M.J. Basso ^{156a}, C.R. Basson ¹⁰¹, R.L. Bates ⁵⁹, S. Batlamous ^{35e}, J.R. Batley ³², B. Batool ¹⁴¹, M. Battaglia ¹³⁶, D. Battulga ¹⁸, M. Baucé ^{75a,75b}, M. Bauer ³⁶, P. Bauer ²⁴, L.T. Bazzano Hurrell ³⁰, J.B. Beacham ⁵¹, T. Beau ¹²⁷, P.H. Beauchemin ¹⁵⁸, F. Becherer ⁵⁴, P. Bechtel ²⁴, H.P. Beck ^{19,s}, K. Becker ¹⁶⁷, A.J. Beddall ⁸², V.A. Bednyakov ³⁸, C.P. Bee ¹⁴⁵, L.J. Beemster ¹⁵, T.A. Beermann ³⁶, M. Begalli ^{83d}, M. Beger ²⁹, A. Behera ¹⁴⁵, J.K. Behr ⁴⁸, J.F. Beirer ⁵⁵, F. Beisiegel ²⁴, M. Belfkir ¹⁵⁹, G. Bella ¹⁵¹, L. Bellagamba ^{23b}, A. Bellerive ³⁴, P. Bellos ²⁰, K. Beloborodov ³⁷, N.L. Belyaev ³⁷, D. Bencheikroun ^{35a}, F. Bendebba ^{35a},

Y. Benhammou [ID151](#), M. Benoit [ID29](#), J.R. Bensingler [ID26](#), S. Bentvelsen [ID114](#), L. Beresford [ID48](#),
 M. Beretta [ID53](#), E. Bergeaas Kuutmann [ID161](#), N. Berger [ID4](#), B. Bergmann [ID132](#), J. Beringer [ID17a](#),
 G. Bernardi [ID5](#), C. Bernius [ID143](#), F.U. Bernlochner [ID24](#), F. Bernon [ID36,102](#), T. Berry [ID95](#), P. Berta [ID133](#),
 A. Berthold [ID50](#), I.A. Bertram [ID91](#), S. Bethke [ID110](#), A. Betti [ID75a,75b](#), A.J. Bevan [ID94](#), M. Bhamjee [ID33c](#),
 S. Bhatta [ID145](#), D.S. Bhattacharya [ID166](#), P. Bhattarai [ID26](#), V.S. Bhopatkar [ID121](#), R. Bi [ID29,am](#),
 R.M. Bianchi [ID129](#), G. Bianco [ID23b,23a](#), O. Biebel [ID109](#), R. Bielski [ID123](#), M. Biglietti [ID77a](#),
 T.R.V. Billoud [ID132](#), M. Bindi [ID55](#), A. Bingul [ID21b](#), C. Bini [ID75a,75b](#), A. Biondini [ID92](#),
 C.J. Birch-sykes [ID101](#), G.A. Bird [ID20,134](#), M. Birman [ID169](#), M. Biros [ID133](#), T. Bisanz [ID49](#),
 E. Bisceglie [ID43b,43a](#), D. Biswas [ID141](#), A. Bitadze [ID101](#), K. Bjørke [ID125](#), I. Bloch [ID48](#), C. Blocker [ID26](#),
 A. Blue [ID59](#), U. Blumenschein [ID94](#), J. Blumenthal [ID100](#), G.J. Bobbink [ID114](#), V.S. Bobrovnikov [ID37](#),
 M. Boehler [ID54](#), B. Boehm [ID166](#), D. Bogavac [ID36](#), A.G. Bogdanchikov [ID37](#), C. Bohm [ID47a](#),
 V. Boisvert [ID95](#), P. Bokaň [ID48](#), T. Bold [ID86a](#), M. Bomben [ID5](#), M. Bona [ID94](#), M. Boonekamp [ID135](#),
 C.D. Booth [ID95](#), A.G. Borbély [ID59](#), I.S. Bordulev [ID37](#), H.M. Borecka-Bielska [ID108](#), L.S. Borgna [ID96](#),
 G. Borissov [ID91](#), D. Bortoletto [ID126](#), D. Boscherini [ID23b](#), M. Bosman [ID13](#), J.D. Bossio Sola [ID36](#),
 K. Bouaouda [ID35a](#), N. Bouchhar [ID163](#), J. Boudreau [ID129](#), E.V. Bouhova-Thacker [ID91](#), D. Boumediene [ID40](#),
 R. Bouquet [ID5](#), A. Boveia [ID119](#), J. Boyd [ID36](#), D. Boye [ID29](#), I.R. Boyko [ID38](#), J. Bracinik [ID20](#),
 N. Brahimī [ID62d](#), G. Brandt [ID171](#), O. Brandt [ID32](#), F. Braren [ID48](#), B. Brau [ID103](#), J.E. Brau [ID123](#),
 R. Brenner [ID169](#), L. Brenner [ID114](#), R. Brenner [ID161](#), S. Bressler [ID169](#), D. Britton [ID59](#), D. Britzger [ID110](#),
 I. Brock [ID24](#), G. Brooijmans [ID41](#), W.K. Brooks [ID137f](#), E. Brost [ID29](#), L.M. Brown [ID165,m](#), L.E. Bruce [ID61](#),
 T.L. Bruckler [ID126](#), P.A. Bruckman de Renstrom [ID87](#), B. Brüers [ID48](#), D. Bruncko [ID28b,*](#), A. Bruni [ID23b](#),
 G. Bruni [ID23b](#), M. Bruschi [ID23b](#), N. Bruscano [ID75a,75b](#), T. Buanes [ID16](#), Q. Buat [ID138](#), D. Buchin [ID110](#),
 A.G. Buckley [ID59](#), M.K. Bugge [ID125](#), O. Bulekov [ID37](#), B.A. Bullard [ID143](#), S. Burdin [ID92](#),
 C.D. Burgard [ID49](#), A.M. Burger [ID40](#), B. Burghgrave [ID8](#), O. Burlayenko [ID54](#), J.T.P. Burr [ID32](#),
 C.D. Burton [ID11](#), J.C. Burzynski [ID142](#), E.L. Busch [ID41](#), V. Büscher [ID100](#), P.J. Bussey [ID59](#),
 J.M. Butler [ID25](#), C.M. Buttar [ID59](#), J.M. Butterworth [ID96](#), W. Buttinger [ID134](#), C.J. Buxo Vazquez [ID107](#),
 A.R. Buzykaev [ID37](#), G. Cabras [ID23b](#), S. Cabrera Urbán [ID163](#), L. Cadamuro [ID66](#), D. Caforio [ID58](#),
 H. Cai [ID129](#), Y. Cai [ID14a,14e](#), V.M.M. Cairo [ID36](#), O. Cakir [ID3a](#), N. Calace [ID36](#), P. Calafiura [ID17a](#),
 G. Calderini [ID127](#), P. Calfayan [ID68](#), G. Callea [ID59](#), L.P. Caloba [ID83b](#), D. Calvet [ID40](#), S. Calvet [ID40](#),
 T.P. Calvet [ID102](#), M. Calvetti [ID74a,74b](#), R. Camacho Toro [ID127](#), S. Camarda [ID36](#), D. Camarero Munoz [ID26](#),
 P. Camarri [ID76a,76b](#), M.T. Camerlingo [ID72a,72b](#), D. Cameron [ID125](#), C. Camincher [ID165](#), M. Campanelli [ID96](#),
 A. Camplani [ID42](#), V. Canale [ID72a,72b](#), A. Canesse [ID104](#), M. Cano Bret [ID80](#), J. Cantero [ID163](#), Y. Cao [ID162](#),
 F. Capocasa [ID26](#), M. Capua [ID43b,43a](#), A. Carbone [ID71a,71b](#), R. Cardarelli [ID76a](#), J.C.J. Cardenas [ID8](#),
 F. Cardillo [ID163](#), T. Carli [ID36](#), G. Carlino [ID72a](#), J.I. Carlotta [ID13](#), B.T. Carlson [ID129,u](#),
 E.M. Carlson [ID165,156a](#), L. Carminati [ID71a,71b](#), A. Carnelli [ID135](#), M. Carnesale [ID75a,75b](#), S. Caron [ID113](#),
 E. Carquin [ID137f](#), S. Carrá [ID71a,71b](#), G. Carratta [ID23b,23a](#), F. Carri Argos [ID33g](#), J.W.S. Carter [ID155](#),
 T.M. Carter [ID52](#), M.P. Casado [ID13,j](#), M. Caspar [ID48](#), E.G. Castiglia [ID172](#), F.L. Castillo [ID4](#),
 L. Castillo Garcia [ID13](#), V. Castillo Gimenez [ID163](#), N.F. Castro [ID130a,130e](#), A. Catinaccio [ID36](#),
 J.R. Catmore [ID125](#), V. Cavaliere [ID29](#), N. Cavalli [ID23b,23a](#), V. Cavasinni [ID74a,74b](#), Y.C. Cekmecelioglu [ID48](#),
 E. Celebi [ID21a](#), F. Celli [ID126](#), M.S. Centonze [ID70a,70b](#), K. Cerny [ID122](#), A.S. Cerqueira [ID83a](#), A. Cerri [ID146](#),
 L. Cerrito [ID76a,76b](#), F. Cerutti [ID17a](#), B. Cervato [ID141](#), A. Cervelli [ID23b](#), G. Cesarini [ID53](#), S.A. Cetin [ID82](#),
 Z. Chadi [ID35a](#), D. Chakraborty [ID115](#), M. Chala [ID130f](#), J. Chan [ID170](#), W.Y. Chan [ID153](#), J.D. Chapman [ID32](#),
 E. Chapon [ID135](#), B. Chargeishvili [ID149b](#), D.G. Charlton [ID20](#), T.P. Charman [ID94](#), M. Chatterjee [ID19](#),
 C. Chauhan [ID133](#), S. Chekanov [ID6](#), S.V. Chekulaev [ID156a](#), G.A. Chelkov [ID38,a](#), A. Chen [ID106](#),
 B. Chen [ID151](#), B. Chen [ID165](#), H. Chen [ID14c](#), H. Chen [ID29](#), J. Chen [ID62c](#), J. Chen [ID142](#), M. Chen [ID126](#),
 S. Chen [ID153](#), S.J. Chen [ID14c](#), X. Chen [ID62c](#), X. Chen [ID14b,aj](#), Y. Chen [ID62a](#), C.L. Cheng [ID170](#),
 H.C. Cheng [ID64a](#), S. Cheong [ID143](#), A. Cheplakov [ID38](#), E. Cheremushkina [ID48](#), E. Cherepanova [ID114](#),
 R. Cherkaoui El Moursli [ID35e](#), E. Cheu [ID7](#), K. Cheung [ID65](#), L. Chevalier [ID135](#), V. Chiarella [ID53](#),

G. Chiarelli ^{74a}, N. Chiedde ¹⁰², G. Chiodini ^{70a}, A.S. Chisholm ²⁰, A. Chitan ^{27b}, M. Chitishvili ¹⁶³, M.V. Chizhov ³⁸, K. Choi ¹¹, A.R. Chomont ^{75a,75b}, Y. Chou ¹⁰³, E.Y.S. Chow ¹¹⁴, T. Chowdhury ^{33g}, K.L. Chu ¹⁶⁹, M.C. Chu ^{64a}, X. Chu ^{14a,14e}, J. Chudoba ¹³¹, J.J. Chwastowski ⁸⁷, D. Cieri ¹¹⁰, K.M. Ciesla ^{86a}, V. Cindro ⁹³, A. Ciocio ^{17a}, F. Cirotto ^{72a,72b}, Z.H. Citron ^{169,n}, M. Citterio ^{71a}, D.A. Ciubotaru ^{27b}, B.M. Ciungu ¹⁵⁵, A. Clark ⁵⁶, P.J. Clark ⁵², J.M. Clavijo Columbie ⁴⁸, S.E. Clawson ⁴⁸, C. Clement ^{47a,47b}, J. Clercx ⁴⁸, L. Clissa ^{23b,23a}, Y. Coadou ¹⁰², M. Cobal ^{69a,69c}, A. Coccaro ^{57b}, R.F. Coelho Barrue ^{130a}, R. Coelho Lopes De Sa ¹⁰³, S. Coelli ^{71a}, H. Cohen ¹⁵¹, A.E.C. Coimbra ^{71a,71b}, B. Cole ⁴¹, J. Collot ⁶⁰, P. Conde Muiño ^{130a,130g}, M.P. Connell ^{33c}, S.H. Connell ^{33c}, I.A. Connelly ⁵⁹, E.I. Conroy ¹²⁶, F. Conventi ^{72a,al}, H.G. Cooke ²⁰, A.M. Cooper-Sarkar ¹²⁶, A. Cordeiro Oudot Choi ¹²⁷, F. Cormier ¹⁶⁴, L.D. Corpe ⁴⁰, M. Corradi ^{75a,75b}, F. Corriveau ^{104,ab}, A. Cortes-Gonzalez ¹⁸, M.J. Costa ¹⁶³, F. Costanza ⁴, D. Costanzo ¹³⁹, B.M. Cote ¹¹⁹, G. Cowan ⁹⁵, K. Cranmer ¹⁷⁰, D. Cremonini ^{23b,23a}, S. Crépe-Renaudin ⁶⁰, F. Crescioli ¹²⁷, M. Cristinziani ¹⁴¹, M. Cristoforetti ^{78a,78b}, V. Croft ¹¹⁴, J.E. Crosby ¹²¹, G. Crosetti ^{43b,43a}, A. Cueto ⁹⁹, T. Cuhadar Donszelmann ¹⁶⁰, H. Cui ^{14a,14e}, Z. Cui ⁷, W.R. Cunningham ⁵⁹, F. Curcio ^{43b,43a}, P. Czodrowski ³⁶, M.M. Czurylo ^{63b}, M.J. Da Cunha Sargedas De Sousa ^{62a}, J.V. Da Fonseca Pinto ^{83b}, C. Da Via ¹⁰¹, W. Dabrowski ^{86a}, T. Dado ⁴⁹, S. Dahbi ^{33g}, T. Dai ¹⁰⁶, C. Dallapiccola ¹⁰³, M. Dam ⁴², G. D'amen ²⁹, V. D'Amico ¹⁰⁹, J. Damp ¹⁰⁰, J.R. Dandoy ¹²⁸, M.F. Daneri ³⁰, M. Danninger ¹⁴², V. Dao ³⁶, G. Darbo ^{57b}, S. Darmora ⁶, S.J. Das ^{29,am}, S. D'Auria ^{71a,71b}, C. David ^{156b}, T. Davidek ¹³³, B. Davis-Purcell ³⁴, I. Dawson ⁹⁴, H.A. Day-hall ¹³², K. De ⁸, R. De Asmundis ^{72a}, N. De Biase ⁴⁸, S. De Castro ^{23b,23a}, N. De Groot ¹¹³, P. de Jong ¹¹⁴, H. De la Torre ¹⁰⁷, A. De Maria ^{14c}, A. De Salvo ^{75a}, U. De Sanctis ^{76a,76b}, A. De Santo ¹⁴⁶, J.B. De Vivie De Regie ⁶⁰, D.V. Dedovich ³⁸, J. Degens ¹¹⁴, A.M. Deiana ⁴⁴, F. Del Corso ^{23b,23a}, J. Del Peso ⁹⁹, F. Del Rio ^{63a}, F. Deliot ¹³⁵, C.M. Delitzsch ⁴⁹, M. Della Pietra ^{72a,72b}, D. Della Volpe ⁵⁶, A. Dell'Acqua ³⁶, L. Dell'Asta ^{71a,71b}, M. Delmastro ⁴, P.A. Delsart ⁶⁰, S. Demers ¹⁷², M. Demichev ³⁸, S.P. Denisov ³⁷, L. D'Eramo ⁴⁰, D. Derendarz ⁸⁷, F. Derue ¹²⁷, P. Dervan ⁹², K. Desch ²⁴, C. Deutsch ²⁴, F.A. Di Bello ^{57b,57a}, A. Di Ciaccio ^{76a,76b}, L. Di Ciaccio ⁴, A. Di Domenico ^{75a,75b}, C. Di Donato ^{72a,72b}, A. Di Girolamo ³⁶, G. Di Gregorio ⁵, A. Di Luca ^{78a,78b}, B. Di Micco ^{77a,77b}, R. Di Nardo ^{77a,77b}, C. Diaconu ¹⁰², F.A. Dias ¹¹⁴, T. Dias Do Vale ¹⁴², M.A. Diaz ^{137a,137b}, F.G. Diaz Capriles ²⁴, M. Didenko ¹⁶³, E.B. Diehl ¹⁰⁶, L. Diehl ⁵⁴, S. Díez Cornell ⁴⁸, C. Diez Pardos ¹⁴¹, C. Dimitriadi ^{24,161}, A. Dimitrievska ^{17a}, J. Dingfelder ²⁴, I-M. Dinu ^{27b}, S.J. Dittmeier ^{63b}, F. Dittus ³⁶, F. Djama ¹⁰², T. Djobava ^{149b}, J.I. Djuvsland ¹⁶, C. Doglioni ^{101,98}, J. Dolejsi ¹³³, Z. Dolezal ¹³³, M. Donadelli ^{83c}, B. Dong ¹⁰⁷, J. Donini ⁴⁰, A. D'Onofrio ^{77a,77b}, M. D'Onofrio ⁹², J. Dopke ¹³⁴, A. Doria ^{72a}, N. Dos Santos Fernandes ^{130a}, M.T. Dova ⁹⁰, A.T. Doyle ⁵⁹, M.A. Draguet ¹²⁶, E. Dreyer ¹⁶⁹, I. Drivas-koulouris ¹⁰, A.S. Drobac ¹⁵⁸, M. Drozdova ⁵⁶, D. Du ^{62a}, T.A. du Pree ¹¹⁴, F. Dubinin ³⁷, M. Dubovsky ^{28a}, E. Duchovni ¹⁶⁹, G. Duckeck ¹⁰⁹, O.A. Ducu ^{27b}, D. Duda ⁵², A. Dudarev ³⁶, E.R. Duden ²⁶, M. D'uffizi ¹⁰¹, L. Duflot ⁶⁶, M. Dührssen ³⁶, C. Dülken ¹⁷¹, A.E. Dumitriu ^{27b}, M. Dunford ^{63a}, S. Dungs ⁴⁹, K. Dunne ^{47a,47b}, A. Duperrin ¹⁰², H. Duran Yildiz ^{3a}, M. Düren ⁵⁸, A. Durglishvili ^{149b}, B.L. Dwyer ¹¹⁵, G.I. Dyckes ^{17a}, M. Dyndal ^{86a}, S. Dysch ¹⁰¹, B.S. Dziedzic ⁸⁷, Z.O. Earnshaw ¹⁴⁶, G.H. Eberwein ¹²⁶, B. Eckerova ^{28a}, S. Eggebrecht ⁵⁵, M.G. Eggleston ⁵¹, E. Egidio Purcino De Souza ¹²⁷, L.F. Ehrke ⁵⁶, G. Eigen ¹⁶, K. Einsweiler ^{17a}, T. Ekelof ¹⁶¹, P.A. Ekman ⁹⁸, S. El Farkh ^{35b}, Y. El Ghazali ^{35b}, H. El Jarrari ^{35e,148}, A. El Moussaouy ^{35a}, V. Ellajosyula ¹⁶¹, M. Ellert ¹⁶¹, F. Ellinghaus ¹⁷¹, A.A. Elliot ⁹⁴, N. Ellis ³⁶, J. Elmsheuser ²⁹, M. Elsing ³⁶, D. Emelianov ¹³⁴, Y. Enari ¹⁵³, I. Ene ^{17a}, S. Epari ¹³, J. Erdmann ⁴⁹,

P.A. Erland ⁸⁷, M. Errenst ¹⁷¹, M. Escalier ⁶⁶, C. Escobar ¹⁶³, E. Etzion ¹⁵¹, G. Evans ^{130a}, H. Evans ⁶⁸, L.S. Evans ⁹⁵, M.O. Evans ¹⁴⁶, A. Ezhilov ³⁷, S. Ezzarqtouni ^{35a}, F. Fabbri ⁵⁹, L. Fabbri ^{23b,23a}, G. Facini ⁹⁶, V. Fadeyev ¹³⁶, R.M. Fakhruddinov ³⁷, S. Falciano ^{75a}, L.F. Falda Ulhoa Coelho ³⁶, P.J. Falke ²⁴, J. Faltova ¹³³, C. Fan ¹⁶², Y. Fan ^{14a}, Y. Fang ^{14a,14e}, M. Fanti ^{71a,71b}, M. Faraj ^{69a,69b}, Z. Farazpay ⁹⁷, A. Farbin ⁸, A. Farilla ^{77a}, T. Farooque ¹⁰⁷, S.M. Farrington ⁵², F. Fassi ^{35e}, D. Fassouliotis ⁹, M. Faucci Giannelli ^{76a,76b}, W.J. Fawcett ³², L. Fayard ⁶⁶, P. Federic ¹³³, P. Federicova ¹³¹, O.L. Fedin ^{37,a}, G. Fedotov ³⁷, M. Feickert ¹⁷⁰, L. Feligioni ¹⁰², D.E. Fellers ¹²³, C. Feng ^{62b}, M. Feng ^{14b}, Z. Feng ¹¹⁴, M.J. Fenton ¹⁶⁰, A.B. Fenyuk ³⁷, L. Ferencz ⁴⁸, R.A.M. Ferguson ⁹¹, S.I. Fernandez Luengo ^{137f}, M.J.V. Fernoux ¹⁰², J. Ferrando ⁴⁸, A. Ferrari ¹⁶¹, P. Ferrari ^{114,113}, R. Ferrari ^{73a}, D. Ferrere ⁵⁶, C. Ferretti ¹⁰⁶, F. Fiedler ¹⁰⁰, A. Filipčič ⁹³, E.K. Filmer ¹, F. Filthaut ¹¹³, M.C.N. Fiolhais ^{130a,130c,d}, L. Fiorini ¹⁶³, W.C. Fisher ¹⁰⁷, T. Fitschen ¹⁰¹, P.M. Fitzhugh ¹³⁵, I. Fleck ¹⁴¹, P. Fleischmann ¹⁰⁶, T. Flick ¹⁷¹, L. Flores ¹²⁸, M. Flores ^{33d,ah}, L.R. Flores Castillo ^{64a}, L. Flores Sanz De Acedo ³⁶, F.M. Follega ^{78a,78b}, N. Fomin ¹⁶, J.H. Foo ¹⁵⁵, B.C. Forland ⁶⁸, A. Formica ¹³⁵, A.C. Forti ¹⁰¹, E. Fortin ³⁶, A.W. Fortman ⁶¹, M.G. Foti ^{17a}, L. Fountas ^{9,k}, D. Fournier ⁶⁶, H. Fox ⁹¹, P. Francavilla ^{74a,74b}, S. Francescato ⁶¹, S. Franchellucci ⁵⁶, M. Franchini ^{23b,23a}, S. Franchino ^{63a}, D. Francis ³⁶, L. Franco ¹¹³, L. Franconi ⁴⁸, M. Franklin ⁶¹, G. Frattari ²⁶, A.C. Freegard ⁹⁴, W.S. Freund ^{83b}, Y.Y. Frid ¹⁵¹, N. Fritzsche ⁵⁰, A. Froch ⁵⁴, D. Froidevaux ³⁶, J.A. Frost ¹²⁶, Y. Fu ^{62a}, M. Fujimoto ¹¹⁸, E. Fullana Torregrosa ^{163,*}, K.Y. Fung ^{64a}, E. Furtado De Simas Filho ^{83b}, M. Furukawa ¹⁵³, J. Fuster ¹⁶³, A. Gabrielli ^{23b,23a}, A. Gabrielli ¹⁵⁵, P. Gadow ⁴⁸, G. Gagliardi ^{57b,57a}, L.G. Gagnon ^{17a}, E.J. Gallas ¹²⁶, B.J. Gallop ¹³⁴, K.K. Gan ¹¹⁹, S. Ganguly ¹⁵³, J. Gao ^{62a}, Y. Gao ⁵², F.M. Garay Walls ^{137a,137b}, B. Garcia ^{29,am}, C. García ¹⁶³, A. Garcia Alonso ¹¹⁴, A.G. Garcia Caffaro ¹⁷², J.E. García Navarro ¹⁶³, M. Garcia-Sciveres ^{17a}, G.L. Gardner ¹²⁸, R.W. Gardner ³⁹, N. Garelli ¹⁵⁸, D. Garg ⁸⁰, R.B. Garg ^{143,r}, J.M. Gargan ⁵², C.A. Garner ¹⁵⁵, S.J. Gasiorowski ¹³⁸, P. Gaspar ^{83b}, G. Gaudio ^{73a}, V. Gautam ¹³, P. Gauzzi ^{75a,75b}, I.L. Gavrilenko ³⁷, A. Gavrilyuk ³⁷, C. Gay ¹⁶⁴, G. Gaycken ⁴⁸, E.N. Gazis ¹⁰, A.A. Geanta ^{27b}, C.M. Gee ¹³⁶, C. Gemme ^{57b}, M.H. Genest ⁶⁰, S. Gentile ^{75a,75b}, S. George ⁹⁵, W.F. George ²⁰, T. Geralis ⁴⁶, P. Gessinger-Befurt ³⁶, M.E. Geyik ¹⁷¹, M. Ghneimat ¹⁴¹, K. Ghorbanian ⁹⁴, A. Ghosal ¹⁴¹, A. Ghosh ¹⁶⁰, A. Ghosh ⁷, B. Giacobbe ^{23b}, S. Giagu ^{75a,75b}, P. Giannetti ^{74a}, A. Giannini ^{62a}, S.M. Gibson ⁹⁵, M. Gignac ¹³⁶, D.T. Gil ^{86b}, A.K. Gilbert ^{86a}, B.J. Gilbert ⁴¹, D. Gillberg ³⁴, G. Gilles ¹¹⁴, N.E.K. Gillwald ⁴⁸, L. Ginabat ¹²⁷, D.M. Gingrich ^{2,ak}, M.P. Giordani ^{69a,69c}, P.F. Giraud ¹³⁵, G. Giugliarelli ^{69a,69c}, D. Giugni ^{71a}, F. Giuli ³⁶, I. Gkialas ^{9,k}, L.K. Gladilin ³⁷, C. Glasman ⁹⁹, G.R. Gledhill ¹²³, M. Glisic ¹²³, I. Gnesi ^{43b,g}, Y. Go ^{29,am}, M. Goblirsch-Kolb ³⁶, B. Gocke ⁴⁹, D. Godin ¹⁰⁸, B. Gokturk ^{21a}, S. Goldfarb ¹⁰⁵, T. Golling ⁵⁶, M.G.D. Gololo ^{33g}, D. Golubkov ³⁷, J.P. Gombas ¹⁰⁷, A. Gomes ^{130a,130b}, G. Gomes Da Silva ¹⁴¹, A.J. Gomez Delegido ¹⁶³, R. Gonçalo ^{130a,130c}, G. Gonella ¹²³, L. Gonella ²⁰, A. Gongadze ³⁸, F. Gonnella ²⁰, J.L. Gonski ⁴¹, R.Y. González Andana ⁵², S. González de la Hoz ¹⁶³, S. Gonzalez Fernandez ¹³, R. Gonzalez Lopez ⁹², C. Gonzalez Renteria ^{17a}, R. Gonzalez Suarez ¹⁶¹, S. Gonzalez-Sevilla ⁵⁶, G.R. Gonzalvo Rodriguez ¹⁶³, L. Goossens ³⁶, P.A. Gorbounov ³⁷, B. Gorini ³⁶, E. Gorini ^{70a,70b}, A. Gorišek ⁹³, T.C. Gosart ¹²⁸, A.T. Goshaw ⁵¹, M.I. Gostkin ³⁸, S. Goswami ¹²¹, C.A. Gottardo ³⁶, M. Gouighri ^{35b}, V. Goumarre ⁴⁸, A.G. Goussiou ¹³⁸, N. Govender ^{33c}, I. Grabowska-Bold ^{86a}, K. Graham ³⁴, E. Gramstad ¹²⁵, S. Grancagnolo ^{70a,70b}, M. Grandi ¹⁴⁶, P.M. Gravila ^{27f}, F.G. Gravili ^{70a,70b}, H.M. Gray ^{17a}, M. Greco ^{70a,70b}, C. Grefe ²⁴, I.M. Gregor ⁴⁸, P. Grenier ¹⁴³, C. Grieco ¹³, A.A. Grillo ¹³⁶, K. Grimm ³¹, S. Grinstein ^{13,x}, J.-F. Grivaz ⁶⁶, E. Gross ¹⁶⁹, J. Grosse-Knetter ⁵⁵, C. Grud ¹⁰⁶, J.C. Grundy ¹²⁶, L. Guan ¹⁰⁶, W. Guan ²⁹, C. Gubbels ¹⁶⁴,

J.G.R. Guerrero Rojas ¹⁶³, G. Guerrieri ^{69a,69b}, F. Guescini ¹¹⁰, R. Gugel ¹⁰⁰, J.A.M. Guhit ¹⁰⁶, A. Guida ¹⁸, T. Guillemin ⁴, E. Guilloton ^{167,134}, S. Guindon ³⁶, F. Guo ^{14a,14e}, J. Guo ^{62c}, L. Guo ⁴⁸, Y. Guo ¹⁰⁶, R. Gupta ⁴⁸, S. Gurbuz ²⁴, S.S. Gurdasani ⁵⁴, G. Gustavino ³⁶, M. Guth ⁵⁶, P. Gutierrez ¹²⁰, L.F. Gutierrez Zagazeta ¹²⁸, C. Gutschow ⁹⁶, C. Gwenlan ¹²⁶, C.B. Gwilliam ⁹², E.S. Haaland ¹²⁵, A. Haas ¹¹⁷, M. Habedank ⁴⁸, C. Haber ^{17a}, H.K. Hadavand ⁸, A. Hadeef ¹⁰⁰, S. Hadzic ¹¹⁰, J.J. Hahn ¹⁴¹, E.H. Haines ⁹⁶, M. Haleem ¹⁶⁶, J. Haley ¹²¹, J.J. Hall ¹³⁹, G.D. Hallewell ¹⁰², L. Halser ¹⁹, K. Hamano ¹⁶⁵, H. Hamdaoui ^{35e}, M. Hamer ²⁴, G.N. Hamity ⁵², E.J. Hampshire ⁹⁵, J. Han ^{62b}, K. Han ^{62a}, L. Han ^{14c}, L. Han ^{62a}, S. Han ^{17a}, Y.F. Han ¹⁵⁵, K. Hanagaki ⁸⁴, M. Hance ¹³⁶, D.A. Hangal ^{41,ag}, H. Hanif ¹⁴², M.D. Hank ¹²⁸, R. Hankache ¹⁰¹, J.B. Hansen ⁴², J.D. Hansen ⁴², P.H. Hansen ⁴², K. Hara ¹⁵⁷, D. Harada ⁵⁶, T. Harenberg ¹⁷¹, S. Harkusha ³⁷, M.L. Harris ¹⁰³, Y.T. Harris ¹²⁶, J. Harrison ¹³, N.M. Harrison ¹¹⁹, P.F. Harrison ¹⁶⁷, N.M. Hartman ¹¹⁰, N.M. Hartmann ¹⁰⁹, Y. Hasegawa ¹⁴⁰, A. Hasib ⁵², S. Haug ¹⁹, R. Hauser ¹⁰⁷, C.M. Hawkes ²⁰, R.J. Hawkins ³⁶, Y. Hayashi ¹⁵³, S. Hayashida ¹¹¹, D. Hayden ¹⁰⁷, C. Hayes ¹⁰⁶, R.L. Hayes ¹¹⁴, C.P. Hays ¹²⁶, J.M. Hays ⁹⁴, H.S. Hayward ⁹², F. He ^{62a}, M. He ^{14a,14e}, Y. He ¹⁵⁴, Y. He ¹²⁷, N.B. Heatley ⁹⁴, V. Hedberg ⁹⁸, A.L. Heggelund ¹²⁵, N.D. Hehir ⁹⁴, C. Heidegger ⁵⁴, K.K. Heidegger ⁵⁴, W.D. Heidorn ⁸¹, J. Heilman ³⁴, S. Heim ⁴⁸, T. Heim ^{17a}, J.G. Heinlein ¹²⁸, J.J. Heinrich ¹²³, L. Heinrich ^{110,ai}, J. Hejbal ¹³¹, L. Helary ⁴⁸, A. Held ¹⁷⁰, S. Hellesund ¹⁶, C.M. Helling ¹⁶⁴, S. Hellman ^{47a,47b}, C. Helsen ³⁶, R.C.W. Henderson ⁹¹, L. Henkelmann ³², A.M. Henriques Correia ³⁶, H. Herde ⁹⁸, Y. Hernández Jiménez ¹⁴⁵, L.M. Herrmann ²⁴, T. Herrmann ⁵⁰, G. Herten ⁵⁴, R. Hertenberger ¹⁰⁹, L. Hervas ³⁶, M.E. Hespings ¹⁰⁰, N.P. Hessey ^{156a}, H. Hibi ⁸⁵, S.J. Hillier ²⁰, J.R. Hinds ¹⁰⁷, F. Hinterkeuser ²⁴, M. Hirose ¹²⁴, S. Hirose ¹⁵⁷, D. Hirschbuehl ¹⁷¹, T.G. Hitchings ¹⁰¹, B. Hiti ⁹³, J. Hobbs ¹⁴⁵, R. Hobincu ^{27e}, N. Hod ¹⁶⁹, M.C. Hodgkinson ¹³⁹, B.H. Hodgkinson ³², A. Hoecker ³⁶, J. Hofer ⁴⁸, T. Holm ²⁴, M. Holzbock ¹¹⁰, L.B.A.H. Hommels ³², B.P. Honan ¹⁰¹, J. Hong ^{62c}, T.M. Hong ¹²⁹, B.H. Hooberman ¹⁶², W.H. Hopkins ⁶, Y. Horii ¹¹¹, S. Hou ¹⁴⁸, A.S. Howard ⁹³, J. Howarth ⁵⁹, J. Hoya ⁶, M. Hrabovsky ¹²², A. Hrynevich ⁴⁸, T. Hryn'ova ⁴, P.J. Hsu ⁶⁵, S.-C. Hsu ¹³⁸, Q. Hu ⁴¹, Y.F. Hu ^{14a,14e}, S. Huang ^{64b}, X. Huang ^{14c}, Y. Huang ^{62a}, Y. Huang ^{14a}, Z. Huang ¹⁰¹, Z. Hubacek ¹³², M. Huebner ²⁴, F. Huegging ²⁴, T.B. Huffman ¹²⁶, C.A. Hugli ⁴⁸, M. Huhtinen ³⁶, S.K. Huiberts ¹⁶, R. Hulsken ¹⁰⁴, N. Huseynov ^{12,a}, J. Huston ¹⁰⁷, J. Huth ⁶¹, R. Hyneman ¹⁴³, G. Iacobucci ⁵⁶, G. Iakovidis ²⁹, I. Ibragimov ¹⁴¹, L. Iconomidou-Fayard ⁶⁶, P. Iengo ^{72a,72b}, R. Iguchi ¹⁵³, T. Iizawa ⁸⁴, Y. Ikegami ⁸⁴, N. Ilic ¹⁵⁵, H. Imam ^{35a}, M. Ince Lezki ⁵⁶, T. Ingebretsen Carlson ^{47a,47b}, G. Introzzi ^{73a,73b}, M. Iodice ^{77a}, V. Ippolito ^{75a,75b}, R.K. Irwin ⁹², M. Ishino ¹⁵³, W. Islam ¹⁷⁰, C. Issever ^{18,48}, S. Istin ^{21a,ao}, H. Ito ¹⁶⁸, J.M. Iturbe Ponce ^{64a}, R. Iuppa ^{78a,78b}, A. Ivina ¹⁶⁹, J.M. Izen ⁴⁵, V. Izzo ^{72a}, P. Jacka ^{131,132}, P. Jackson ¹, R.M. Jacobs ⁴⁸, B.P. Jaeger ¹⁴², C.S. Jagfeld ¹⁰⁹, P. Jain ⁵⁴, G. Jäkel ¹⁷¹, K. Jakobs ⁵⁴, T. Jakoubek ¹⁶⁹, J. Jamieson ⁵⁹, K.W. Janas ^{86a}, A.E. Jaspán ⁹², M. Javurkova ¹⁰³, F. Jeanneau ¹³⁵, L. Jeanty ¹²³, J. Jejelava ^{149a,ae}, P. Jenni ^{54,h}, C.E. Jessiman ³⁴, S. Jézéquel ⁴, C. Jia ^{62b}, J. Jia ¹⁴⁵, X. Jia ⁶¹, X. Jia ^{14a,14e}, Z. Jia ^{14c}, Y. Jiang ^{62a}, S. Jiggins ⁴⁸, J. Jimenez Pena ¹³, S. Jin ^{14c}, A. Jinaru ^{27b}, O. Jinnouchi ¹⁵⁴, P. Johansson ¹³⁹, K.A. Johns ⁷, J.W. Johnson ¹³⁶, D.M. Jones ³², E. Jones ⁴⁸, P. Jones ³², R.W.L. Jones ⁹¹, T.J. Jones ⁹², R. Joshi ¹¹⁹, J. Jovicevic ¹⁵, X. Ju ^{17a}, J.J. Junggeburth ³⁶, T. Junkermann ^{63a}, A. Juste Rozas ^{13,x}, M.K. Juzek ⁸⁷, S. Kabana ^{137e}, A. Kaczmarzka ⁸⁷, M. Kado ¹¹⁰, H. Kagan ¹¹⁹, M. Kagan ¹⁴³, A. Kahn ⁴¹, A. Kahn ¹²⁸, C. Kahra ¹⁰⁰, T. Kaji ¹⁶⁸, E. Kajomovitz ¹⁵⁰, N. Kakati ¹⁶⁹, I. Kalaitzidou ⁵⁴, C.W. Kalderon ²⁹, A. Kamenshchikov ¹⁵⁵, S. Kanayama ¹⁵⁴, N.J. Kang ¹³⁶, D. Kar ^{33g}, K. Karava ¹²⁶, M.J. Kareem ^{156b}, E. Karentzos ⁵⁴, I. Karknias ¹⁵², O. Karkout ¹¹⁴, S.N. Karpov ³⁸, Z.M. Karpova ³⁸, V. Kartvelishvili ⁹¹,

A.N. Karyukhin ³⁷, E. Kasimi ¹⁵², J. Katzy ⁴⁸, S. Kaur ³⁴, K. Kawade ¹⁴⁰, T. Kawamoto ¹³⁵,
 E.F. Kay ³⁶, F.I. Kaya ¹⁵⁸, S. Kazakos ¹⁰⁷, V.F. Kazanin ³⁷, Y. Ke ¹⁴⁵, J.M. Keaveney ^{33a},
 R. Keeler ¹⁶⁵, G.V. Kehris ⁶¹, J.S. Keller ³⁴, A.S. Kelly ⁹⁶, J.J. Kempster ¹⁴⁶, K.E. Kennedy ⁴¹,
 P.D. Kennedy ¹⁰⁰, O. Kepka ¹³¹, B.P. Kerridge ¹⁶⁷, S. Kersten ¹⁷¹, B.P. Kerševan ⁹³,
 S. Keshri ⁶⁶, L. Keszezhova ^{28a}, S. Ketabchi Haghghat ¹⁵⁵, M. Khandoga ¹²⁷, A. Khanov ¹²¹,
 A.G. Kharlamov ³⁷, T. Kharlamova ³⁷, E.E. Khoda ¹³⁸, T.J. Khoo ¹⁸, G. Khorauli ¹⁶⁶,
 J. Khubua ^{149b}, Y.A.R. Khwaira ⁶⁶, M. Kiehn ³⁶, A. Kilgallon ¹²³, D.W. Kim ^{47a,47b},
 Y.K. Kim ³⁹, N. Kimura ⁹⁶, A. Kirchhoff ⁵⁵, C. Kirfel ²⁴, F. Kirfel ²⁴, J. Kirk ¹³⁴,
 A.E. Kiryunin ¹¹⁰, C. Kitsaki ¹⁰, O. Kivernyk ²⁴, M. Klassen ^{63a}, C. Klein ³⁴, L. Klein ¹⁶⁶,
 M.H. Klein ¹⁰⁶, M. Klein ⁹², S.B. Klein ⁵⁶, U. Klein ⁹², P. Klimek ³⁶, A. Klimentov ²⁹,
 T. Klioutchnikova ³⁶, P. Kluit ¹¹⁴, S. Kluth ¹¹⁰, E. Kneringer ⁷⁹, T.M. Knight ¹⁵⁵, A. Knue ⁵⁴,
 R. Kobayashi ⁸⁸, S.F. Koch ¹²⁶, M. Kocian ¹⁴³, P. Kodyš ¹³³, D.M. Koeck ¹²³, P.T. Koenig ²⁴,
 T. Koffas ³⁴, M. Kolb ¹³⁵, I. Koletsou ⁴, T. Komarek ¹²², K. Köneke ⁵⁴, A.X.Y. Kong ¹,
 T. Kono ¹¹⁸, N. Konstantinidis ⁹⁶, B. Konya ⁹⁸, R. Kopeliansky ⁶⁸, S. Koperny ^{86a}, K. Korcyl ⁸⁷,
 K. Kordas ^{152,f}, G. Koren ¹⁵¹, A. Korn ⁹⁶, S. Korn ⁵⁵, I. Korolkov ¹³, N. Korotkova ³⁷,
 B. Kortman ¹¹⁴, O. Kortner ¹¹⁰, S. Kortner ¹¹⁰, W.H. Kostecka ¹¹⁵, V.V. Kostyukhin ¹⁴¹,
 A. Kotsokechagia ¹³⁵, A. Kotwal ⁵¹, A. Koulouris ³⁶, A. Kourkoumeli-Charalampidi ^{73a,73b},
 C. Kourkoumelis ⁹, E. Kourlitis ⁶, O. Kovanda ¹⁴⁶, R. Kowalewski ¹⁶⁵, W. Kozanecki ¹³⁵,
 A.S. Kozhin ³⁷, V.A. Kramarenko ³⁷, G. Kramberger ⁹³, P. Kramer ¹⁰⁰, M.W. Krasny ¹²⁷,
 A. Krasznahorkay ³⁶, J.W. Kraus ¹⁷¹, J.A. Kremer ¹⁰⁰, T. Kresse ⁵⁰, J. Kretschmar ⁹²,
 K. Kreul ¹⁸, P. Krieger ¹⁵⁵, S. Krishnamurthy ¹⁰³, M. Krivos ¹³³, K. Krizka ²⁰,
 K. Kroeninger ⁴⁹, H. Kroha ¹¹⁰, J. Kroll ¹³¹, J. Kroll ¹²⁸, K.S. Krowpman ¹⁰⁷, U. Kruchonak ³⁸,
 H. Krüger ²⁴, N. Krumnack ⁸¹, M.C. Kruse ⁵¹, J.A. Krzysiak ⁸⁷, O. Kuchinskaia ³⁷, S. Kuday ^{3a},
 S. Kuehn ³⁶, R. Kuesters ⁵⁴, T. Kuhl ⁴⁸, V. Kukhtin ³⁸, Y. Kulchitsky ^{37,a}, S. Kuleshov ^{137d,137b},
 M. Kumar ^{33g}, N. Kumari ¹⁰², A. Kupco ¹³¹, T. Kupfer ⁴⁹, A. Kupich ³⁷, O. Kuprash ⁵⁴,
 H. Kurashige ⁸⁵, L.L. Kurchaninov ^{156a}, O. Kurdysh ⁶⁶, Y.A. Kurochkin ³⁷, A. Kurova ³⁷,
 M. Kuze ¹⁵⁴, A.K. Kvam ¹⁰³, J. Kvita ¹²², T. Kwan ¹⁰⁴, N.G. Kyriacou ¹⁰⁶, L.A.O. Laatu ¹⁰²,
 C. Lacasta ¹⁶³, F. Lacava ^{75a,75b}, H. Lacker ¹⁸, D. Lacour ¹²⁷, N.N. Lad ⁹⁶, E. Ladygin ³⁸,
 B. Laforge ¹²⁷, T. Lagouri ^{137e}, S. Lai ⁵⁵, I.K. Lakomic ^{86a}, N. Lalloue ⁶⁰, J.E. Lambert ^{165,m},
 S. Lammers ⁶⁸, W. Lampl ⁷, C. Lampoudis ^{152,f}, A.N. Lancaster ¹¹⁵, E. Lançon ²⁹,
 U. Landgraf ⁵⁴, M.P.J. Landon ⁹⁴, V.S. Lang ⁵⁴, R.J. Langenberg ¹⁰³, O.K.B. Langrekken ¹²⁵,
 A.J. Lankford ¹⁶⁰, F. Lanni ³⁶, K. Lantzsch ²⁴, A. Lanza ^{73a}, A. Lapertosa ^{57b,57a},
 J.F. Laporte ¹³⁵, T. Lari ^{71a}, F. Lasagni Manghi ^{23b}, M. Lassnig ³⁶, V. Latonova ¹³¹,
 A. Laudrain ¹⁰⁰, A. Laurier ¹⁵⁰, S.D. Lawlor ⁹⁵, Z. Lawrence ¹⁰¹, M. Lazzaroni ^{71a,71b}, B. Le ¹⁰¹,
 E.M. Le Boulicaut ⁵¹, B. Leban ⁹³, A. Lebedev ⁸¹, M. LeBlanc ³⁶, F. Ledroit-Guillon ⁶⁰,
 A.C.A. Lee ⁹⁶, S.C. Lee ¹⁴⁸, S. Lee ^{47a,47b}, T.F. Lee ⁹², L.L. Leeuw ^{33c}, H.P. Lefebvre ⁹⁵,
 M. Lefebvre ¹⁶⁵, C. Leggett ^{17a}, G. Lehmann Miotto ³⁶, M. Leigh ⁵⁶, W.A. Leight ¹⁰³,
 W. Leinonen ¹¹³, A. Leisos ^{152,w}, M.A.L. Leite ^{83c}, C.E. Leitgeb ⁴⁸, R. Leitner ¹³³,
 K.J.C. Leney ⁴⁴, T. Lenz ²⁴, S. Leone ^{74a}, C. Leonidopoulos ⁵², A. Leopold ¹⁴⁴, C. Leroy ¹⁰⁸,
 R. Les ¹⁰⁷, C.G. Lester ³², M. Levchenko ³⁷, J. Levêque ⁴, D. Levin ¹⁰⁶, L.J. Levinson ¹⁶⁹,
 M.P. Lewicki ⁸⁷, D.J. Lewis ⁴, A. Li ⁵, B. Li ^{62b}, C. Li ^{62a}, C-Q. Li ^{62c}, H. Li ^{62a}, H. Li ^{62b},
 H. Li ^{14c}, H. Li ^{62b}, K. Li ¹³⁸, L. Li ^{62c}, M. Li ^{14a,14e}, Q.Y. Li ^{62a}, S. Li ^{14a,14e}, S. Li ^{62d,62c,e},
 T. Li ^{5,c}, X. Li ¹⁰⁴, Z. Li ¹²⁶, Z. Li ¹⁰⁴, Z. Li ⁹², Z. Li ^{14a,14e}, Z. Liang ^{14a}, M. Liberatore ⁴⁸,
 B. Liberti ^{76a}, K. Lie ^{64c}, J. Lieber Marin ^{83b}, H. Lien ⁶⁸, K. Lin ¹⁰⁷, R.E. Lindley ⁷,
 J.H. Lindon ², A. Lins ⁴⁸, E. Lipeles ¹²⁸, A. Lipniacka ¹⁶, A. Lister ¹⁶⁴, J.D. Little ⁴,
 B. Liu ^{14a}, B.X. Liu ¹⁴², D. Liu ^{62d,62c}, J.B. Liu ^{62a}, J.K.K. Liu ³², K. Liu ^{62d,62c}, M. Liu ^{62a},
 M.Y. Liu ^{62a}, P. Liu ^{14a}, Q. Liu ^{62d,138,62c}, X. Liu ^{62a}, Y. Liu ^{14d,14e}, Y.L. Liu ¹⁰⁶, Y.W. Liu ^{62a},

J. Llorente Merino ¹⁴², S.L. Lloyd ⁹⁴, E.M. Lobodzinska ⁴⁸, P. Loch ⁷, S. Loffredo ^{76a,76b},
 T. Lohse ¹⁸, K. Lohwasser ¹³⁹, E. Loiacono ⁴⁸, M. Lokajicek ^{131,*}, J.D. Lomas ²⁰,
 J.D. Long ¹⁶², I. Longarini ¹⁶⁰, L. Longo ^{70a,70b}, R. Longo ¹⁶², I. Lopez Paz ⁶⁷,
 A. Lopez Solis ⁴⁸, J. Lorenz ¹⁰⁹, N. Lorenzo Martinez ⁴, A.M. Lory ¹⁰⁹, O. Loseva ³⁷,
 X. Lou ^{47a,47b}, X. Lou ^{14a,14e}, A. Lounis ⁶⁶, J. Love ⁶, P.A. Love ⁹¹, G. Lu ^{14a,14e}, M. Lu ⁸⁰,
 S. Lu ¹²⁸, Y.J. Lu ⁶⁵, H.J. Lubatti ¹³⁸, C. Luci ^{75a,75b}, F.L. Lucio Alves ^{14c}, A. Lucotte ⁶⁰,
 F. Luehring ⁶⁸, I. Luise ¹⁴⁵, O. Lukianchuk ⁶⁶, O. Lundberg ¹⁴⁴, B. Lund-Jensen ¹⁴⁴,
 N.A. Luongo ¹²³, M.S. Lutz ¹⁵¹, D. Lynn ²⁹, H. Lyons ⁹², R. Lysak ¹³¹, E. Lytken ⁹⁸,
 V. Lyubushkin ³⁸, T. Lyubushkina ³⁸, M.M. Lyukova ¹⁴⁵, H. Ma ²⁹, K. Ma ^{62a}, L.L. Ma ^{62b},
 Y. Ma ¹²¹, D.M. Mac Donell ¹⁶⁵, G. Maccarrone ⁵³, J.C. MacDonald ¹⁰⁰, R. Madar ⁴⁰,
 W.F. Mader ⁵⁰, J. Maeda ⁸⁵, T. Maeno ²⁹, M. Maerker ⁵⁰, H. Maguire ¹³⁹, V. Maiboroda ¹³⁵,
 A. Maio ^{130a,130b,130d}, K. Maj ^{86a}, O. Majersky ⁴⁸, S. Majewski ¹²³, N. Makovec ⁶⁶,
 V. Maksimovic ¹⁵, B. Malaescu ¹²⁷, Pa. Malecki ⁸⁷, V.P. Maleev ³⁷, F. Malek ⁶⁰, M. Mali ⁹³,
 D. Malito ^{95,q}, U. Mallik ⁸⁰, S. Maltezos ¹⁰, S. Malyukov ³⁸, J. Mamuzic ¹³, G. Mancini ⁵³,
 G. Manco ^{73a,73b}, J.P. Mandalia ⁹⁴, I. Mandić ⁹³, L. Manhaes de Andrade Filho ^{83a},
 I.M. Maniatis ¹⁶⁹, J. Manjarres Ramos ^{102,af}, D.C. Mankad ¹⁶⁹, A. Mann ¹⁰⁹, B. Mansoulie ¹³⁵,
 S. Manzoni ³⁶, A. Marantis ^{152,w}, G. Marchiori ⁵, M. Marcisovsky ¹³¹, C. Marcon ^{71a,71b},
 M. Marinescu ²⁰, M. Marjanovic ¹²⁰, E.J. Marshall ⁹¹, Z. Marshall ^{17a}, S. Marti-Garcia ¹⁶³,
 T.A. Martin ¹⁶⁷, V.J. Martin ⁵², B. Martin dit Latour ¹⁶, L. Martinelli ^{75a,75b}, M. Martinez ^{13,x},
 P. Martinez Agullo ¹⁶³, V.I. Martinez Outschoorn ¹⁰³, P. Martinez Suarez ¹³, S. Martin-Haugh ¹³⁴,
 V.S. Martoiu ^{27b}, A.C. Martyniuk ⁹⁶, A. Marzin ³⁶, D. Mascione ^{78a,78b}, L. Masetti ¹⁰⁰,
 T. Mashimo ¹⁵³, J. Masik ¹⁰¹, A.L. Maslennikov ³⁷, L. Massa ^{23b}, P. Massarotti ^{72a,72b},
 P. Mastrandrea ^{74a,74b}, A. Mastroberardino ^{43b,43a}, T. Masubuchi ¹⁵³, T. Mathisen ¹⁶¹,
 J. Matousek ¹³³, N. Matsuzawa ¹⁵³, J. Maurer ^{27b}, B. Maček ⁹³, D.A. Maximov ³⁷, R. Mazini ¹⁴⁸,
 I. Maznas ¹⁵², M. Mazza ¹⁰⁷, S.M. Mazza ¹³⁶, E. Mazzeo ^{71a,71b}, C. Mc Ginn ²⁹,
 J.P. Mc Gowan ¹⁰⁴, S.P. Mc Kee ¹⁰⁶, E.F. McDonald ¹⁰⁵, A.E. McDougall ¹¹⁴, J.A. Mcfayden ¹⁴⁶,
 R.P. McGovern ¹²⁸, G. Mchedlidze ^{149b}, R.P. Mckenzie ^{33g}, T.C. McLachlan ⁴⁸,
 D.J. McLaughlin ⁹⁶, K.D. McLean ¹⁶⁵, S.J. McMahon ¹³⁴, P.C. McNamara ¹⁰⁵,
 C.M. Mcpartland ⁹², R.A. McPherson ^{165,ab}, S. Mehlhase ¹⁰⁹, A. Mehta ⁹², D. Melini ¹⁵⁰,
 B.R. Mellado Garcia ^{33g}, A.H. Melo ⁵⁵, F. Meloni ⁴⁸, A.M. Mendes Jacques Da Costa ¹⁰¹,
 H.Y. Meng ¹⁵⁵, L. Meng ⁹¹, S. Menke ¹¹⁰, M. Mentink ³⁶, E. Meoni ^{43b,43a}, C. Merlassino ¹²⁶,
 L. Merola ^{72a,72b}, C. Meroni ^{71a,71b}, G. Merz ¹⁰⁶, O. Meshkov ³⁷, J. Metcalfe ⁶, A.S. Mete ⁶,
 C. Meyer ⁶⁸, J-P. Meyer ¹³⁵, R.P. Middleton ¹³⁴, L. Mijović ⁵², G. Mikenberg ¹⁶⁹,
 M. Mikestikova ¹³¹, M. Mikuž ⁹³, H. Mildner ¹⁰⁰, A. Milic ³⁶, C.D. Milke ⁴⁴, D.W. Miller ³⁹,
 L.S. Miller ³⁴, A. Milov ¹⁶⁹, D.A. Milstead ^{47a,47b}, T. Min ^{14c}, A.A. Minaenko ³⁷,
 I.A. Minashvili ^{149b}, L. Mince ⁵⁹, A.I. Mincer ¹¹⁷, B. Mindur ^{86a}, M. Mineev ³⁸, Y. Mino ⁸⁸,
 L.M. Mir ¹³, M. Miralles Lopez ¹⁶³, M. Mironova ^{17a}, A. Mishima ¹⁵³, M.C. Missio ¹¹³,
 T. Mitani ¹⁶⁸, A. Mitra ¹⁶⁷, V.A. Mitsou ¹⁶³, O. Miu ¹⁵⁵, P.S. Miyagawa ⁹⁴, Y. Miyazaki ⁸⁹,
 A. Mizukami ⁸⁴, T. Mkrtchyan ^{63a}, M. Mlinarevic ⁹⁶, T. Mlinarevic ⁹⁶, M. Mlynarikova ³⁶,
 S. Mobius ¹⁹, K. Mochizuki ¹⁰⁸, P. Moder ⁴⁸, P. Mogg ¹⁰⁹, A.F. Mohammed ^{14a,14e},
 S. Mohapatra ⁴¹, G. Mokgatitwane ^{33g}, L. Moleri ¹⁶⁹, B. Mondal ¹⁴¹, S. Mondal ¹³²,
 G. Monig ¹⁴⁶, K. Mönig ⁴⁸, E. Monnier ¹⁰², L. Monsonis Romero ¹⁶³, J. Montejo Berlingen ^{13,84},
 M. Montella ¹¹⁹, F. Montekali ^{77a,77b}, F. Monticelli ⁹⁰, S. Monzani ^{69a,69c}, N. Morange ⁶⁶,
 A.L. Moreira De Carvalho ^{130a}, M. Moreno Llácer ¹⁶³, C. Moreno Martinez ⁵⁶, P. Morettini ^{57b},
 S. Morgenstern ³⁶, M. Morii ⁶¹, M. Morinaga ¹⁵³, A.K. Morley ³⁶, F. Morodei ^{75a,75b},
 L. Morvaj ³⁶, P. Moschovakos ³⁶, B. Moser ³⁶, M. Mosidze ^{149b}, T. Moskalets ⁵⁴,
 P. Moskvitina ¹¹³, J. Moss ^{31,o}, E.J.W. Moyse ¹⁰³, O. Mtintsilana ^{33g}, S. Muanza ¹⁰²,

J. Mueller ¹²⁹, D. Muenstermann ⁹¹, R. Müller ¹⁹, G.A. Mullier ¹⁶¹, A.J. Mullin³², J.J. Mullin¹²⁸, D.P. Mungo ¹⁵⁵, D. Munoz Perez ¹⁶³, F.J. Munoz Sanchez ¹⁰¹, M. Murin ¹⁰¹, W.J. Murray ^{167,134}, A. Murrone ^{71a,71b}, J.M. Muse ¹²⁰, M. Muškinja ^{17a}, C. Mwewa ²⁹, A.G. Myagkov ^{37,a}, A.J. Myers ⁸, A.A. Myers¹²⁹, G. Myers ⁶⁸, M. Myska ¹³², B.P. Nachman ^{17a}, O. Nackenhorst ⁴⁹, A. Nag ⁵⁰, K. Nagai ¹²⁶, K. Nagano ⁸⁴, J.L. Nagle ^{29,am}, E. Nagy ¹⁰², A.M. Nairz ³⁶, Y. Nakahama ⁸⁴, K. Nakamura ⁸⁴, K. Nakkalil ⁵, H. Nanjo ¹²⁴, R. Narayan ⁴⁴, E.A. Narayanan ¹¹², I. Naryshkin ³⁷, M. Naseri ³⁴, S. Nasri ¹⁵⁹, C. Nass ²⁴, G. Navarro ^{22a}, J. Navarro-Gonzalez ¹⁶³, R. Nayak ¹⁵¹, A. Nayaz ¹⁸, P.Y. Nechaeva ³⁷, F. Nechansky ⁴⁸, L. Nedic ¹²⁶, T.J. Neep ²⁰, A. Negri ^{73a,73b}, M. Negrini ^{23b}, C. Nellist ¹¹⁴, C. Nelson ¹⁰⁴, K. Nelson ¹⁰⁶, S. Nemecek ¹³¹, M. Nessi ^{36,i}, M.S. Neubauer ¹⁶², F. Neuhaus ¹⁰⁰, J. Neundorf ⁴⁸, R. Newhouse ¹⁶⁴, P.R. Newman ²⁰, C.W. Ng ¹²⁹, Y.W.Y. Ng ⁴⁸, B. Ngair ^{35e}, H.D.N. Nguyen ¹⁰⁸, R.B. Nickerson ¹²⁶, R. Nicolaidou ¹³⁵, J. Nielsen ¹³⁶, M. Niemeyer ⁵⁵, J. Niermann ^{55,36}, N. Nikiforou ³⁶, V. Nikolaenko ^{37,a}, I. Nikolic-Audit ¹²⁷, K. Nikolopoulos ²⁰, P. Nilsson ²⁹, I. Ninca ⁴⁸, H.R. Nindhito ⁵⁶, G. Ninio ¹⁵¹, A. Nisati ^{75a}, N. Nishu ², R. Nisius ¹¹⁰, J-E. Nitschke ⁵⁰, E.K. Nkadimeng ^{33g}, S.J. Noacco Rosende ⁹⁰, T. Nobe ¹⁵³, D.L. Noel ³², T. Nommensen ¹⁴⁷, M.B. Norfolk ¹³⁹, R.R.B. Norisam ⁹⁶, B.J. Norman ³⁴, J. Novak ⁹³, T. Novak ⁴⁸, L. Novotny ¹³², R. Novotny ¹¹², L. Nozka ¹²², K. Ntekas ¹⁶⁰, N.M.J. Nunes De Moura Junior ^{83b}, E. Nurse⁹⁶, J. Ocariz ¹²⁷, A. Ochi ⁸⁵, I. Ochoa ^{130a}, S. Oerdeek ¹⁶¹, J.T. Offermann ³⁹, A. Ogrodnik ¹³³, A. Oh ¹⁰¹, C.C. Ohm ¹⁴⁴, H. Oide ⁸⁴, R. Oishi ¹⁵³, M.L. Ojeda ⁴⁸, Y. Okazaki ⁸⁸, M.W. O'Keefe⁹², Y. Okumura ¹⁵³, L.F. Oleiro Seabra ^{130a}, S.A. Olivares Pino ^{137d}, D. Oliveira Damazio ²⁹, D. Oliveira Goncalves ^{83a}, J.L. Oliver ¹⁶⁰, A. Olszewski ⁸⁷, Ö.O. Öncel ⁵⁴, D.C. O'Neil ¹⁴², A.P. O'Neill ¹⁹, A. Onofre ^{130a,130e}, P.U.E. Onyisi ¹¹, M.J. Oreglia ³⁹, G.E. Orellana ⁹⁰, D. Orestano ^{77a,77b}, N. Orlando ¹³, R.S. Orr ¹⁵⁵, V. O'Shea ⁵⁹, L.M. Osojnak ¹²⁸, R. Ospanov ^{62a}, G. Otero y Garzon ³⁰, H. Otono ⁸⁹, P.S. Ott ^{63a}, G.J. Ottino ^{17a}, M. Ouchrif ^{35d}, J. Ouellette ²⁹, F. Ould-Saada ¹²⁵, M. Owen ⁵⁹, R.E. Owen ¹³⁴, K.Y. Oyulmaz ^{21a}, V.E. Ozcan ^{21a}, N. Ozturk ⁸, S. Ozturk ⁸², H.A. Pacey ³², A. Pacheco Pages ¹³, C. Padilla Aranda ¹³, G. Padovano ^{75a,75b}, S. Pagan Griso ^{17a}, G. Palacino ⁶⁸, A. Palazzo ^{70a,70b}, S. Palestini ³⁶, J. Pan ¹⁷², T. Pan ^{64a}, D.K. Panchal ¹¹, C.E. Pandini ¹¹⁴, J.G. Panduro Vazquez ⁹⁵, H. Pang ^{14b}, P. Pani ⁴⁸, G. Panizzo ^{69a,69c}, L. Paolozzi ⁵⁶, C. Papadatos ¹⁰⁸, S. Parajuli ⁴⁴, A. Paramonov ⁶, C. Paraskevopoulos ¹⁰, D. Paredes Hernandez ^{64b}, T.H. Park ¹⁵⁵, M.A. Parker ³², F. Parodi ^{57b,57a}, E.W. Parrish ¹¹⁵, V.A. Parrish ⁵², J.A. Parsons ⁴¹, U. Parzefall ⁵⁴, B. Pascual Dias ¹⁰⁸, L. Pascual Dominguez ¹⁵¹, F. Pasquali ¹¹⁴, E. Pasqualucci ^{75a}, S. Passaggio ^{57b}, F. Pastore ⁹⁵, P. Pasuwan ^{47a,47b}, P. Patel ⁸⁷, U.M. Patel ⁵¹, J.R. Pater ¹⁰¹, T. Pauly ³⁶, J. Pearkes ¹⁴³, M. Pedersen ¹²⁵, R. Pedro ^{130a}, S.V. Peleganchuk ³⁷, O. Penc ³⁶, E.A. Pender ⁵², H. Peng ^{62a}, K.E. Pensi ¹⁰⁹, M. Penzin ³⁷, B.S. Peralva ^{83d}, A.P. Pereira Peixoto ⁶⁰, L. Pereira Sanchez ^{47a,47b}, D.V. Perepelitsa ^{29,am}, E. Perez Codina ^{156a}, M. Perganti ¹⁰, L. Perini ^{71a,71b,*}, H. Pernegger ³⁶, A. Perrevoort ¹¹³, O. Perrin ⁴⁰, K. Peters ⁴⁸, R.F.Y. Peters ¹⁰¹, B.A. Petersen ³⁶, T.C. Petersen ⁴², E. Petit ¹⁰², V. Petousis ¹³², C. Petridou ^{152,f}, A. Petrukhin ¹⁴¹, M. Pettee ^{17a}, N.E. Pettersson ³⁶, A. Petukhov ³⁷, K. Petukhova ¹³³, A. Peyaud ¹³⁵, R. Pezoa ^{137f}, L. Pezzotti ³⁶, G. Pezzullo ¹⁷², T.M. Pham ¹⁷⁰, T. Pham ¹⁰⁵, P.W. Phillips ¹³⁴, G. Piacquadio ¹⁴⁵, E. Pianori ^{17a}, F. Piazza ^{71a,71b}, R. Piegai ³⁰, D. Pietreanu ^{27b}, A.D. Pilkington ¹⁰¹, M. Pinamonti ^{69a,69c}, J.L. Pinfeld ², B.C. Pinheiro Pereira ^{130a}, A.E. Pinto Pinoargote ¹³⁵, K.M. Piper ¹⁴⁶, A. Pirttikoski ⁵⁶, C. Pitman Donaldson⁹⁶, D.A. Pizzi ³⁴, L. Pizzimento ^{76a,76b}, A. Pizzini ¹¹⁴, M.-A. Pleier ²⁹, V. Plesanovs⁵⁴, V. Pleskot ¹³³, E. Plotnikova³⁸, G. Poddar ⁴, R. Poettgen ⁹⁸, L. Poggioli ¹²⁷, I. Pokharel ⁵⁵, S. Polacek ¹³³, G. Polesello ^{73a}, A. Poley ^{142,156a}, R. Polifka ¹³², A. Polini ^{23b}, C.S. Pollard ¹⁶⁷, Z.B. Pollock ¹¹⁹, V. Polychronakos ²⁹,

E. Pompa Pacchi [id75a,75b](#), D. Ponomarenko [id113](#), L. Pontecorvo [id36](#), S. Popa [id27a](#), G.A. Popeneciu [id27d](#),
 A. Poreba [id36](#), D.M. Portillo Quintero [id156a](#), S. Pospisil [id132](#), M.A. Postill [id139](#), P. Postolache [id27c](#),
 K. Potamianos [id167](#), P.A. Potepa [id86a](#), I.N. Potrap [id38](#), C.J. Potter [id32](#), H. Potti [id1](#), T. Poulsen [id48](#),
 J. Poveda [id163](#), M.E. Pozo Astigarraga [id36](#), A. Prades Ibanez [id163](#), J. Pretel [id54](#), D. Price [id101](#),
 M. Primavera [id70a](#), M.A. Principe Martin [id99](#), R. Privara [id122](#), T. Procter [id59](#), M.L. Proffitt [id138](#),
 N. Proklova [id128](#), K. Prokofiev [id64c](#), G. Proto [id110](#), S. Protopopescu [id29](#), J. Proudfoot [id6](#),
 M. Przybycien [id86a](#), W.W. Przygoda [id86b](#), J.E. Puddefoot [id139](#), D. Pudzha [id37](#), D. Pyatiizbyantseva [id37](#),
 J. Qian [id106](#), D. Qichen [id101](#), Y. Qin [id101](#), T. Qiu [id52](#), A. Quadt [id55](#), M. Queitsch-Maitland [id101](#),
 G. Quetant [id56](#), G. Rabanal Bolanos [id61](#), D. Rafanoharana [id54](#), F. Ragusa [id71a,71b](#), J.L. Rainbolt [id39](#),
 J.A. Raine [id56](#), S. Rajagopalan [id29](#), E. Ramakoti [id37](#), K. Ran [id48,14e](#), N.P. Rapheeha [id33g](#),
 H. Rasheed [id27b](#), V. Raskina [id127](#), D.F. Rassloff [id63a](#), S. Rave [id100](#), B. Ravina [id55](#), I. Ravinovich [id169](#),
 M. Raymond [id36](#), A.L. Read [id125](#), N.P. Readioff [id139](#), D.M. Rebutzi [id73a,73b](#), G. Redlinger [id29](#),
 A.S. Reed [id110](#), K. Reeves [id26](#), J.A. Reidelsturz [id171,v](#), D. Reikher [id151](#), A. Rej [id141](#), C. Rembser [id36](#),
 A. Renardi [id48](#), M. Renda [id27b](#), M.B. Rendel [id110](#), F. Renner [id48](#), A.G. Rennie [id59](#), S. Resconi [id71a](#),
 M. Ressegotti [id57b,57a](#), S. Rettie [id36](#), J.G. Reyes Rivera [id107](#), B. Reynolds [id119](#), E. Reynolds [id17a](#),
 O.L. Rezanova [id37](#), P. Reznicek [id133](#), N. Ribaric [id91](#), E. Ricci [id78a,78b](#), R. Richter [id110](#),
 S. Richter [id47a,47b](#), E. Richter-Was [id86b](#), M. Ridel [id127](#), S. Ridouani [id35d](#), P. Rieck [id117](#), P. Riedler [id36](#),
 M. Rijssenbeek [id145](#), A. Rimoldi [id73a,73b](#), M. Rimoldi [id48](#), L. Rinaldi [id23b,23a](#), T.T. Rinn [id29](#),
 M.P. Rinnagel [id109](#), G. Ripellino [id161](#), I. Riu [id13](#), P. Rivadeneira [id48](#), J.C. Rivera Vergara [id165](#),
 F. Rizatdinova [id121](#), E. Rizvi [id94](#), B.A. Roberts [id167](#), B.R. Roberts [id17a](#), S.H. Robertson [id104,ab](#),
 M. Robin [id48](#), D. Robinson [id32](#), C.M. Robles Gajardo [id137f](#), M. Robles Manzano [id100](#), A. Robson [id59](#),
 A. Rocchi [id76a,76b](#), C. Roda [id74a,74b](#), S. Rodriguez Bosca [id63a](#), Y. Rodriguez Garcia [id22a](#),
 A. Rodriguez Rodriguez [id54](#), A.M. Rodríguez Vera [id156b](#), S. Roe [id36](#), J.T. Roemer [id160](#),
 A.R. Roepe-Gier [id136](#), J. Roggel [id171](#), O. Røhne [id125](#), R.A. Rojas [id103](#), C.P.A. Roland [id68](#), J. Roloff [id29](#),
 A. Romaniouk [id37](#), E. Romano [id73a,73b](#), M. Romano [id23b](#), A.C. Romero Hernandez [id162](#),
 N. Rompotis [id92](#), L. Roos [id127](#), S. Rosati [id75a](#), B.J. Rosser [id39](#), E. Rossi [id126](#), E. Rossi [id72a,72b](#),
 L.P. Rossi [id57b](#), L. Rossini [id48](#), R. Rosten [id119](#), M. Rotaru [id27b](#), B. Rottler [id54](#), C. Rougier [id102,af](#),
 D. Rousseau [id66](#), D. Rousso [id32](#), A. Roy [id162](#), S. Roy-Garand [id155](#), A. Rozanov [id102](#), Y. Rozen [id150](#),
 X. Ruan [id33g](#), A. Rubio Jimenez [id163](#), A.J. Ruby [id92](#), V.H. Ruelas Rivera [id18](#), T.A. Ruggeri [id1](#),
 A. Ruggiero [id126](#), A. Ruiz-Martinez [id163](#), A. Rummler [id36](#), Z. Rurikova [id54](#), N.A. Rusakovich [id38](#),
 H.L. Russell [id165](#), G. Russo [id75a,75b](#), J.P. Rutherford [id7](#), S. Rutherford Colmenares [id32](#), K. Rybacki [id91](#),
 M. Rybar [id133](#), E.B. Rye [id125](#), A. Ryzhov [id44](#), J.A. Sabater Iglesias [id56](#), P. Sabatini [id163](#),
 L. Sabetta [id75a,75b](#), H.F-W. Sadrozinski [id136](#), F. Safai Tehrani [id75a](#), B. Safarzadeh Samani [id146](#),
 M. Safdari [id143](#), S. Saha [id165](#), M. Sahinsoy [id110](#), M. Saimpert [id135](#), M. Saito [id153](#), T. Saito [id153](#),
 D. Salamani [id36](#), A. Salnikov [id143](#), J. Salt [id163](#), A. Salvador Salas [id13](#), D. Salvatore [id43b,43a](#),
 F. Salvatore [id146](#), A. Salzburger [id36](#), D. Sammel [id54](#), D. Sampsonidis [id152,f](#), D. Sampsonidou [id123](#),
 J. Sánchez [id163](#), A. Sanchez Pineda [id4](#), V. Sanchez Sebastian [id163](#), H. Sandaker [id125](#), C.O. Sander [id48](#),
 J.A. Sandesara [id103](#), M. Sandhoff [id171](#), C. Sandoval [id22b](#), D.P.C. Sankey [id134](#), T. Sano [id88](#),
 A. Sansoni [id53](#), L. Santi [id75a,75b](#), C. Santoni [id40](#), H. Santos [id130a,130b](#), S.N. Santpur [id17a](#), A. Santra [id169](#),
 K.A. Saoucha [id139](#), J.G. Saraiva [id130a,130d](#), J. Sardain [id7](#), O. Sasaki [id84](#), K. Sato [id157](#), C. Sauer [id63b](#),
 F. Sauerburger [id54](#), E. Sauvan [id4](#), P. Savard [id155,ak](#), R. Sawada [id153](#), C. Sawyer [id134](#), L. Sawyer [id97](#),
 I. Sayago Galvan [id163](#), C. Sbarra [id23b](#), A. Sbrizzi [id23b,23a](#), T. Scanlon [id96](#), J. Schaarschmidt [id138](#),
 P. Schacht [id110](#), D. Schaefer [id39](#), U. Schäfer [id100](#), A.C. Schaffer [id66,44](#), D. Schaile [id109](#),
 R.D. Schamberger [id145](#), C. Scharf [id18](#), M.M. Schefer [id19](#), V.A. Schegelsky [id37](#), D. Scheirich [id133](#),
 F. Schenck [id18](#), M. Schernau [id160](#), C. Scheulen [id55](#), C. Schiavi [id57b,57a](#), E.J. Schioppa [id70a,70b](#),
 M. Schioppa [id43b,43a](#), B. Schlag [id143,r](#), K.E. Schleicher [id54](#), S. Schlenker [id36](#), J. Schmeing [id171](#),
 M.A. Schmidt [id171](#), K. Schmieden [id100](#), C. Schmitt [id100](#), S. Schmitt [id48](#), L. Schoeffel [id135](#),

A. Schoening [id](#)^{63b}, P.G. Scholer [id](#)⁵⁴, E. Schopf [id](#)¹²⁶, M. Schott [id](#)¹⁰⁰, J. Schovancova [id](#)³⁶,
 S. Schramm [id](#)⁵⁶, F. Schroeder [id](#)¹⁷¹, T. Schroer [id](#)⁵⁶, H-C. Schultz-Coulon [id](#)^{63a}, M. Schumacher [id](#)⁵⁴,
 B.A. Schumm [id](#)¹³⁶, Ph. Schune [id](#)¹³⁵, A.J. Schuy [id](#)¹³⁸, H.R. Schwartz [id](#)¹³⁶, A. Schwartzman [id](#)¹⁴³,
 T.A. Schwarz [id](#)¹⁰⁶, Ph. Schwemling [id](#)¹³⁵, R. Schwienhorst [id](#)¹⁰⁷, A. Sciandra [id](#)¹³⁶, G. Sciolla [id](#)²⁶,
 F. Scuri [id](#)^{74a}, C.D. Sebastiani [id](#)⁹², K. Sedlaczek [id](#)¹¹⁵, P. Seema [id](#)¹⁸, S.C. Seidel [id](#)¹¹², A. Seiden [id](#)¹³⁶,
 B.D. Seidlitz [id](#)⁴¹, C. Seitz [id](#)⁴⁸, J.M. Seixas [id](#)^{83b}, G. Sekhniadze [id](#)^{72a}, S.J. Sekula [id](#)⁴⁴, L. Selem [id](#)⁶⁰,
 N. Semprini-Cesari [id](#)^{23b,23a}, D. Sengupta [id](#)⁵⁶, V. Senthilkumar [id](#)¹⁶³, L. Serin [id](#)⁶⁶, L. Serkin [id](#)^{69a,69b},
 M. Sessa [id](#)^{76a,76b}, H. Severini [id](#)¹²⁰, F. Sforza [id](#)^{57b,57a}, A. Sfyrla [id](#)⁵⁶, E. Shabalina [id](#)⁵⁵, R. Shaheen [id](#)¹⁴⁴,
 J.D. Shahinian [id](#)¹²⁸, D. Shaked Renous [id](#)¹⁶⁹, L.Y. Shan [id](#)^{14a}, M. Shapiro [id](#)^{17a}, A. Sharma [id](#)³⁶,
 A.S. Sharma [id](#)¹⁶⁴, P. Sharma [id](#)⁸⁰, S. Sharma [id](#)⁴⁸, P.B. Shatalov [id](#)³⁷, K. Shaw [id](#)¹⁴⁶, S.M. Shaw [id](#)¹⁰¹,
 A. Shcherbakova [id](#)³⁷, Q. Shen [id](#)^{62c,5}, P. Sherwood [id](#)⁹⁶, L. Shi [id](#)⁹⁶, X. Shi [id](#)^{14a}, C.O. Shimmin [id](#)¹⁷²,
 Y. Shimogama [id](#)¹⁶⁸, J.D. Shinner [id](#)⁹⁵, I.P.J. Shipsey [id](#)¹²⁶, S. Shirabe [id](#)^{56,i}, M. Shiyakova [id](#)^{38,z},
 J. Shlomi [id](#)¹⁶⁹, M.J. Shochet [id](#)³⁹, J. Shojaii [id](#)¹⁰⁵, D.R. Shope [id](#)¹²⁵, B. Shrestha [id](#)¹²⁰, S. Shrestha [id](#)^{119,an},
 E.M. Shrif [id](#)^{33g}, M.J. Shroff [id](#)¹⁶⁵, P. Sicho [id](#)¹³¹, A.M. Sickles [id](#)¹⁶², E. Sideras Haddad [id](#)^{33g},
 A. Sidoti [id](#)^{23b}, F. Siegert [id](#)⁵⁰, Dj. Sijacki [id](#)¹⁵, R. Sikora [id](#)^{86a}, F. Sili [id](#)⁹⁰, J.M. Silva [id](#)²⁰,
 M.V. Silva Oliveira [id](#)²⁹, S.B. Silverstein [id](#)^{47a}, S. Simion [id](#)⁶⁶, R. Simoniello [id](#)³⁶, E.L. Simpson [id](#)⁵⁹,
 H. Simpson [id](#)¹⁴⁶, L.R. Simpson [id](#)¹⁰⁶, N.D. Simpson [id](#)⁹⁸, S. Simsek [id](#)⁸², S. Sindhu [id](#)⁵⁵, P. Sinervo [id](#)¹⁵⁵,
 S. Singh [id](#)¹⁵⁵, S. Sinha [id](#)⁴⁸, S. Sinha [id](#)¹⁰¹, M. Sioli [id](#)^{23b,23a}, I. Siral [id](#)³⁶, E. Sitnikova [id](#)⁴⁸,
 S.Yu. Sivoklokov [id](#)^{37,*}, J. Sjölin [id](#)^{47a,47b}, A. Skaf [id](#)⁵⁵, E. Skorda [id](#)⁹⁸, P. Skubic [id](#)¹²⁰, M. Slawinska [id](#)⁸⁷,
 V. Smakhtin [id](#)¹⁶⁹, B.H. Smart [id](#)¹³⁴, J. Smiesko [id](#)³⁶, S.Yu. Smirnov [id](#)³⁷, Y. Smirnov [id](#)³⁷,
 L.N. Smirnova [id](#)^{37,a}, O. Smirnova [id](#)⁹⁸, A.C. Smith [id](#)⁴¹, E.A. Smith [id](#)³⁹, H.A. Smith [id](#)¹²⁶,
 J.L. Smith [id](#)⁹², R. Smith [id](#)¹⁴³, M. Smizanska [id](#)⁹¹, K. Smolek [id](#)¹³², A.A. Snesarev [id](#)³⁷, S.R. Snider [id](#)¹⁵⁵,
 H.L. Snoek [id](#)¹¹⁴, S. Snyder [id](#)²⁹, R. Sobie [id](#)^{165,ab}, A. Soffer [id](#)¹⁵¹, C.A. Solans Sanchez [id](#)³⁶,
 E.Yu. Soldatov [id](#)³⁷, U. Soldevila [id](#)¹⁶³, A.A. Solodkov [id](#)³⁷, S. Solomon [id](#)²⁶, A. Soloshenko [id](#)³⁸,
 K. Solovieva [id](#)⁵⁴, O.V. Solovyanov [id](#)⁴⁰, V. Solovyev [id](#)³⁷, P. Sommer [id](#)³⁶, A. Sonay [id](#)¹³,
 W.Y. Song [id](#)^{156b}, J.M. Sonneveld [id](#)¹¹⁴, A. Sopczak [id](#)¹³², A.L. Soppio [id](#)⁹⁶, F. Sopkova [id](#)^{28b},
 V. Sothilingam [id](#)^{63a}, S. Sottocornola [id](#)⁶⁸, R. Soualah [id](#)^{116b}, Z. Soumami [id](#)^{35e}, D. South [id](#)⁴⁸,
 S. Spagnolo [id](#)^{70a,70b}, M. Spalla [id](#)¹¹⁰, D. Sperlich [id](#)⁵⁴, G. Spigo [id](#)³⁶, M. Spina [id](#)¹⁴⁶, S. Spinali [id](#)⁹¹,
 D.P. Spiteri [id](#)⁵⁹, M. Spousta [id](#)¹³³, E.J. Staats [id](#)³⁴, A. Stabile [id](#)^{71a,71b}, R. Stamen [id](#)^{63a},
 M. Stamenkovic [id](#)¹¹⁴, A. Stampekis [id](#)²⁰, M. Standke [id](#)²⁴, E. Stanecka [id](#)⁸⁷, M.V. Stange [id](#)⁵⁰,
 B. Stanislaus [id](#)^{17a}, M.M. Stanitzki [id](#)⁴⁸, B. Stapf [id](#)⁴⁸, E.A. Starchenko [id](#)³⁷, G.H. Stark [id](#)¹³⁶,
 J. Stark [id](#)^{102,af}, D.M. Starko [id](#)^{156b}, P. Staroba [id](#)¹³¹, P. Starovoitov [id](#)^{63a}, S. Stärz [id](#)¹⁰⁴, R. Staszewski [id](#)⁸⁷,
 G. Stavropoulos [id](#)⁴⁶, J. Steentoft [id](#)¹⁶¹, P. Steinberg [id](#)²⁹, B. Stelzer [id](#)^{142,156a}, H.J. Stelzer [id](#)¹²⁹,
 O. Stelzer-Chilton [id](#)^{156a}, H. Stenzel [id](#)⁵⁸, T.J. Stevenson [id](#)¹⁴⁶, G.A. Stewart [id](#)³⁶, J.R. Stewart [id](#)¹²¹,
 M.C. Stockton [id](#)³⁶, G. Stoicea [id](#)^{27b}, M. Stolarski [id](#)^{130a}, S. Stonjek [id](#)¹¹⁰, A. Straessner [id](#)⁵⁰,
 J. Strandberg [id](#)¹⁴⁴, S. Strandberg [id](#)^{47a,47b}, M. Strauss [id](#)¹²⁰, T. Strebler [id](#)¹⁰², P. Strizenec [id](#)^{28b},
 R. Ströhmer [id](#)¹⁶⁶, D.M. Strom [id](#)¹²³, L.R. Strom [id](#)⁴⁸, R. Stroynowski [id](#)⁴⁴, A. Strubig [id](#)^{47a,47b},
 S.A. Stucci [id](#)²⁹, B. Stugu [id](#)¹⁶, J. Stupak [id](#)¹²⁰, N.A. Styles [id](#)⁴⁸, D. Su [id](#)¹⁴³, S. Su [id](#)^{62a}, W. Su [id](#)^{62d},
 X. Su [id](#)^{62a,66}, K. Sugizaki [id](#)¹⁵³, V.V. Sulin [id](#)³⁷, M.J. Sullivan [id](#)⁹², D.M.S. Sultan [id](#)^{78a,78b},
 L. Sultanliyeva [id](#)³⁷, S. Sultansoy [id](#)^{3b}, T. Sumida [id](#)⁸⁸, S. Sun [id](#)¹⁰⁶, S. Sun [id](#)¹⁷⁰,
 O. Sunneborn Gudnadottir [id](#)¹⁶¹, N. Sur [id](#)¹⁰², M.R. Sutton [id](#)¹⁴⁶, H. Suzuki [id](#)¹⁵⁷, M. Svatos [id](#)¹³¹,
 M. Swiatlowski [id](#)^{156a}, T. Swirski [id](#)¹⁶⁶, I. Sykora [id](#)^{28a}, M. Sykora [id](#)¹³³, T. Sykora [id](#)¹³³, D. Ta [id](#)¹⁰⁰,
 K. Tackmann [id](#)^{48,y}, A. Taffard [id](#)¹⁶⁰, R. Tafirout [id](#)^{156a}, J.S. Tafoya Vargas [id](#)⁶⁶, E.P. Takeva [id](#)⁵²,
 Y. Takubo [id](#)⁸⁴, M. Talby [id](#)¹⁰², A.A. Talyshev [id](#)³⁷, K.C. Tam [id](#)^{64b}, N.M. Tamir [id](#)¹⁵¹, A. Tanaka [id](#)¹⁵³,
 J. Tanaka [id](#)¹⁵³, R. Tanaka [id](#)⁶⁶, M. Tanasini [id](#)^{57b,57a}, Z. Tao [id](#)¹⁶⁴, S. Tapia Araya [id](#)^{137f},
 S. Tapprogge [id](#)¹⁰⁰, A. Tarek Abouelfadl Mohamed [id](#)¹⁰⁷, S. Tarem [id](#)¹⁵⁰, K. Tariq [id](#)^{14a}, G. Tarna [id](#)^{102,27b},
 G.F. Tartarelli [id](#)^{71a}, P. Tas [id](#)¹³³, M. Tasevsky [id](#)¹³¹, E. Tassi [id](#)^{43b,43a}, A.C. Tate [id](#)¹⁶², G. Tateno [id](#)¹⁵³,

Y. Tayalati ^{35e,aa}, G.N. Taylor ¹⁰⁵, W. Taylor ^{156b}, H. Teagle ⁹², A.S. Tee ¹⁷⁰,
 R. Teixeira De Lima ¹⁴³, P. Teixeira-Dias ⁹⁵, J.J. Teoh ¹⁵⁵, K. Terashi ¹⁵³, J. Terron ⁹⁹,
 S. Terzo ¹³, M. Testa ⁵³, R.J. Teuscher ^{155,ab}, A. Thaler ⁷⁹, O. Theiner ⁵⁶, N. Themistokleous ⁵²,
 T. Thevenaux-Pelzer ¹⁰², O. Thielmann ¹⁷¹, D.W. Thomas ⁹⁵, J.P. Thomas ²⁰, E.A. Thompson ^{17a},
 P.D. Thompson ²⁰, E. Thomson ¹²⁸, Y. Tian ⁵⁵, V. Tikhomirov ^{37,a}, Yu.A. Tikhonov ³⁷,
 S. Timoshenko ³⁷, D. Timoshyn ¹³³, E.X.L. Ting ¹, P. Tipton ¹⁷², S.H. Tlou ^{33g}, A. Tnourji ⁴⁰,
 K. Todome ^{23b,23a}, S. Todorova-Nova ¹³³, S. Todt ⁵⁰, M. Togawa ⁸⁴, J. Tojo ⁸⁹, S. Tokár ^{28a},
 K. Tokushuku ⁸⁴, O. Toldaiev ⁶⁸, R. Tombs ³², M. Tomoto ^{84,111}, L. Tompkins ^{143,r},
 K.W. Topolnicki ^{86b}, E. Torrence ¹²³, H. Torres ^{102,af}, E. Torró Pastor ¹⁶³, M. Toscani ³⁰,
 C. Tosciri ³⁹, M. Tost ¹¹, D.R. Tovey ¹³⁹, A. Traeet ¹⁶, I.S. Trandafir ^{27b}, T. Trefzger ¹⁶⁶,
 A. Tricoli ²⁹, I.M. Trigger ^{156a}, S. Trincaz-Duvoid ¹²⁷, D.A. Trischuk ²⁶, B. Trocmé ⁶⁰,
 C. Troncon ^{71a}, L. Truong ^{33c}, M. Trzebinski ⁸⁷, A. Trzupek ⁸⁷, F. Tsai ¹⁴⁵, M. Tsai ¹⁰⁶,
 A. Tsiamis ^{152,f}, P.V. Tsiarehka ³⁷, S. Tsigaridas ^{156a}, A. Tsigotis ^{152,w}, V. Tsiskaridze ¹⁵⁵,
 E.G. Tskhadadze ^{149a}, M. Tsopoulou ^{152,f}, Y. Tsujikawa ⁸⁸, I.I. Tsukerman ³⁷, V. Tsulaia ^{17a},
 S. Tsuno ⁸⁴, O. Tsur ¹⁵⁰, K. Tsurii ¹¹⁸, D. Tsybychev ¹⁴⁵, Y. Tu ^{64b}, A. Tudorache ^{27b},
 V. Tudorache ^{27b}, A.N. Tuna ³⁶, S. Turchikhin ³⁸, I. Turk Cakir ^{3a}, R. Turra ^{71a},
 T. Turtuvshin ^{38,ac}, P.M. Tuts ⁴¹, S. Tzamaras ^{152,f}, P. Tzanis ¹⁰, E. Tzovara ¹⁰⁰, K. Uchida ¹⁵³,
 F. Ukegawa ¹⁵⁷, P.A. Ulloa Poblete ^{137c,137b}, E.N. Umaka ²⁹, G. Unal ³⁶, M. Unal ¹¹,
 A. Undrus ²⁹, G. Unel ¹⁶⁰, J. Urban ^{28b}, P. Urquijo ¹⁰⁵, G. Usai ⁸, R. Ushioda ¹⁵⁴,
 M. Usman ¹⁰⁸, Z. Uysal ^{21b}, L. Vacavant ¹⁰², V. Vacek ¹³², B. Vachon ¹⁰⁴, K.O.H. Vadla ¹²⁵,
 T. Vafeiadis ³⁶, A. Vaitkus ⁹⁶, C. Valderanis ¹⁰⁹, E. Valdes Santurio ^{47a,47b}, M. Valente ^{156a},
 S. Valentinetti ^{23b,23a}, A. Valero ¹⁶³, E. Valiente Moreno ¹⁶³, A. Vallier ^{102,af},
 J.A. Valls Ferrer ¹⁶³, D.R. Van Arneman ¹¹⁴, T.R. Van Daalen ¹³⁸, A. Van Der Graaf ⁴⁹,
 P. Van Gemmeren ⁶, M. Van Rijnbach ^{125,36}, S. Van Stroud ⁹⁶, I. Van Vulpen ¹¹⁴,
 M. Vanadia ^{76a,76b}, W. Vandelli ³⁶, M. Vandenbroucke ¹³⁵, E.R. Vandewall ¹²¹, D. Vannicola ¹⁵¹,
 L. Vannoli ^{57b,57a}, R. Vari ^{75a}, E.W. Varnes ⁷, C. Varni ^{17a}, T. Varol ¹⁴⁸, D. Varouchas ⁶⁶,
 L. Varriale ¹⁶³, K.E. Varvell ¹⁴⁷, M.E. Vasile ^{27b}, L. Vaslin ⁴⁰, G.A. Vasquez ¹⁶⁵, F. Vazeille ⁴⁰,
 T. Vazquez Schroeder ³⁶, J. Veatch ³¹, V. Vecchio ¹⁰¹, M.J. Veen ¹⁰³, I. Veliscek ¹²⁶,
 L.M. Veloce ¹⁵⁵, F. Veloso ^{130a,130c}, S. Veneziano ^{75a}, A. Ventura ^{70a,70b}, A. Verbytskyi ¹¹⁰,
 M. Verducci ^{74a,74b}, C. Vergis ²⁴, M. Verissimo De Araujo ^{83b}, W. Verkerke ¹¹⁴,
 J.C. Vermeulen ¹¹⁴, C. Vernieri ¹⁴³, P.J. Verschuuren ⁹⁵, M. Vessella ¹⁰³, M.C. Vetterli ^{142,ak},
 A. Vgenopoulos ^{152,f}, N. Viaux Maira ^{137f}, T. Vickey ¹³⁹, O.E. Vickey Boeriu ¹³⁹,
 G.H.A. Viehhauser ¹²⁶, L. Vigani ^{63b}, M. Villa ^{23b,23a}, M. Villaplana Perez ¹⁶³, E.M. Villhauer ⁵²,
 E. Vilucchi ⁵³, M.G. Vincter ³⁴, G.S. Virdee ²⁰, A. Vishwakarma ⁵², A. Visibile ¹¹⁴, C. Vittori ³⁶,
 I. Vivarelli ¹⁴⁶, V. Vladimirov ¹⁶⁷, E. Voevodina ¹¹⁰, F. Vogel ¹⁰⁹, P. Vokac ¹³², J. Von Ahnen ⁴⁸,
 E. Von Toerne ²⁴, B. Vormwald ³⁶, V. Vorobel ¹³³, K. Vorobev ³⁷, M. Vos ¹⁶³, K. Voss ¹⁴¹,
 J.H. Vossebeld ⁹², M. Vozak ¹¹⁴, L. Vozdecky ⁹⁴, N. Vranjes ¹⁵, M. Vranjes Milosavljevic ¹⁵,
 M. Vreeswijk ¹¹⁴, R. Vuillermet ³⁶, O. Vujinovic ¹⁰⁰, I. Vukotic ³⁹, S. Wada ¹⁵⁷, C. Wagner ¹⁰³,
 J.M. Wagner ^{17a}, W. Wagner ¹⁷¹, S. Wahdan ¹⁷¹, H. Wahlberg ⁹⁰, R. Wakasa ¹⁵⁷,
 M. Wakida ¹¹¹, J. Walder ¹³⁴, R. Walker ¹⁰⁹, W. Walkowiak ¹⁴¹, A. Wall ¹²⁸, T. Wamorkar ⁶,
 A.Z. Wang ¹⁷⁰, C. Wang ¹⁰⁰, C. Wang ^{62c}, H. Wang ^{17a}, J. Wang ^{64a}, R.-J. Wang ¹⁰⁰,
 R. Wang ⁶¹, R. Wang ⁶, S.M. Wang ¹⁴⁸, S. Wang ^{62b}, T. Wang ^{62a}, W.T. Wang ⁸⁰,
 W. Wang ^{14a}, X. Wang ^{14c}, X. Wang ¹⁶², X. Wang ^{62c}, Y. Wang ^{62d}, Y. Wang ^{14c}, Z. Wang ¹⁰⁶,
 Z. Wang ^{62d,51,62c}, Z. Wang ¹⁰⁶, A. Warburton ¹⁰⁴, R.J. Ward ²⁰, N. Warrack ⁵⁹, A.T. Watson ²⁰,
 H. Watson ⁵⁹, M.F. Watson ²⁰, E. Watton ^{59,134}, G. Watts ¹³⁸, B.M. Waugh ⁹⁶, C. Weber ²⁹,
 H.A. Weber ¹⁸, M.S. Weber ¹⁹, S.M. Weber ^{63a}, C. Wei ^{62a}, Y. Wei ¹²⁶, A.R. Weidberg ¹²⁶,
 E.J. Weik ¹¹⁷, J. Weingarten ⁴⁹, M. Weirich ¹⁰⁰, C. Weiser ⁵⁴, C.J. Wells ⁴⁸, T. Wenaus ²⁹,

B. Wendland ⁴⁹, T. Wengler ³⁶, N.S. Wenke¹¹⁰, N. Wermes ²⁴, M. Wessels ^{63a}, K. Whalen ¹²³, A.M. Wharton ⁹¹, A.S. White ⁶¹, A. White ⁸, M.J. White ¹, D. Whiteson ¹⁶⁰, L. Wickremasinghe ¹²⁴, W. Wiedenmann ¹⁷⁰, C. Wiel ⁵⁰, M. Wieler ¹³⁴, C. Wiglesworth ⁴², D.J. Wilbern¹²⁰, H.G. Wilkens ³⁶, D.M. Williams ⁴¹, H.H. Williams¹²⁸, S. Williams ³², S. Willocq ¹⁰³, B.J. Wilson ¹⁰¹, P.J. Windischhofer ³⁹, F.I. Winkel ³⁰, F. Winklmeier ¹²³, B.T. Winter ⁵⁴, J.K. Winter ¹⁰¹, M. Wittgen¹⁴³, M. Wobisch ⁹⁷, Z. Wolffs ¹¹⁴, R. Wölker ¹²⁶, J. Wollrath¹⁶⁰, M.W. Wolter ⁸⁷, H. Wolters ^{130a,130c}, A.F. Wongel ⁴⁸, S.D. Worm ⁴⁸, B.K. Wosiek ⁸⁷, K.W. Woźniak ⁸⁷, S. Wozniowski ⁵⁵, K. Wraight ⁵⁹, C. Wu ²⁰, J. Wu ^{14a,14e}, M. Wu ^{64a}, M. Wu ¹¹³, S.L. Wu ¹⁷⁰, X. Wu ⁵⁶, Y. Wu ^{62a}, Z. Wu ¹³⁵, J. Wuerzinger ¹¹⁰, T.R. Wyatt ¹⁰¹, B.M. Wynne ⁵², S. Xella ⁴², L. Xia ^{14c}, M. Xia ^{14b}, J. Xiang ^{64c}, X. Xiao ¹⁰⁶, M. Xie ^{62a}, X. Xie ^{62a}, S. Xin ^{14a,14e}, J. Xiong ^{17a}, D. Xu ^{14a}, H. Xu ^{62a}, L. Xu ^{62a}, R. Xu ¹²⁸, T. Xu ¹⁰⁶, Y. Xu ^{14b}, Z. Xu ⁵², Z. Xu ^{14a}, B. Yabsley ¹⁴⁷, S. Yacoob ^{33a}, N. Yamaguchi ⁸⁹, Y. Yamaguchi ¹⁵⁴, E. Yamashita ¹⁵³, H. Yamauchi ¹⁵⁷, T. Yamazaki ^{17a}, Y. Yamazaki ⁸⁵, J. Yan ^{62c}, S. Yan ¹²⁶, Z. Yan ²⁵, H.J. Yang ^{62c,62d}, H.T. Yang ^{62a}, S. Yang ^{62a}, T. Yang ^{64c}, X. Yang ^{62a}, X. Yang ^{14a}, Y. Yang ⁴⁴, Y. Yang ^{62a}, Z. Yang ^{62a}, W-M. Yao ^{17a}, Y.C. Yap ⁴⁸, H. Ye ^{14c}, H. Ye ⁵⁵, J. Ye ⁴⁴, S. Ye ²⁹, X. Ye ^{62a}, Y. Yeh ⁹⁶, I. Yeletsikh ³⁸, B.K. Yeo ^{17a}, M.R. Yexley ⁹⁶, P. Yin ⁴¹, K. Yorita ¹⁶⁸, S. Younas ^{27b}, C.J.S. Young ⁵⁴, C. Young ¹⁴³, Y. Yu ^{62a}, M. Yuan ¹⁰⁶, R. Yuan ^{62b,1}, L. Yue ⁹⁶, M. Zaazoua ^{62a}, B. Zabinski ⁸⁷, E. Zaid⁵², T. Zakareishvili ^{149b}, N. Zakharchuk ³⁴, S. Zambito ⁵⁶, J.A. Zamora Saa ^{137d,137b}, J. Zang ¹⁵³, D. Zanzi ⁵⁴, O. Zaplatilek ¹³², C. Zeitnitz ¹⁷¹, H. Zeng ^{14a}, J.C. Zeng ¹⁶², D.T. Zenger Jr ²⁶, O. Zenin ³⁷, T. Ženiš ^{28a}, S. Zenz ⁹⁴, S. Zerradi ^{35a}, D. Zerwas ⁶⁶, M. Zhai ^{14a,14e}, B. Zhang ^{14c}, D.F. Zhang ¹³⁹, J. Zhang ^{62b}, J. Zhang ⁶, K. Zhang ^{14a,14e}, L. Zhang ^{14c}, P. Zhang ^{14a,14e}, R. Zhang ¹⁷⁰, S. Zhang ¹⁰⁶, T. Zhang ¹⁵³, X. Zhang ^{62c}, X. Zhang ^{62b}, Y. Zhang ^{62c,5}, Y. Zhang ⁹⁶, Z. Zhang ^{17a}, Z. Zhang ⁶⁶, H. Zhao ¹³⁸, P. Zhao ⁵¹, T. Zhao ^{62b}, Y. Zhao ¹³⁶, Z. Zhao ^{62a}, A. Zhemchugov ³⁸, K. Zheng ¹⁶², X. Zheng ^{62a}, Z. Zheng ¹⁴³, D. Zhong ¹⁶², B. Zhou¹⁰⁶, H. Zhou ⁷, N. Zhou ^{62c}, Y. Zhou⁷, C.G. Zhu ^{62b}, J. Zhu ¹⁰⁶, Y. Zhu ^{62c}, Y. Zhu ^{62a}, X. Zhuang ^{14a}, K. Zhukov ³⁷, V. Zhulanov ³⁷, N.I. Zimine ³⁸, J. Zinsser ^{63b}, M. Ziolkowski ¹⁴¹, L. Živković ¹⁵, A. Zoccoli ^{23b,23a}, K. Zoch ⁵⁶, T.G. Zorbas ¹³⁹, O. Zormpa ⁴⁶, W. Zou ⁴¹, L. Zwalinski ³⁶.

¹Department of Physics, University of Adelaide, Adelaide; Australia.

²Department of Physics, University of Alberta, Edmonton AB; Canada.

³(^a)Department of Physics, Ankara University, Ankara; (^b)Division of Physics, TOBB University of Economics and Technology, Ankara; Türkiye.

⁴LAPP, Université Savoie Mont Blanc, CNRS/IN2P3, Annecy; France.

⁵APC, Université Paris Cité, CNRS/IN2P3, Paris; France.

⁶High Energy Physics Division, Argonne National Laboratory, Argonne IL; United States of America.

⁷Department of Physics, University of Arizona, Tucson AZ; United States of America.

⁸Department of Physics, University of Texas at Arlington, Arlington TX; United States of America.

⁹Physics Department, National and Kapodistrian University of Athens, Athens; Greece.

¹⁰Physics Department, National Technical University of Athens, Zografou; Greece.

¹¹Department of Physics, University of Texas at Austin, Austin TX; United States of America.

¹²Institute of Physics, Azerbaijan Academy of Sciences, Baku; Azerbaijan.

¹³Institut de Física d'Altes Energies (IFAE), Barcelona Institute of Science and Technology, Barcelona; Spain.

¹⁴(^a)Institute of High Energy Physics, Chinese Academy of Sciences, Beijing; (^b)Physics Department, Tsinghua University, Beijing; (^c)Department of Physics, Nanjing University, Nanjing; (^d)School of Science,

Shenzhen Campus of Sun Yat-sen University;^(e) University of Chinese Academy of Science (UCAS), Beijing; China.

¹⁵Institute of Physics, University of Belgrade, Belgrade; Serbia.

¹⁶Department for Physics and Technology, University of Bergen, Bergen; Norway.

¹⁷(^a) Physics Division, Lawrence Berkeley National Laboratory, Berkeley CA; (^b) University of California, Berkeley CA; United States of America.

¹⁸Institut für Physik, Humboldt Universität zu Berlin, Berlin; Germany.

¹⁹Albert Einstein Center for Fundamental Physics and Laboratory for High Energy Physics, University of Bern, Bern; Switzerland.

²⁰School of Physics and Astronomy, University of Birmingham, Birmingham; United Kingdom.

²¹(^a) Department of Physics, Bogazici University, Istanbul; (^b) Department of Physics Engineering, Gaziantep University, Gaziantep; (^c) Department of Physics, Istanbul University, Istanbul; Türkiye.

²²(^a) Facultad de Ciencias y Centro de Investigaciones, Universidad Antonio Nariño, Bogotá; (^b) Departamento de Física, Universidad Nacional de Colombia, Bogotá; (^c) Pontificia Universidad Javeriana, Bogota; Colombia.

²³(^a) Dipartimento di Fisica e Astronomia A. Righi, Università di Bologna, Bologna; (^b) INFN Sezione di Bologna; Italy.

²⁴Physikalisches Institut, Universität Bonn, Bonn; Germany.

²⁵Department of Physics, Boston University, Boston MA; United States of America.

²⁶Department of Physics, Brandeis University, Waltham MA; United States of America.

²⁷(^a) Transilvania University of Brasov, Brasov; (^b) Horia Hulubei National Institute of Physics and Nuclear Engineering, Bucharest; (^c) Department of Physics, Alexandru Ioan Cuza University of Iasi, Iasi; (^d) National Institute for Research and Development of Isotopic and Molecular Technologies, Physics Department, Cluj-Napoca; (^e) University Politehnica Bucharest, Bucharest; (^f) West University in Timisoara, Timisoara; (^g) Faculty of Physics, University of Bucharest, Bucharest; Romania.

²⁸(^a) Faculty of Mathematics, Physics and Informatics, Comenius University, Bratislava; (^b) Department of Subnuclear Physics, Institute of Experimental Physics of the Slovak Academy of Sciences, Kosice; Slovak Republic.

²⁹Physics Department, Brookhaven National Laboratory, Upton NY; United States of America.

³⁰Universidad de Buenos Aires, Facultad de Ciencias Exactas y Naturales, Departamento de Física, y CONICET, Instituto de Física de Buenos Aires (IFIBA), Buenos Aires; Argentina.

³¹California State University, CA; United States of America.

³²Cavendish Laboratory, University of Cambridge, Cambridge; United Kingdom.

³³(^a) Department of Physics, University of Cape Town, Cape Town; (^b) iThemba Labs, Western

Cape; (^c) Department of Mechanical Engineering Science, University of Johannesburg,

Johannesburg; (^d) National Institute of Physics, University of the Philippines Diliman

(Philippines); (^e) University of South Africa, Department of Physics, Pretoria; (^f) University of Zululand, KwaDlangezwa; (^g) School of Physics, University of the Witwatersrand, Johannesburg; South Africa.

³⁴Department of Physics, Carleton University, Ottawa ON; Canada.

³⁵(^a) Faculté des Sciences Ain Chock, Réseau Universitaire de Physique des Hautes Energies - Université Hassan II, Casablanca; (^b) Faculté des Sciences, Université Ibn-Tofail, Kénitra; (^c) Faculté des Sciences Semlalia, Université Cadi Ayyad, LPHEA-Marrakech; (^d) LPMR, Faculté des Sciences, Université Mohamed Premier, Oujda; (^e) Faculté des sciences, Université Mohammed V, Rabat; (^f) Institute of Applied Physics, Mohammed VI Polytechnic University, Ben Guerir; Morocco.

³⁶CERN, Geneva; Switzerland.

³⁷Affiliated with an institute covered by a cooperation agreement with CERN.

³⁸Affiliated with an international laboratory covered by a cooperation agreement with CERN.

- ³⁹Enrico Fermi Institute, University of Chicago, Chicago IL; United States of America.
- ⁴⁰LPC, Université Clermont Auvergne, CNRS/IN2P3, Clermont-Ferrand; France.
- ⁴¹Nevis Laboratory, Columbia University, Irvington NY; United States of America.
- ⁴²Niels Bohr Institute, University of Copenhagen, Copenhagen; Denmark.
- ⁴³(^a)Dipartimento di Fisica, Università della Calabria, Rende; (^b)INFN Gruppo Collegato di Cosenza, Laboratori Nazionali di Frascati; Italy.
- ⁴⁴Physics Department, Southern Methodist University, Dallas TX; United States of America.
- ⁴⁵Physics Department, University of Texas at Dallas, Richardson TX; United States of America.
- ⁴⁶National Centre for Scientific Research "Demokritos", Agia Paraskevi; Greece.
- ⁴⁷(^a)Department of Physics, Stockholm University; (^b)Oskar Klein Centre, Stockholm; Sweden.
- ⁴⁸Deutsches Elektronen-Synchrotron DESY, Hamburg and Zeuthen; Germany.
- ⁴⁹Fakultät Physik , Technische Universität Dortmund, Dortmund; Germany.
- ⁵⁰Institut für Kern- und Teilchenphysik, Technische Universität Dresden, Dresden; Germany.
- ⁵¹Department of Physics, Duke University, Durham NC; United States of America.
- ⁵²SUPA - School of Physics and Astronomy, University of Edinburgh, Edinburgh; United Kingdom.
- ⁵³INFN e Laboratori Nazionali di Frascati, Frascati; Italy.
- ⁵⁴Physikalisches Institut, Albert-Ludwigs-Universität Freiburg, Freiburg; Germany.
- ⁵⁵II. Physikalisches Institut, Georg-August-Universität Göttingen, Göttingen; Germany.
- ⁵⁶Département de Physique Nucléaire et Corpusculaire, Université de Genève, Genève; Switzerland.
- ⁵⁷(^a)Dipartimento di Fisica, Università di Genova, Genova; (^b)INFN Sezione di Genova; Italy.
- ⁵⁸II. Physikalisches Institut, Justus-Liebig-Universität Giessen, Giessen; Germany.
- ⁵⁹SUPA - School of Physics and Astronomy, University of Glasgow, Glasgow; United Kingdom.
- ⁶⁰LPSC, Université Grenoble Alpes, CNRS/IN2P3, Grenoble INP, Grenoble; France.
- ⁶¹Laboratory for Particle Physics and Cosmology, Harvard University, Cambridge MA; United States of America.
- ⁶²(^a)Department of Modern Physics and State Key Laboratory of Particle Detection and Electronics, University of Science and Technology of China, Hefei; (^b)Institute of Frontier and Interdisciplinary Science and Key Laboratory of Particle Physics and Particle Irradiation (MOE), Shandong University, Qingdao; (^c)School of Physics and Astronomy, Shanghai Jiao Tong University, Key Laboratory for Particle Astrophysics and Cosmology (MOE), SKLPPC, Shanghai; (^d)Tsung-Dao Lee Institute, Shanghai; China.
- ⁶³(^a)Kirchhoff-Institut für Physik, Ruprecht-Karls-Universität Heidelberg, Heidelberg; (^b)Physikalisches Institut, Ruprecht-Karls-Universität Heidelberg, Heidelberg; Germany.
- ⁶⁴(^a)Department of Physics, Chinese University of Hong Kong, Shatin, N.T., Hong Kong; (^b)Department of Physics, University of Hong Kong, Hong Kong; (^c)Department of Physics and Institute for Advanced Study, Hong Kong University of Science and Technology, Clear Water Bay, Kowloon, Hong Kong; China.
- ⁶⁵Department of Physics, National Tsing Hua University, Hsinchu; Taiwan.
- ⁶⁶IJCLab, Université Paris-Saclay, CNRS/IN2P3, 91405, Orsay; France.
- ⁶⁷Centro Nacional de Microelectrónica (IMB-CNM-CSIC), Barcelona; Spain.
- ⁶⁸Department of Physics, Indiana University, Bloomington IN; United States of America.
- ⁶⁹(^a)INFN Gruppo Collegato di Udine, Sezione di Trieste, Udine; (^b)ICTP, Trieste; (^c)Dipartimento Politecnico di Ingegneria e Architettura, Università di Udine, Udine; Italy.
- ⁷⁰(^a)INFN Sezione di Lecce; (^b)Dipartimento di Matematica e Fisica, Università del Salento, Lecce; Italy.
- ⁷¹(^a)INFN Sezione di Milano; (^b)Dipartimento di Fisica, Università di Milano, Milano; Italy.
- ⁷²(^a)INFN Sezione di Napoli; (^b)Dipartimento di Fisica, Università di Napoli, Napoli; Italy.
- ⁷³(^a)INFN Sezione di Pavia; (^b)Dipartimento di Fisica, Università di Pavia, Pavia; Italy.
- ⁷⁴(^a)INFN Sezione di Pisa; (^b)Dipartimento di Fisica E. Fermi, Università di Pisa, Pisa; Italy.
- ⁷⁵(^a)INFN Sezione di Roma; (^b)Dipartimento di Fisica, Sapienza Università di Roma, Roma; Italy.

- ^{76(a)}INFN Sezione di Roma Tor Vergata;^(b)Dipartimento di Fisica, Università di Roma Tor Vergata, Roma; Italy.
- ^{77(a)}INFN Sezione di Roma Tre;^(b)Dipartimento di Matematica e Fisica, Università Roma Tre, Roma; Italy.
- ^{78(a)}INFN-TIFPA;^(b)Università degli Studi di Trento, Trento; Italy.
- ⁷⁹Universität Innsbruck, Department of Astro and Particle Physics, Innsbruck; Austria.
- ⁸⁰University of Iowa, Iowa City IA; United States of America.
- ⁸¹Department of Physics and Astronomy, Iowa State University, Ames IA; United States of America.
- ⁸²Istinye University, Sariyer, Istanbul; Türkiye.
- ^{83(a)}Departamento de Engenharia Elétrica, Universidade Federal de Juiz de Fora (UFJF), Juiz de Fora;^(b)Universidade Federal do Rio De Janeiro COPPE/EE/IF, Rio de Janeiro;^(c)Instituto de Física, Universidade de São Paulo, São Paulo;^(d)Rio de Janeiro State University, Rio de Janeiro; Brazil.
- ⁸⁴KEK, High Energy Accelerator Research Organization, Tsukuba; Japan.
- ⁸⁵Graduate School of Science, Kobe University, Kobe; Japan.
- ^{86(a)}AGH University of Krakow, Faculty of Physics and Applied Computer Science, Krakow;^(b)Marian Smoluchowski Institute of Physics, Jagiellonian University, Krakow; Poland.
- ⁸⁷Institute of Nuclear Physics Polish Academy of Sciences, Krakow; Poland.
- ⁸⁸Faculty of Science, Kyoto University, Kyoto; Japan.
- ⁸⁹Research Center for Advanced Particle Physics and Department of Physics, Kyushu University, Fukuoka ; Japan.
- ⁹⁰Instituto de Física La Plata, Universidad Nacional de La Plata and CONICET, La Plata; Argentina.
- ⁹¹Physics Department, Lancaster University, Lancaster; United Kingdom.
- ⁹²Oliver Lodge Laboratory, University of Liverpool, Liverpool; United Kingdom.
- ⁹³Department of Experimental Particle Physics, Jožef Stefan Institute and Department of Physics, University of Ljubljana, Ljubljana; Slovenia.
- ⁹⁴School of Physics and Astronomy, Queen Mary University of London, London; United Kingdom.
- ⁹⁵Department of Physics, Royal Holloway University of London, Egham; United Kingdom.
- ⁹⁶Department of Physics and Astronomy, University College London, London; United Kingdom.
- ⁹⁷Louisiana Tech University, Ruston LA; United States of America.
- ⁹⁸Fysiska institutionen, Lunds universitet, Lund; Sweden.
- ⁹⁹Departamento de Física Teórica C-15 and CIAFF, Universidad Autónoma de Madrid, Madrid; Spain.
- ¹⁰⁰Institut für Physik, Universität Mainz, Mainz; Germany.
- ¹⁰¹School of Physics and Astronomy, University of Manchester, Manchester; United Kingdom.
- ¹⁰²CPPM, Aix-Marseille Université, CNRS/IN2P3, Marseille; France.
- ¹⁰³Department of Physics, University of Massachusetts, Amherst MA; United States of America.
- ¹⁰⁴Department of Physics, McGill University, Montreal QC; Canada.
- ¹⁰⁵School of Physics, University of Melbourne, Victoria; Australia.
- ¹⁰⁶Department of Physics, University of Michigan, Ann Arbor MI; United States of America.
- ¹⁰⁷Department of Physics and Astronomy, Michigan State University, East Lansing MI; United States of America.
- ¹⁰⁸Group of Particle Physics, University of Montreal, Montreal QC; Canada.
- ¹⁰⁹Fakultät für Physik, Ludwig-Maximilians-Universität München, München; Germany.
- ¹¹⁰Max-Planck-Institut für Physik (Werner-Heisenberg-Institut), München; Germany.
- ¹¹¹Graduate School of Science and Kobayashi-Maskawa Institute, Nagoya University, Nagoya; Japan.
- ¹¹²Department of Physics and Astronomy, University of New Mexico, Albuquerque NM; United States of America.
- ¹¹³Institute for Mathematics, Astrophysics and Particle Physics, Radboud University/Nikhef, Nijmegen;

Netherlands.

¹¹⁴Nikhef National Institute for Subatomic Physics and University of Amsterdam, Amsterdam; Netherlands.

¹¹⁵Department of Physics, Northern Illinois University, DeKalb IL; United States of America.

¹¹⁶(^a)New York University Abu Dhabi, Abu Dhabi; (^b)University of Sharjah, Sharjah; United Arab Emirates.

¹¹⁷Department of Physics, New York University, New York NY; United States of America.

¹¹⁸Ochanomizu University, Otsuka, Bunkyo-ku, Tokyo; Japan.

¹¹⁹Ohio State University, Columbus OH; United States of America.

¹²⁰Homer L. Dodge Department of Physics and Astronomy, University of Oklahoma, Norman OK; United States of America.

¹²¹Department of Physics, Oklahoma State University, Stillwater OK; United States of America.

¹²²Palacký University, Joint Laboratory of Optics, Olomouc; Czech Republic.

¹²³Institute for Fundamental Science, University of Oregon, Eugene, OR; United States of America.

¹²⁴Graduate School of Science, Osaka University, Osaka; Japan.

¹²⁵Department of Physics, University of Oslo, Oslo; Norway.

¹²⁶Department of Physics, Oxford University, Oxford; United Kingdom.

¹²⁷LPNHE, Sorbonne Université, Université Paris Cité, CNRS/IN2P3, Paris; France.

¹²⁸Department of Physics, University of Pennsylvania, Philadelphia PA; United States of America.

¹²⁹Department of Physics and Astronomy, University of Pittsburgh, Pittsburgh PA; United States of America.

¹³⁰(^a)Laboratório de Instrumentação e Física Experimental de Partículas - LIP, Lisboa; (^b)Departamento de Física, Faculdade de Ciências, Universidade de Lisboa, Lisboa; (^c)Departamento de Física, Universidade de Coimbra, Coimbra; (^d)Centro de Física Nuclear da Universidade de Lisboa, Lisboa; (^e)Departamento de Física, Universidade do Minho, Braga; (^f)Departamento de Física Teórica y del Cosmos, Universidad de Granada, Granada (Spain); (^g)Departamento de Física, Instituto Superior Técnico, Universidade de Lisboa, Lisboa; Portugal.

¹³¹Institute of Physics of the Czech Academy of Sciences, Prague; Czech Republic.

¹³²Czech Technical University in Prague, Prague; Czech Republic.

¹³³Charles University, Faculty of Mathematics and Physics, Prague; Czech Republic.

¹³⁴Particle Physics Department, Rutherford Appleton Laboratory, Didcot; United Kingdom.

¹³⁵IRFU, CEA, Université Paris-Saclay, Gif-sur-Yvette; France.

¹³⁶Santa Cruz Institute for Particle Physics, University of California Santa Cruz, Santa Cruz CA; United States of America.

¹³⁷(^a)Departamento de Física, Pontificia Universidad Católica de Chile, Santiago; (^b)Millennium Institute for Subatomic physics at high energy frontier (SAPHIR), Santiago; (^c)Instituto de Investigación Multidisciplinario en Ciencia y Tecnología, y Departamento de Física, Universidad de La Serena; (^d)Universidad Andres Bello, Department of Physics, Santiago; (^e)Instituto de Alta Investigación, Universidad de Tarapacá, Arica; (^f)Departamento de Física, Universidad Técnica Federico Santa María, Valparaíso; Chile.

¹³⁸Department of Physics, University of Washington, Seattle WA; United States of America.

¹³⁹Department of Physics and Astronomy, University of Sheffield, Sheffield; United Kingdom.

¹⁴⁰Department of Physics, Shinshu University, Nagano; Japan.

¹⁴¹Department Physik, Universität Siegen, Siegen; Germany.

¹⁴²Department of Physics, Simon Fraser University, Burnaby BC; Canada.

¹⁴³SLAC National Accelerator Laboratory, Stanford CA; United States of America.

¹⁴⁴Department of Physics, Royal Institute of Technology, Stockholm; Sweden.

- ¹⁴⁵Departments of Physics and Astronomy, Stony Brook University, Stony Brook NY; United States of America.
- ¹⁴⁶Department of Physics and Astronomy, University of Sussex, Brighton; United Kingdom.
- ¹⁴⁷School of Physics, University of Sydney, Sydney; Australia.
- ¹⁴⁸Institute of Physics, Academia Sinica, Taipei; Taiwan.
- ¹⁴⁹^(a)E. Andronikashvili Institute of Physics, Iv. Javakhishvili Tbilisi State University, Tbilisi; ^(b)High Energy Physics Institute, Tbilisi State University, Tbilisi; ^(c)University of Georgia, Tbilisi; Georgia.
- ¹⁵⁰Department of Physics, Technion, Israel Institute of Technology, Haifa; Israel.
- ¹⁵¹Raymond and Beverly Sackler School of Physics and Astronomy, Tel Aviv University, Tel Aviv; Israel.
- ¹⁵²Department of Physics, Aristotle University of Thessaloniki, Thessaloniki; Greece.
- ¹⁵³International Center for Elementary Particle Physics and Department of Physics, University of Tokyo, Tokyo; Japan.
- ¹⁵⁴Department of Physics, Tokyo Institute of Technology, Tokyo; Japan.
- ¹⁵⁵Department of Physics, University of Toronto, Toronto ON; Canada.
- ¹⁵⁶^(a)TRIUMF, Vancouver BC; ^(b)Department of Physics and Astronomy, York University, Toronto ON; Canada.
- ¹⁵⁷Division of Physics and Tomonaga Center for the History of the Universe, Faculty of Pure and Applied Sciences, University of Tsukuba, Tsukuba; Japan.
- ¹⁵⁸Department of Physics and Astronomy, Tufts University, Medford MA; United States of America.
- ¹⁵⁹United Arab Emirates University, Al Ain; United Arab Emirates.
- ¹⁶⁰Department of Physics and Astronomy, University of California Irvine, Irvine CA; United States of America.
- ¹⁶¹Department of Physics and Astronomy, University of Uppsala, Uppsala; Sweden.
- ¹⁶²Department of Physics, University of Illinois, Urbana IL; United States of America.
- ¹⁶³Instituto de Física Corpuscular (IFIC), Centro Mixto Universidad de Valencia - CSIC, Valencia; Spain.
- ¹⁶⁴Department of Physics, University of British Columbia, Vancouver BC; Canada.
- ¹⁶⁵Department of Physics and Astronomy, University of Victoria, Victoria BC; Canada.
- ¹⁶⁶Fakultät für Physik und Astronomie, Julius-Maximilians-Universität Würzburg, Würzburg; Germany.
- ¹⁶⁷Department of Physics, University of Warwick, Coventry; United Kingdom.
- ¹⁶⁸Waseda University, Tokyo; Japan.
- ¹⁶⁹Department of Particle Physics and Astrophysics, Weizmann Institute of Science, Rehovot; Israel.
- ¹⁷⁰Department of Physics, University of Wisconsin, Madison WI; United States of America.
- ¹⁷¹Fakultät für Mathematik und Naturwissenschaften, Fachgruppe Physik, Bergische Universität Wuppertal, Wuppertal; Germany.
- ¹⁷²Department of Physics, Yale University, New Haven CT; United States of America.
- ^a Also Affiliated with an institute covered by a cooperation agreement with CERN.
- ^b Also at An-Najah National University, Nablus; Palestine.
- ^c Also at APC, Université Paris Cité, CNRS/IN2P3, Paris; France.
- ^d Also at Borough of Manhattan Community College, City University of New York, New York NY; United States of America.
- ^e Also at Center for High Energy Physics, Peking University; China.
- ^f Also at Center for Interdisciplinary Research and Innovation (CIRI-AUTH), Thessaloniki; Greece.
- ^g Also at Centro Studi e Ricerche Enrico Fermi; Italy.
- ^h Also at CERN, Geneva; Switzerland.
- ⁱ Also at Département de Physique Nucléaire et Corpusculaire, Université de Genève, Genève; Switzerland.
- ^j Also at Departament de Física de la Universitat Autònoma de Barcelona, Barcelona; Spain.
- ^k Also at Department of Financial and Management Engineering, University of the Aegean, Chios; Greece.

^l Also at Department of Physics and Astronomy, Michigan State University, East Lansing MI; United States of America.

^m Also at Department of Physics and Astronomy, University of Victoria, Victoria BC; Canada.

ⁿ Also at Department of Physics, Ben Gurion University of the Negev, Beer Sheva; Israel.

^o Also at Department of Physics, California State University, Sacramento; United States of America.

^p Also at Department of Physics, King's College London, London; United Kingdom.

^q Also at Department of Physics, Royal Holloway University of London, Egham; United Kingdom.

^r Also at Department of Physics, Stanford University, Stanford CA; United States of America.

^s Also at Department of Physics, University of Fribourg, Fribourg; Switzerland.

^t Also at Department of Physics, University of Thessaly; Greece.

^u Also at Department of Physics, Westmont College, Santa Barbara; United States of America.

^v Also at Fakultät für Mathematik und Naturwissenschaften, Fachgruppe Physik, Bergische Universität Wuppertal, Wuppertal; Germany.

^w Also at Hellenic Open University, Patras; Greece.

^x Also at Institutio Catalana de Recerca i Estudis Avancats, ICREA, Barcelona; Spain.

^y Also at Institut für Experimentalphysik, Universität Hamburg, Hamburg; Germany.

^z Also at Institute for Nuclear Research and Nuclear Energy (INRNE) of the Bulgarian Academy of Sciences, Sofia; Bulgaria.

^{aa} Also at Institute of Applied Physics, Mohammed VI Polytechnic University, Ben Guerir; Morocco.

^{ab} Also at Institute of Particle Physics (IPP); Canada.

^{ac} Also at Institute of Physics and Technology, Ulaanbaatar; Mongolia.

^{ad} Also at Institute of Physics, Azerbaijan Academy of Sciences, Baku; Azerbaijan.

^{ae} Also at Institute of Theoretical Physics, Iliia State University, Tbilisi; Georgia.

^{af} Also at L2IT, Université de Toulouse, CNRS/IN2P3, UPS, Toulouse; France.

^{ag} Also at Lawrence Livermore National Laboratory, Livermore; United States of America.

^{ah} Also at National Institute of Physics, University of the Philippines Diliman (Philippines); Philippines.

^{ai} Also at Technical University of Munich, Munich; Germany.

^{aj} Also at The Collaborative Innovation Center of Quantum Matter (CICQM), Beijing; China.

^{ak} Also at TRIUMF, Vancouver BC; Canada.

^{al} Also at Università di Napoli Parthenope, Napoli; Italy.

^{am} Also at University of Colorado Boulder, Department of Physics, Colorado; United States of America.

^{an} Also at Washington College, Chestertown, MD; United States of America.

^{ao} Also at Yeditepe University, Physics Department, Istanbul; Türkiye.

* Deceased